IFITM1 Modulates Circadian Rhythm by Regulating CRY1 Stability

by

Melis Çelik

A Dissertation Submitted to the
Graduate School of Sciences and Engineering
in Partial Fulfillment of the Requirements for
the Degree of

Master of Science

in

Molecular Biology and Genetics

July, 2022

IFITM1 Modulates Circadian Rhythm by Regulating CRY1 Stability

Koç University

Graduate School of Sciences and Engineering

This is to certify that I have examined this copy of a master's thesis by

Melis Çelik

and have found that it is complete and satisfactory in all respects,
and that any and all revisions required by the final
examining committee have been made.

Committee Members:

Prof. İ. Halil Kavaklı

Assist. Prof. Cihan Aydın

Prof. Nuri Öztürk

Assist. Prof. Hasan Demirci

Assist. Prof. Serkan Kır

Date: 26/07/2022

Dedicated to my mother, father, and sweet sister, who always supported and encouraged me to be determined, hardworking, and brave in this journey.

ABSTRACT

Circadian rhythm, generated by the central and peripheral clocks, regulates nearly all physiological and behavioral processes by synchronizing internal time to the earth's rotation within a period of 24 hours. Hence, disruption of circadian rhythm causes different types of diseases such as cancer, cognitive impairments, metabolic diseases, psychiatric illnesses, and immune system-related disorders. At the molecular level, the circadian clock is controlled by the interlocking of positive and negative transcriptional-translational feedback loops (TTFL). In the positive loop, BMAL1 and CLOCK form a heterodimer and initiate the transcription of clock-controlled genes (*CCG*), including *Per* and *Cry,* by binding E-BOX elements. In the negative loop of TTFL, Later, a heterodimer of CRY and PER interact with casein kinase Iε (CKIε) and translocates to the nucleus to repress the transactivation of BMAL1:CLOCK, thus transcription of *CCG.*

In this thesis, I demonstrated that IFITM1, a transmembrane protein taking a role in the immune defense under viral attack and identified by machine learning, functionally interacts with CRY1 through the C-terminal domain of CRY1 in the nucleus. Knockout of *IFITM1* by CRISPR/Cas9 in U2-OS *Bmal1-dluc* cells leads to period lengthening by 1.28 h and dampening of the amplitude. Further, biochemical studies showed that IFITM1 increases the half-life of CRY1 significantly and represses the BMAL1:CLOCK-driven transcription, hence modulating circadian rhythmicity. Moreover, treatment of U2OS cells with poly (I: C) result in an increased level of IFITM1 and a change in circadian period length. This suggests that IFITM1-CRY1 interaction may be important for regulating cellular circadian physiology and circadian clock-driven immune system regulation.

ÖZETÇE

Merkezi ve çevresel saatler tarafından üretilen sirkadiyen ritim, içsel zamanı 24 saatlik bir süre içinde Dünya'nın dönüşüne göre senkronize ederek neredeyse tüm fizyolojik ve davranışsal süreçleri düzenler. Dolayısıyla sirkadiyen ritmin bozulması kanser, bilişsel ve metabolik bozukluklar, psikiyatrik rahatsızlıklar ve bağışıklık sistemi ile ilgili sorunların ortaya çıkmasına neden olur. Moleküler düzeyde, sirkadiyen saat, iç içe geçmiş pozitif ve negatif transkripsiyonel-translasyonel geri besleme döngüleri (TTFL) tarafından kontrol edilir. Pozitif döngüde, BMAL1 ve CLOCK bir heterodimer oluşturur ve E-BOX kutucuğuna bağlanarak, *Per* ve *Cry* dahil olmak üzere saat tarafından kontrol edilen genlerin (*CCG*) transkripsiyonunu başlatır. TTFL'nin negatif döngüsünde ise CRY ve PER heterodimeri kazein kinaz I ε (CKIε) ile etkileşime girerek çekirdeğe taşınır ve BMAL1:CLOCK'un transaktivasyonunu, dolayısıyla *CCG'*nin transkripsiyonunu baskılar.

Bu tezde, viral saldırı altında bağışıklık savunmasında rol oynayan ve makine öğrenme stratejileri ile tanımlanmış bir transmembran protein olan IFITM1'in, çekirdekte CRY1'in C-terminal bölgesi aracılığıyla fonksiyonel olarak CRY1 ile etkileşime girdiğini gösterdim. U2-OS *Bmal1-dluc* hücrelerinde IFITM1'in CRISPR/Cas9 uygulanarak devre dışı bırakılması sonucunda, sürenin 1,28 saat uzamasına ve genliğin azalmasına neden olmuştur. Ayrıca biyokimyasal çalışmalar, IFITM1'in CRY1'in yarılanma ömrünü önemli ölçüde arttırdığını ve BMAL1:CLOCK kontrollü transkripsiyonu baskıladığını, dolayısıyla sirkadiyen ritmikliği modüle ettiğini göstermiştir. Ayrıca, U2-OS hücrelerinin Poli (I: C) ile müdahalesi sonucunda, IFITM1 seviyesinin artmasına ve sirkadiyen periyot uzunluğunun değişmesine neden olduğu gözlemlenmiştir. Elde edilen bulgular sonucunda, IFITM1-CRY1 etkileşiminin, hücresel sirkadiyen fizyolojisinin çalışmasında ve sirkadiyen saate bağlı olarak bağışıklık sistemin düzenlenmesinde önemli olabileceğini düşündürmektedir.

ACKNOWLEDGMENTS

First and foremost, I would like to express my sincere appreciation to my thesis advisor Prof. İ. Halil Kavaklı, for his guidance during my master's and for accepting me into the lab by seeing my potential even though I was a first-year undergraduate student six years before, which is a milestone in my life. Besides, I would like to thank Assist. Prof. Cihan Aydın for his support, patience, mentorship, and generosity in sharing his knowledge since 2018. I am grateful for his efforts to raise me as a good scholar and teach me his scientific attitude. I am thankful for giving me the freedom to try new ideas and make mistakes by saying, *"We don't make mistakes; we have happy accidents."*

I want to thank my thesis committee members, Prof. Nuri Öztürk, Asst. Prof. Hasan Demirci and Asst. Prof. Serkan Kır for their insightful comments and their time on my thesis. I would like to sincerely thank Dr. İbrahim Barış for patiently listening to me at every turn.

I owe my sincere thanks to my dear friend Zeynep Melis Gül, *kankimmmm*, who always held my hand during these three years and was the honorary guide of this project. As I always say, you are one of the best things this lab has given me. I am grateful for the patience and support you have shown me throughout this process. I don't think any word I can use in English can express my gratitude. Thank you for doing RNA isolation with me until 3 am, for being with me in every problem, for your unique understanding and hospitality, for greeting the sun together, for being just you, and many more. It is an honor to watch the scientist you are and witness your achievements. As the famous philosopher Pooh said, "*I knew when I met you an adventure was going to happen*." Don't forget that we will be friends "*even longer than forever*."

It was not an easy process to experiment and adapt to another lab due to the pandemic. At this point, getting to know the sociologist and microbiologist Gülşen Günel was another turning point in my thesis and my life. *Bacım*, it's not easy to write "thank you" words for you because I cannot express the sacrifices you made for me. Thank you for looking for microscopes with me all over Istanbul, making BiFC results available, supporting all experiments as if they were your own, teaching me microbiology, paving my way with your existence, and being with me in all my psychological processes. You are the secret hero of this study and mine. I feel so lucky to have you in my life forever.

Also, I would like to thank other CA Lab and BİLTAM members; Kader Kubat, who will be a great scientist, no doubt, for their assistance; Sevinç Baba for support and motivation; Dr. Şükrü Sadık Öner and his team for helps and generosity.

My dear Şafak, I think the experiments we did together by dancing and singing to music at night were the ones I enjoyed the most. You made that complicated process enjoyable with your joy and presence. I am grateful for our motivational phone conversations. You are one of the most scientifically minded people I know. I am very thrilled to see that you will come to very perfect places and to have the privilege of witnessing this journey closely. As an Italian family, we will always be together.

I would like to thank my dear Barış Çakılkaya for our friendship and lab partnership starting from 2014 until today. It is a different feeling to end this adventure we started with you. I have always been proud of your efforts and achievements, and I do not doubt that I will continue to do so. I would like to thank Onur Özcan for his scientific guidance and our coffee chats. Thank you for rebelling against all my problems with the same motivation as me. I would like to sincerely thank my lab mate and home mate Çağla Çakmak for her support, companionship, and touch on my life with her perseverance and opinions; and Bilge Bahar Çamur for our cheerful coffee times waiting for PCR. I am pleased to know both of you. I also want to thank Gizem Çağla Parlak for her friendship and assistance during my genotyping process. A special thanks to Çisel Kemahlı Aytekin for behaving like an older sister and for her support.

Thanks to Dr. Selma Bulut and Dr. Sibel Çal Kayıtmazbatır who welcomed me to the lab with understanding and patiently shared their knowledge. Another person who deserves special thanks is Dr. Tuba Korkmaz Ünal, mentoring me throughout the whole process and supported me. I consider myself very lucky to have the privilege of knowing you. Thanks to all beautiful people of HK lab, Çağla Ergün, Saliha Sürme, Yağmur Doruk, Begüm Baybalı, Ufuk Solmaz, Nadire Efenti, Başak Velioğlu.

Last but not least, I would like to thank my dear sister Ece, my mother and father...I could not do without you. Your endless support, patience, and love made everything much more manageable and achievable. You are my biggest chance in life. Thank you very much for waking up with me, for the time you left your work and spent with me on the roads, and for supporting my education and me in every way. Thank you for the effort you put into raising me. I love you so much, and I will always do.

This project has been supported by Tubitak 3501 program between September 2019 and July 2022. The last year of the study was completed in a collaboration with İstanbul Medeniyet University under the supervision of Assist. Prof. Cihan Aydın.

TABLE OF CONTENTS

ABSTRACT ..... **iv**

ÖZETÇE ..... **v**

ACKNOWLEDGMENTS ..... **vi**

LIST OF TABLES ..... **xii**

LIST OF FIGURES ..... **xiii**

ABBREVIATIONS ..... **xv**

Chapter 1: INTRODUCTION **1**

Chapter 2: LITERATURE REVIEW **3**

2.1 The Family of Biological Rhythms 3
2.2 Historical Background of Circadian Clock 5
2.3 Master and Peripheral Circadian Clock in Mammalian Organisms 7
2.4 The Molecular Architecture of Circadian Rhythm 8
2.5 The Significance of Circadian Rhythm in Human Physiology and Health 10
2.6 The Communication between Circadian Rhythm and Immune System 11
2.7 Interferon Inducible Transmembrane (IFITM) Protein Family 13
2.8 Significance of Novel Clock Component Discovery Research 14

Chapter 3: MATERIALS AND METHODS **15**

3.1 Plasmid Constructs and Molecular Cloning 15
3.1.1 Annealed Oligo Cloning 15
3.1.2 PCR Based Cloning 15
3.1.3 Cloning by Restriction Digest 16
3.2 Cell Lines and Regular Maintenance Procedure 16
3.3 Generation of IFITM1 Overexpressed and CRISPR Knock-out Stable Cell Lines 16
3.3.1 Determination of Optimal Selection Antibiotic Concentration 16
3.3.2 Lentivirus Production to Generate IFITM1 Overexpression and CRISPR Knock-out Stable Cell Lines 17

3.3.3 Establishment of Overexpressed Stable Cell Lines 17
3.3.4 Establishment of CRISPR Knock-out Stable Cell Lines 18
3.3.5 Monoclonal Expansion via Limiting Dilution 19
3.3.6 T7 Endonuclease Assay 19
3.4 Cell-Based Circadian Assay 20
3.5 Bimolecular Fluorescence Complementation Assay and Colocalization Analysis in Fluorescence Microscope 20
3.6 Protein Isolation and Western Blotting 21
3.6.1 Protein Isolation from Mammalian Cells 21
3.6.2 SDS PAGE and Western Blotting 22
3.6.3 Visualizing via Homemade ECL Solution 23
3.7 RNA Isolation and Real-Time PCR 23
3.7.1 RNA Isolation from Cell Pellet 23
3.7.2 cDNA Synthesis from Isolated RNA 24
3.7.3 Real-Time PCR 24
3.8 Cytosol-Nuclear Fractionation 24
3.9 Poly(I: C) Induction 25

Chapter 4: RESULTS 26

4.1 The Expression Profile of IFITM1 Shows the Oscillation in Synchronized Cells 26
4.2 Cloning of Human cDNAs of IFITMs and CRYs into Mammalian Expression Vector 28
4.3 Generating and Verifying IFITM1 Overexpression and CRISPR/Cas9 Knock-out Stable Cell Lines 31
4.4 IFITM1 KO affects the circadian rhythmicity of U2-OS Bmal1-dluc by extending the period and dampening the amplitude. 33
4.5 IFITM1 and CRY1 physically interact and co-localize in the nucleus, but not CRY2. 35
4.6 The effect of IFITM1 on the half-life of CRY1. 38
4.7 The relative mRNA expressions of core clock genes are altered in IFITM1 overexpressed (OE) and knock-out (KO) cell lines. 39
4.8 IFITM1 is strongly upregulated by type I and type II IFNs through Poly(I: C) in induced U2-OS Bmal1-dluc. 41

4.9 When the immune system is triggered via Poly(I: C), circadian oscillations are modulated. 42
4.10 When the immune system is triggered via Poly(I: C), mRNA expression of core clock genes is changed. 44

Chapter 5: DISCUSSION 46

BIBLIOGRAPHY 52

APPENDICES 64

APPENDIX A : SUPPLEMENTARY DATA 64
APPENDIX B: PRIMER SEQUENCES 66
APPENDIX C: DNA and Protein Ladder 68
APPENDIX D: Plasmid Maps 69
APPENDIX E: Permissions and Copyrights 70

LIST OF TABLES

Table 3. 1: Phosphorylation and Annealing Incubation Times for T4 PNK 15
Table 3. 2: Sequence of oligo pairs and name of constructs used for knocking out the target gene via CRISPR 18
Table 4. 1: Plasmids and genes that used in the cloning of this study.....30
Table A. 1: The regions were amplified via PCR by adding specific Restriction Sites for subcloning into pJET-v2.....67
Table A. 2: qRT-PCR Primer List……...68

LIST OF FIGURES

Figure 2. 1: Schematic representation of biological rhythms 4
Figure 2. 2: Schematic representation of parameters defining continuous periodic oscillation 5
Figure 2. 3: Schematic representation of internal circadian clock synchronized by peripheral and master clock and entrainment. 7
Figure 2. 4: Representation of molecular mechanism of circadian rhythm controlled by interlocked transcriptions and translation feedback loops. 10
Figure 2. 5: Schematic representation of molecular associations between circadian clock components and immune system elements. 12
Figure 3. 1: Schematic representation of BiFC (Bimolecular Fluorescent Complementation Assay) and co-localization working principle 21
Figure 4. 1: RT-qPCR detection of *IFITM1* mRNA amount oscillation in 4 hours intervals for 20 hours after synchronization with Dexamethasone. 27
Figure 4. 2: The circadian expression pattern of *Ifitm1* in mouse tissues. 27
Figure 4. 3: Diagnostic restriction digest products were run on an 0.8% agarose gel to verify the correct orientation and as well as a correct insert in the plasmids. In the figure, the plasmid names are written above each gel. 29
Figure 4. 4: Western Blot verification of pCMV-Sport6-FLAG-*IFITM* recombinant constructs.. 29
Figure 4. 5: Protein Level Verification of Overexpression and CRISPR/Cas9 constructs by Western Blot. 31
Figure 4. 6: Western Blot verification of monoclonal selected colonies from *IFITM1* KO U2-OS and U2-OS *Bmal1-dluc* bulk population. 32
Figure 4. 7: Schematic and result of T7 Endonuclease I assay to verify CRISPR *IFITM1* KO U2-OS cell lines. 33
Figure 4. 8: *IFITM1* KO and OE modulate the rhythmicity of U2-OS *Bmal1-dluc* cell lines. 34
Figure 4. 9: Bi-FC (Bimolecular Fluorescent Complementation) assay shows IFITM1 interacts with CRY1 in the nucleus but not CRY2 35

Figure 4. 10: The subcellular fractionation shows IFITM1 is found in the nuclear field to a large extent..... 37
Figure 4. 11: CRY1 is more stable when IFITM1 is overexpressed in the *IFITM1* OE and WT U2-OS *Bmal1*:d*luc*.. 38
Figure 4. 12: The mRNA expressions of core clock genes are modulated when IFITM1 is overexpressed or knockout. 40
Figure 4. 13: Poly(I: C) induces the expression of IFITM1 significantly in *U2OS Bmal1-dluc.*. 42
Figure 4. 14: Circadian phenotype was altered because of immune response stimulated by Poly(I: C). 44
Figure 4. 15: The mRNA expressions of core clock genes are modulated when viral stress was mimicked via Poly(I: C) in *IFITM1* OE, KO, and WT U2-OS *Bmal1-dluc* cell lines. 45
Figure 5. 1: Schematic representation of IFITM1 and CRY1 communication under pathogenic stress..... 50
Figure A. 1: Subcellular localization of IFITM and CRY in HEK 293 cell lines.....65
Figure A. 2: IFITM1 physically interacts with CRY1 but not CRY2 by co-Immunoprecipitation in IFITM1 OE and KO U2-OS Bmal1-dluc cell lines.....66
Figure C. 1: 1 kb and 100 bp DNA Ladder for agarose gel electrophoresis.....69
Figure C. 2: Protein ladder for SDS-PAGE and Western Blotting.....69
Figure D. 1: Some plasmid constructs in the project.....70

ABBREVIATIONS

AMPK	AMP-Activated Protein Kinase
ARNTL-1	Aryl hydrocarbon receptor nuclear translocator-like protein 1
bHLH	Basic Helix-Loop-Helix
BiFC	Bi-molecular Fluorescence Complementation
BMAL1	Brain-Muscle-Arnt-like protein 1
Bmal1-dluc	Luciferase expression under *Bmal1* promotor
CCGs	Clock Controlled Genese
CHX	Cycloheximide
CK1δ	Casein kinase 1 delta
CK1ε	Casein kinase 1 epsilon
CKIε	Casein Kinase 1ε
CLOCK	Circadian Locomotor Output Cycles Kaput
Co-IP	Co-Immunoprecipitation
CRY1/2	Cryptochrome1/2
CT	Circadian Time
DBP	D-Box Binding Protein
DMEM	Dulbecco's Modified Eagle Medium
DNA	Deoxyribonucleic acid
ECL	Enhanced Chemiluminescence
FBS	Fetal Bovine Serum
FBXL3/21	F-Box and leucine-rich repeat protein 3/21
HAT	Histone Acetyltransferase
HEK 293T	Human Embryonic Kidney Cells
HPA	Hypothalamic–pituitary–adrenal axis
HRP	Horseradish peroxidase
IFITM1	Interferon Induced Transmembrane Protein 1
IFITM3	Interferon Induced Transmembrane Protein 3
ipRGC	Intrinsically Photoreceptive Retinal Ganglion Cell
KO	Knock-out
LB	Luria Bertani
LUC	Luciferase

NFIL3	Nuclear Factor Interleukin 3
NPAS2	Neuronal PAS domain protein 2
OE	Overexpress
PAS	Per-Arnt-Single-minded
PBS	Phosphate Buffered Saline
PCR	Polymerase Chain Reaction
PER	Period
PHR	Photolyase Homology Region
PMSF	Phenylmethanesulfonylfluoride
REM	Rapid Eye Movement
REV-ERB	Nuclear Receptor Subfamily 1, Group 1
RNA	Ribonucleic acid
ROR	RAR-related orphan receptor
RORE	Receptor-related orphan receptor response elements
SCF	SKP1-CUL1-F-box
SCN	Suprachiasmatic Nucleus
SDS	Sodium Dodecyl Sulphate
SDS-PAGE	Sodium Dodecyl Sulphate Polyacrylamide Gel Electrophoresis
TBS	Tris Buffered Saline
TNFα	Tumour Necrosis Factor A
TTFL	Transcription Translational Feedback Loop
U2OS	Human osteosarcoma cells
WT	Wild type
ZT	Zeitgeber Time

CHAPTER 1:
INTRODUCTION

The circadian clock regulates lots of behavioral and physiological processes such as alertness, memory, blood pressure, psychological state, and immune responses (Eckel-Mahan & Storm, 2009; Franken & Dijk, 2009; Kyriacou & Hastings, 2010; Wirz-Justice, 2006). Associations between clock proteins and immunity occur in a reciprocal manner. Any disturbance of circadian components causes severe diseases and pathologies in the immune system (Hergenhan et al., 2020). Immune diseases, in turn, can alter locomotor activity, decreases behavioral oscillations, and modulates the expression of molecular clock genes (Cavadini et al., 2007).

At the molecular level, the circadian clock consists of intertwined tripartite transcription translational feedback loop in mammalians. Brain and Muscle ARNT-Like-1 (BMAL1) and Circadian Locomotor Output Cycles Kaput (CLOCK), transcription factors regulating the positive arm, heterodimerized and bind to E-BOX elements (CACGTG) to initiate the transcription of clock-controlled genes, including negative regulatory elements *Period* (Per) and *Cryptochrome* (Cry). PER and CRY proteins translocate to the nucleus after binding with casein kinase Iε (CKI) ε to repress their own and BMAL1:CLOCK driven transcription (Kavakli, Ozturk, et al., 2022). The degradation of CRY and PER proteins renew the BMAL1:CLOCK-driven transcription by diminishing the repression effect of CRY: PER heterodimer.

Recent *in vivo, in vitro, and in silico* studies demonstrate that there is an obvious communication between clock modulating factors and additional clock components (Anafi et al., 2014; Cal-Kayitmazbatir et al., 2021; Robles et al., 2010). Clock proteins as transcription factors can regulate gene transcription and also play role in recruiting enzymes to the promoter of immune-associated genes (Hergenhan et al., 2020). Additionally, circadian clock components also physically interact with inflammatory molecules to regulate immune elements in a circadian-dependent manner (Scheiermann et al., 2013).

IFITM1 (Interferon-Induced Transmembrane Protein 1) is a member of the interferon-induced transmembrane protein family (Narayana et al., 2015). IFITM1, induced by type I and II interferons, functions as a critical antiviral component in the

innate immune system by changing the structure and the fluidly of the cell membrane to suppress the entrance of several viruses such as influenza A virus (IAV), West Nile virus, dengue virus, SARS coronavirus, filoviruses, VSV, and HCV among others (Brass et al., 2009; Narayana et al., 2015; Sun et al., 2020). The absence of endogenous IFITM1 enhances the sensitivity to a range of viral infections (Shi et al., 2021; Yanez et al., 2020).

Here, we have identified Interferon-Induced Transmembrane Protein 1 (IFITM1) as a novel circadian clock component that stabilizes CRY1 by interacting specifically through the C-terminal intrinsically disordered domain of CRY1, but not CRY2, in the nucleus. Hence, it modulates BMAL1:CLOCK-driven transcription of core clock genes. Knockout of *IFITM1* by CRISPR in U2OS *Bmal1-dluc* cell lines resulted in a lengthened period and dampening of the amplitude. To evaluate the communication between IFITM1 and circadian clock genes under viral attack at the physiological level, Poly(I: C), a synthetic double-strand RNA analog mimicking pathogenic stress in the cell, was treated into *IFITM1* KO, OE, and WT *U2OS Bmal1-dluc*. Alterations in both circadian rhythmicity and the mRNA level of some clock genes were observed. With this study, we suggest a new role for IFITM1, which is antiviral cell-intrinsic restriction factors, as a clock candidate gene.

Chapter 2 introduces the literature about the history and features of the biological clock, the molecular architecture of the circadian clock, and the relationship between the immune system and the circadian rhythm.

Chapter 3 of the thesis explains the materials and methods applied in this work.

In chapter 4, we give a detailed explanation of all results obtained throughout this work which prompted us to conclude that IFITM1-CRY1 interaction stabilizes CRY1, but not CRY2, by interacting C terminal of CRY1 in the nucleus, hence modulating the expression of core clock genes and circadian rhythmicity under the pathogenic stress.

Chapter 5 provides a discussion about all results obtained throughout the study and points out future directions to further understand the role of IFITM1 in the circadian clock.

CHAPTER 2:
LITERATURE REVIEW

2.1 The Family of Biological Rhythms

As a result of the fact that the Earth rotates on its axis about every 24 hours, organisms in the world encounter fluctuations of several cues such as light, temperature, and humidity (Dunlap et al., 2004). A wide variety of species, from cyanobacteria to mammalians, evolved endogenous biological cycles, which enable them to anticipate the cyclic alterations of light, food availability, and the risk of predators. (Yi et al., 2022). These biological rhythms can be classified into three categories based on periodicity: ultradian, infradian, and circadian rhythms **(Figure 2. 1)**. Ultradian rhythms involve biological events taking less than 24 hours (Lamont & Amir, 2017). The events such as cell division, metabolic cycling, and human sleep cycles (REM and non-REM) are the scope of ultradian rhythms that repeatedly exhibit a period of seconds, minutes, or hours each day (Lloyd & Murray, 2005; Moszczynski & Murray, 2012). Infradian rhythms describe events that oscillate for a more extended period than 24 hours, lengthening from days to weeks, months, and years (Lamont & Amir, 2017). These biological processes can be exemplified as the human menstrual cycle and hibernation. Lastly, circadian rhythms regulate physiological processes in mammalian organisms like the sleep-wake cycle, heart rate, blood pressure, feeding, brain activity, and photosynthesis, having a period of 24 hours approximately (Gachon et al., 2004). Disruption of this circadian cycle established by the biological clock regulating a range of physiological events can lead to issues in the health of the organisms (Vitaterna et al., 2001).

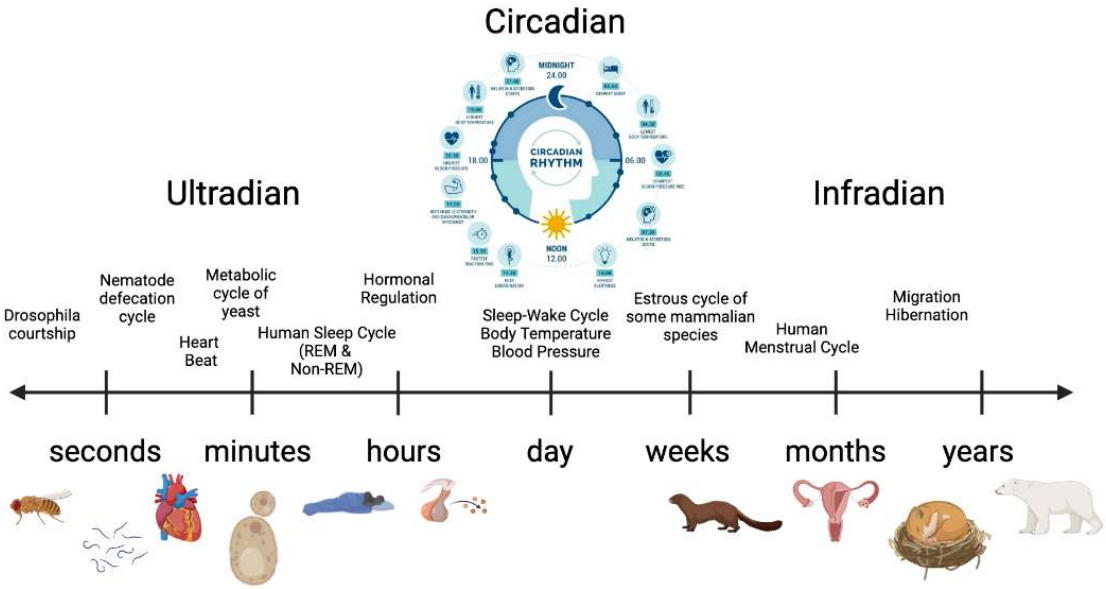

Figure 2. 1: Schematic representation of biological rhythms. Ultradian, circadian, and infradian rhythms with some biological examples are demonstrated. The figure is adapted from (Lamont & Amir, 2017). The figure was illustrated via BioRender.

Circadian rhythm can be unified by several distinct characteristic properties in different organisms at a functional level. First, a typical feature of circadian rhythm is to exist self-sustained nature, approximately 24 hours, which means the persistence of circadian rhythm devoid of the dark-light cycle or other exogenous time signals, with a period of 24 hours (Merrow et al., 2005). The period of circadian rhythm under constant conditions is defined as a free-running period. In addition, these free-running periods can range from 23 to 25 hours in different organisms (Wever, 1986). This phenomenon indicates the presence of an endogenous time-keeping mechanism or biological clock (Vitaterna et al., 2001). Secondly, another feature of circadian rhythms is exhibiting compensation corresponding with environmental changes, which can play roles as *zeitgebers* (Kuhlman et al., 2018). Clock function is regulated by a sum of biochemical reactions. However, it oscillates with the same period over a wide range of physiological temperatures, which is defined as temperature compensation, despite the synchronization of the circadian clock by temperature cycling within 24 hours period (Brown et al., 2002). Lastly, the rhythm can be entrained by several external cues like light, feeding, emotional changes, social communications, and temperature (Asher et al., 2010; Damiola et al., 2000; Mohawk et al., 2012). The extrinsic factors applied to entrain a rhythm are called *Zeitgeber* (in German means time-giver) (Merrow et al., 2005; Pittendrigh, 1960).

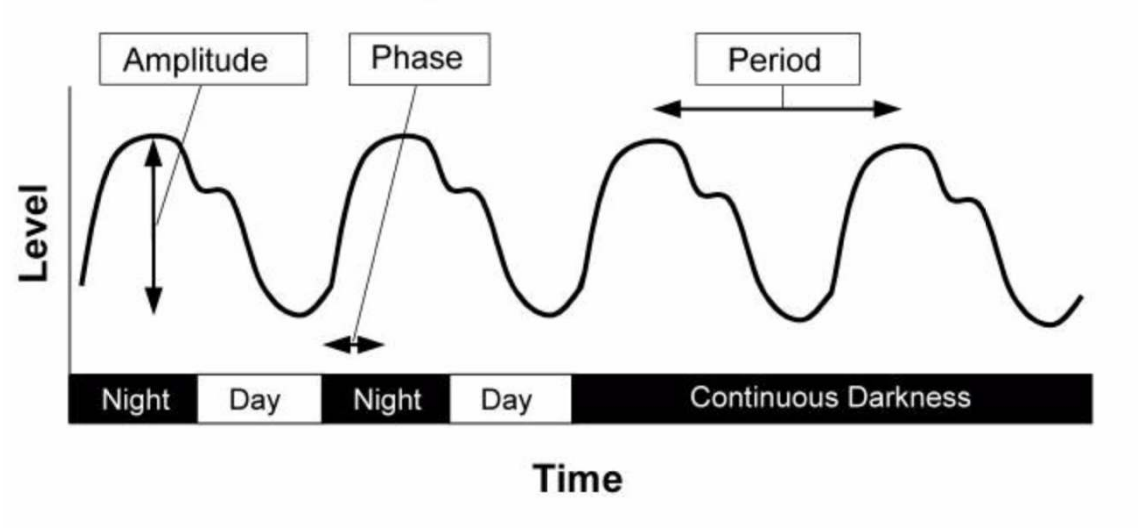

Figure 2. 2: Schematic representation of parameters defining continuous periodic oscillation. The period, amplitude, and phase were depicted under a light-dark cycle and free-running (under continuous darkness)**.** The figure is adapted from (Vitaterna et al., 2001)**.**

Alterations in circadian rhythm can be demonstrated based on some parameters defining the features of continuous periodic oscillation, such as amplitude, period, and phase **(Figure 2. 2)**. All wave and rhythmic events are described by these parameters, which facilitate evaluating the differences between organisms and conditions (Vitaterna et al., 2001). *Amplitude* is defined as the distance between peak (highest) and trough (lowest) values. The amplitude can be altered corresponding with aging, different conditions, and immune changes. The time length between two peaks is called the *period*, while the *phase* is the timing difference between the reference point in the oscillation and the fixed events (Reppert & Weaver, 2002). Stimulus-induced shifts in the phase can be calculated and visualized by Phase Response Curve (PRC).

2.2 Historical Background of Circadian Clock

In circadian biology, the first known experiment goes back to the observation of Jean-Jacques d'Ortous de Mairan, an astronomer, on the daily leaf movement of heliotrope plants (*Mimosa pudica*) in1729 (de Mairan, 1729). He provided evidence for the presence of circadian rhythm by observing that the leaves of the plant opened in the daytime while closed at night in constant darkness (Fuhr et al., 2015). He proposed this phenomenon as the existence of an endogenous mechanism generating time, corresponding with geophysical timing. Later, Augustin Pyramus de Candolle, a Swiss scientist, supported Jacques d'Ortous de Mairan's findings by demonstrating that a period of leaf movement

was approximately 22-23 hours under constant light, which indicates an endogenous rhythm (Bünning, 1960). He claimed that this shortened period (less than 24 hours) is a result not only controlled by environmental cues but also by an endogenous clock.

After two centuries of this observation, the genetic basis of circadian rhythm was shown based on Erwin Bünning's bean experiment (Kuhlman et al., 2018). He noticed that the period length of offspring varies within the range of the period lengths of their ancestors (McClung, 2006). Later, Franz Halberg used the term "circadian" (*circa* and *dies* "about a day") first time to define the observed rhythm in 1959. With circadian researchers from different disciplines, such as experimental, mathematical, and computational, come together, the foundations of circadian biology research were laid to pave the way for chronobiology (Aschoff, 1960; Fuhr et al., 2015).

After these preliminary studies, the strong basis of modern chronobiology originated from keen observations of the co-founders and pioneers of the field: Jürgen Aschoff and Colin Pittendrigh. Colin Pittendrigh described the features of the circadian clock in fruit flies (*Drosophila pseudoobscura*) by explaining how circadian rhythm was synchronized by the light-dark cycle. He suggested the necessity of time-keeping mechanisms that are insensitive to fluctuations in temperature (Pittendrigh, 1954). Jürgen Aschoff focused on the entrainability of the circadian rhythm (Daan, 2000). Also, he showed endogenous rhythm in humans by monitoring different biological events such as the sleep-wake cycle, body temperature, and urinary excretion (Aschoff, 1965).

Until 1971, the underlying molecular mechanism of circadian rhythm was an unidentified challenge. In 1971, Ronald J. Konopka and Seymour Benzer defined the first core clock gene "*Period*" in *Drosophila melanogaster* by analyzing pupal eclosion and locomotor activity of mutagenized flies (Konopka & Benzer, 1971). By the 1990s, an essential milestone for chronobiology was reached by identifying the suprachiasmatic nucleus SCN as the central circadian pacemaker in mammals (Ralph et al., 1990). In 1994 Joseph S. Takahashi discovered the *Circadian Locomotor Output Cycles Kaput* (*Clock*) gene by screening mutant mice exhibiting period-lengthening mutation (Siepka et al., 2007). Brain and Muscle Arntl-like-1 protein (BMAL1) was discovered by John B. Hogenesch in 1997 (McIntosh et al., 2010). Later, Cryptochromes (CRYs) were identified as circadian clock regulators (Horst et al., 1999; Vitaterna et al., 1999).

2.3 Master and Peripheral Circadian Clock in Mammalian Organisms

In mammals, the circadian clock is composed of two interrelated oscillators and feedback loops; and is divided into two units as the central (master) clock located in the suprachiasmatic nucleus (SCN) of the hypothalamus and the peripheral clock residing in a range of tissues in the body **(Figure 2. 3)** (Mohawk et al., 2012; Richards & Gumz, 2012). SCN works on synchronizing and conducting the proper functioning of the peripheral clocks by transmitting neural and humoral messages (Kavakli & Sancar, 2002; Reppert & Weaver, 2002).

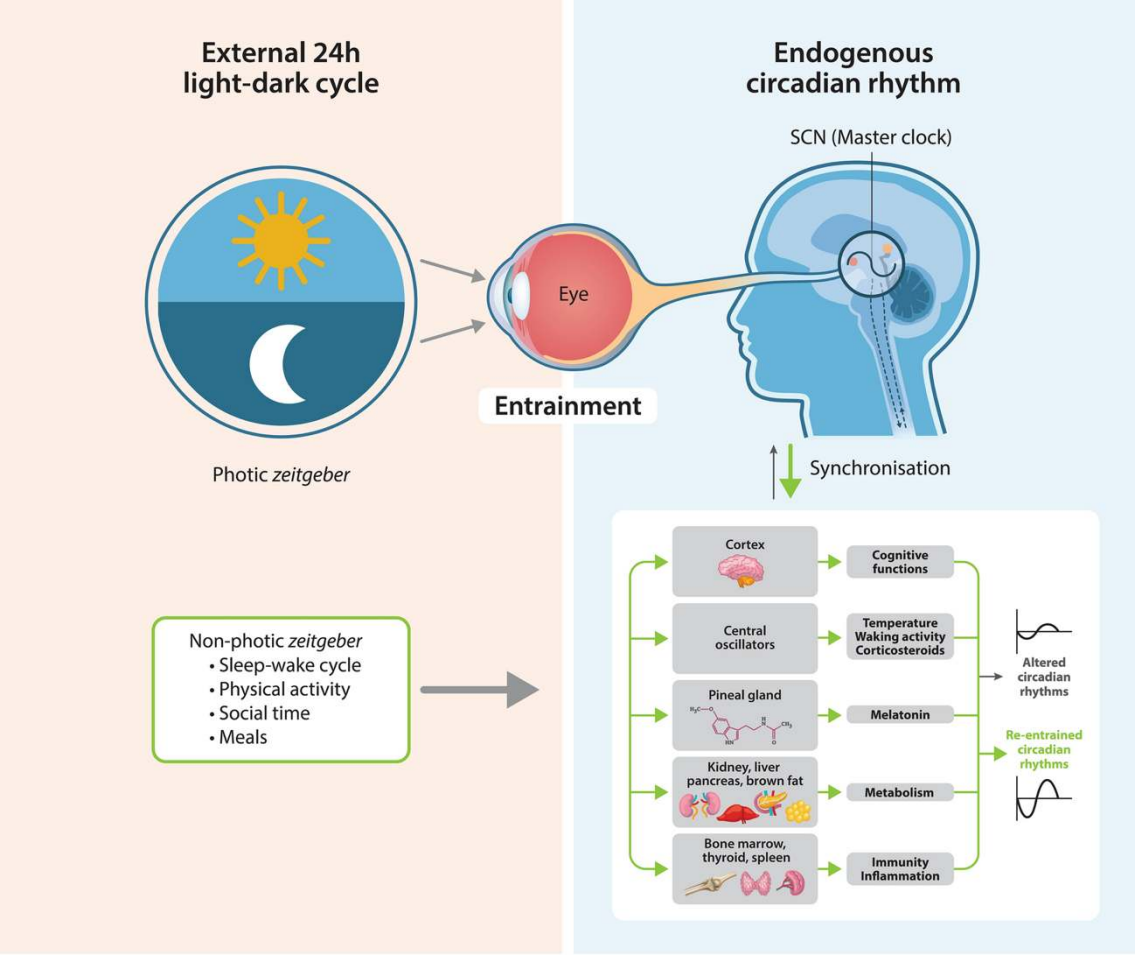

Figure 2. 3: Schematic representation of internal circadian clock synchronized by peripheral and master clock and entrainment. Photic input is transmitted through the suprachiasmatic nucleus (SCN), while other non-photic cues exhibit rhythmic alterations. Therefore, the SCN and peripheral clocks within 24 hours can be entrained. The figure is retrieved from (Janse van Rensburg et al., 2021). Permission is attached in the appendix.

SCN, as a central pacemaker, consists of about 20.000 neurons (Herzog et al., 2017; Van Gelder, 2003). Each of the neurons is considered to have cell-autonomous circadian

periods ranging from 22 hours to 20 hours, which make phase lability and phase plasticity possible. (Ko et al., 2010; Liu et al., 1997; Mohawk et al., 2012; Welsh et al., 1995). Light input, which is an important *Zeitgeber*, is received through the eye to intrinsically photosensitive retinal ganglion cells (ipRGCs), where photo-pigment melanopsin is found, to transmit photic input to the SCN (Kofuji et al., 2016).

Alongside a central pacemaker, SCN, in the hypothalamus, all tissues have their own rhythmic and insistent gene expression pattern, which are defined as the peripheral clocks. The master clock orchestrates and facilitates maintaining the coherence of the peripheral clock through several factors such as physical activity, resting, feeding, socialization, neural and humoral signals, alterations in the body temperature, and the cycle of hormones and metabolites (Cuninkova & Brown, 2008; Damiola et al., 2000; Gamble et al., 2014; Schwartz & Zeltser, 2013). Although molecular clock mechanisms work in the same manner in different tissues, the proper functioning of the peripheral clock is vital to regulating the expression of specific genes and physiological events (Yamazaki et al., 2000; Yoo et al., 2004).

2.4 The Molecular Architecture of Circadian Rhythm

The circadian clock consists of both master and many peripheral clocks in mammalians. Master clock is found in the suprachiasmatic nucleus (SCN), while peripheral clocks are found within cells except for SCN. Both master and peripheral clocks have the same molecular architecture, although SCN can send signals and synchronize peripheral clocks (Mohawk et al., 2012). At the molecular level, the circadian clock consists of three interlocking transcription-translation (TTFL) feedback loops **(Figure 2. 4)** (Dunlap et al., 2004). The main loop is driven by activators BMAL1 and CLOCK (and its paralogue NPAS2), forming heterodimer in the daytime through bHLH-PAS (Period-Arnt-Single) to regulate the transcription of repressors, PER1-3 and CRY1-2, by binding E-box elements in the afternoon (Hogenesch et al., 1997; Kume et al., 1999). In the late afternoon or evening, PER and CRY proteins are accumulated in the cytoplasm. Later, heterodimerized PER and CRY proteins bind with the serine/threonine kinase casein kinase 1δ (CK1δ) and CK1ε to translocate into the nucleus at night (Takahashi, 2017; Vielhaber et al., 2001). Then this complex bind to BMAL1:CLOCK heterodimer to inhibit their own transcription. In the second loop, nuclear receptors RAR- related orphan receptor (ROR) and REV-ERB (also known as NR1D1 and NR1D2) bind to

receptor-related orphan receptor response elements (ROREs) in the promoter of *Bmal1*. The expression of BMAL1 is activated by RORs while repressed by REV-ERBs. The third loop involves the transcriptional activator albumin D-box binding protein (DBP) is controlled through its E-box and the nuclear factor interleukin 3 (NFIL3), repressing the expression of DBP regulated via a RORE (Preitner et al., 2002). Then, these two circadian components synergistically regulate the expression of D-box-controlled genes like Per.

Besides these interlocked TTFL mechanisms, the precision of the molecular clock is controlled also by different post-translational modifications like phosphorylation regulated by kinases (e.g., the casein kinases (CKIα, CK1δ, and CKIε), phosphatases (PP1 and PP5) (Hirano et al., 2016). The stability and turnover via proper degradation of repressor elements CRY and PER proteins are essential to maintain robust rhythmicity in mammalians (Busino et al., 2007; Nangle et al., 2014). They are regulated by several degradation pathways. For CRY proteins, it is controlled by two paralogues of FBXL3 and FBXL21. FBXL3 is an F-box-type ubiquitin ligase subunit. It recognizes CRY at the flavin adenine dinucleotide (FAD) binding pocket to advocate proteasomal degradation of CRY. On the other hand, FBXL21 functions as an antagonist of FBXL3 by binding with CRY, thereby protecting it from FBXL3-based ubiquitination (Yoo et al., 2013). Despite the fact that SCF^{FBXL21} exhibit less activity than SCF^{FBXL3} in ubiquitination of CRY, FBXL21 binds more strongly than FBXL3 with CRY so that it can protect CRY against degradation based SCF^{FBXL3} (Hirano et al., 2013). In addition, while FBXL3 functions as the primary E3 ligase for CRY in the nucleus, FBXL21 works in the cytoplasm (Hirano et al., 2013; Yoo et al., 2013). The stability and turnover of PER proteins are regulated by CK1δ and CK1ε and phosphotase1 and 5 (Takahashi, 2017). While kinases (CKIα, CKIδ, and CKIε) determine the degradation or translocation into nucleus rates for PER: CRY heterodimer, phosphatases work in an opposite manner.

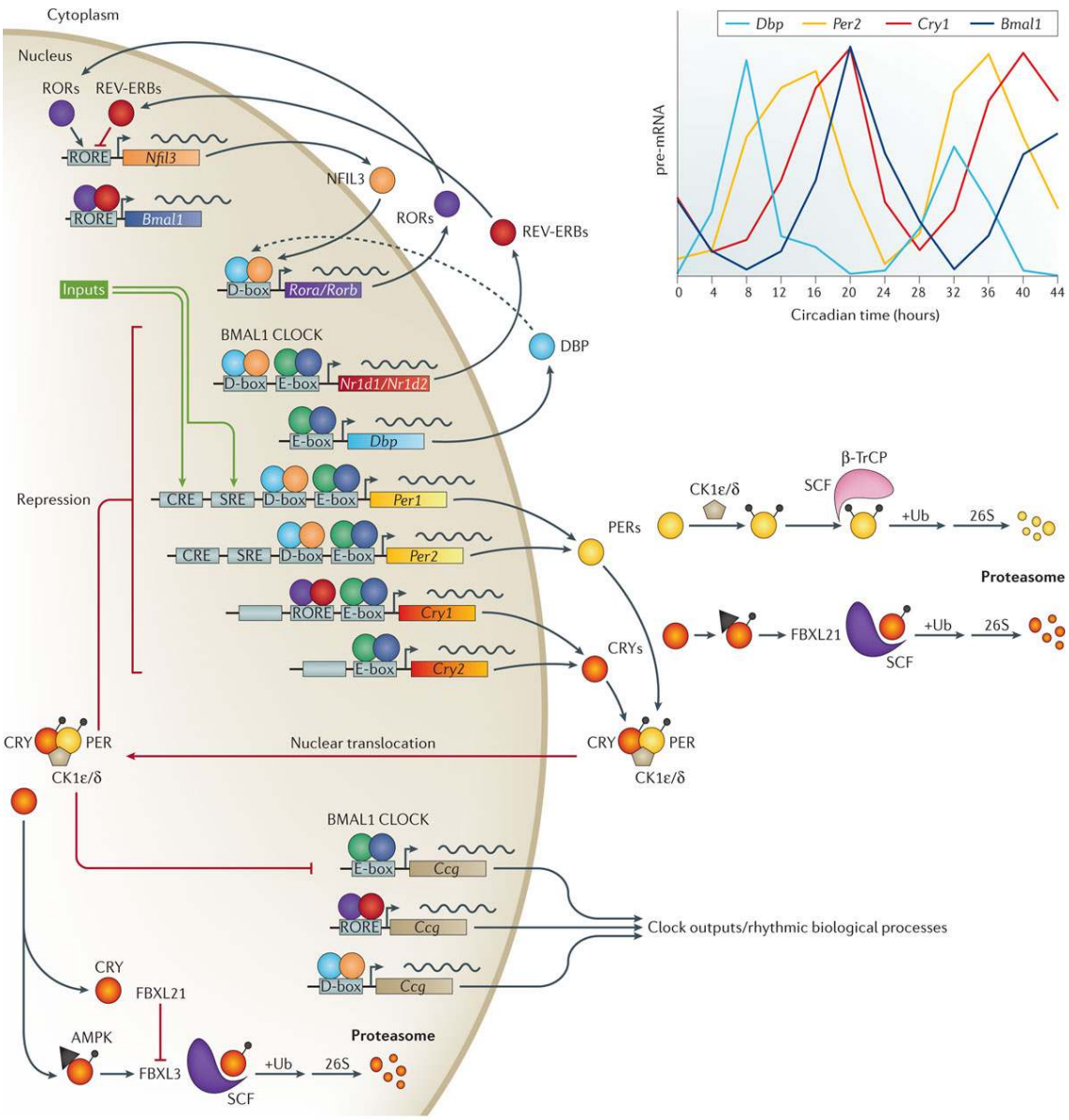

Figure 2. 4: Representation of molecular mechanism of circadian rhythm controlled by interlocked transcriptions and translation feedback loops. The figure is retrieved from (Takahashi, 2017). Permission is attached in the appendix.

2.5 The Significance of Circadian Rhythm in Human Physiology and Health

The circadian clock evolved to facilitate humans to fit into environmental alterations and integrate these cues with internal physiologies. When the importance of the circadian clock to regulate phycological events is considered, the proper functioning of the circadian clock is essential to health and well-being. Circadian disruption is directly associated with sleep issues and made susceptible to psychiatric disorders, cognitive dysfunction, cancer, metabolic syndromes, aging, diabetes, obesity, and inevitably immune system (Evans & Davidson, 2013; Gauger & Sancar, 2005).

Sleep behavior is directly related to circadian mechanisms because based on the melatonin secretion at night, it is regulated. A familial advanced sleep disorder (FASPD) is a result of mutation of the core clock gene, *PER2,* which alters the sleep cycle (Toh et al., 2001).

The intact circadian clock in the immune cells exhibits an immunoprotective role, thereby a healthy state provided in the organisms (Nguyen et al., 2013). Therefore, any genetic disruption in the clock control genes can prevent the proper functioning of the immune system factors and generate immune responses by organisms (Druzd et al., 2017; Fortier et al., 2011; Nobis et al., 2019)

2.6 The Communication between Circadian Rhythm and Immune System

The immune system is controlled by circadian clock mechanisms via neural and humoral signals transmitted from SCN (Curtis et al., 2014). Core clock proteins work as transcription factors to regulate the gene of the immune system and interaction partners of several inflammatory molecules, while immune response elements affect circadian clock functioning. The inflammatory NFκB pathway is a prominent instance showing the link between the immune system and circadian rhythm (Hergenhan et al., 2020). Therefore, there is a reciprocal control between circadian clock components and immune factors.

BMAL1 is the central mediator between circadian rhythm and the immune system. It plays an anti-inflammatory role, heterodimerizes with CLOCK, and binds to E-box to repress the expression of several chemotactic cytokines such as CCL2 and CCL8 (Nguyen et al., 2013). Moreover, BMAL1, in response to pathogenic stress, plays a crucial role in host immune defense. BMAL1 binds to the promoter of a pattern recognition receptor for intracellular pathogen-associated molecular pattern, toll-like receptor 9 (TLR9), to upregulate its transcription (Silver et al., 2012). In addition to the BMAL1-driven transcription regulation on immune system elements, BMAL1 can affect the immune system on a molecular level by interacting directly with a subunit of the proinflammatory transcription factor NFκB (Bellet et al., 2012).

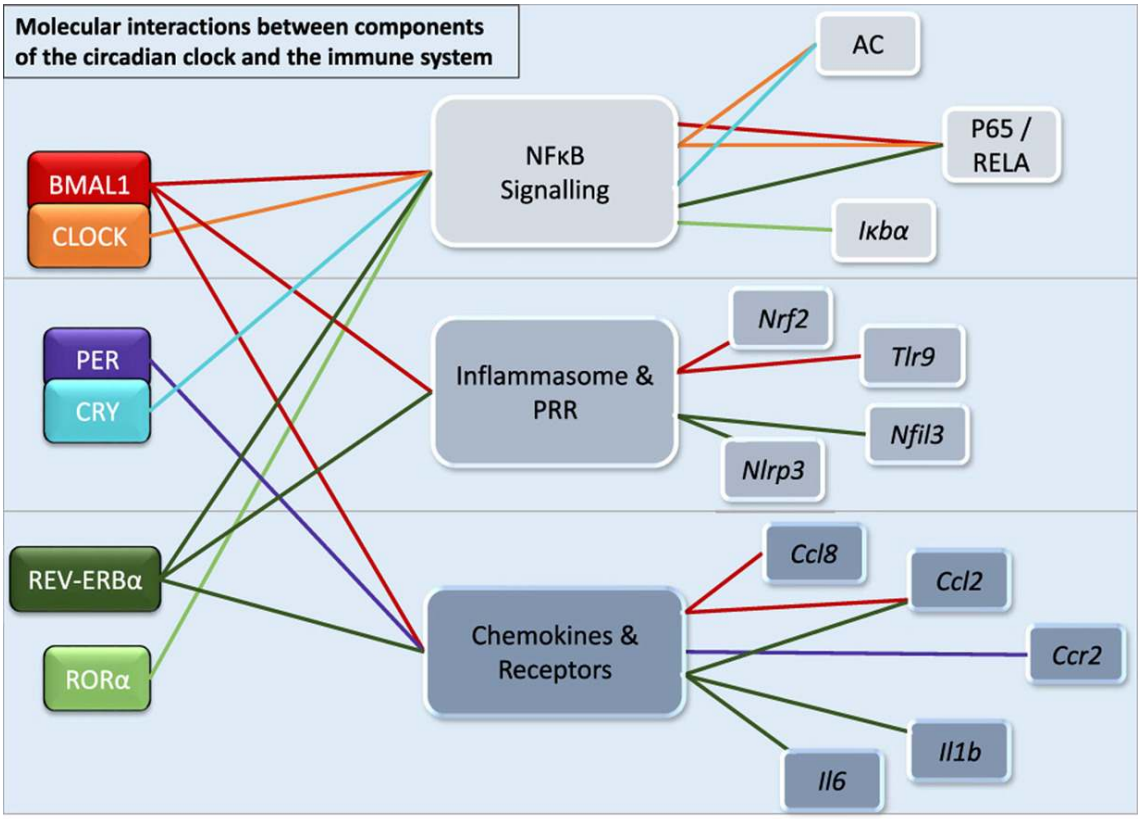

Figure 2. 5: Schematic representation of molecular associations between circadian clock components and immune system elements. Core clock components directly regulate the cytokines, chemokines, and immune regulatory proteins taking the role in NF-κB signaling, inflammasome, pattern recognition receptors, and chemokines. The figure is retrieved from (Hergenhan et al., 2020) with permission.

The proper functioning of CLOCK is critical to the regulation of period and locomotor activity in a range of organisms (Vitaterna et al., 1994). In addition to its regulatory function in molecular clock mechanisms, CLOCK enhances the activity of the immune system by complexation with NFκB subunit p65 (Spengler et al., 2012). These findings showed that CLOCK has a proinflammatory role as a mediator by interacting with the components of the NFκB pathway in addition to its transactivation function with BMAL1 (Hergenhan et al., 2020)

Although the role of PER proteins in the immune system regulation is complicated, PER1 takes a role in anti-inflammatory regulation, whereas PER2 is claimed to work as a positive regulatory factor for proinflammatory cytokines. For instance, the regulation of the inflammatory chemokine receptor CCR2 expression is regulated by PER1 (Wang et al., 2016). In addition to that, PER2 can form a complex with nuclear receptors while both PER1 and PER2 interact with GRα (glucocorticoid-receptor alpha), which affects

the response against inflammation, apoptosis, growth, and development in organisms (Schmutz et al., 2010). Similar to PER, CRYs play an anti-inflammatory role in the control of the intensity of immune response generated by organisms by downregulating the level of inflammatory cytokines.

REV-ERB and ROR exhibit anti-inflammatory effects. REV-ERBα drives the differentiation of the Th17 immune factor by binding to a consensus sequence of *Nfil3* to inhibit its transcription (Yu et al., 2013). Also, deficiency of REV-ERBα, triggers the higher expression of *Nfil3;* on the other hand, RORγ induces T cells to produce and leads the development of Th17 cells (Yu et al., 2013).

2.7 Interferon Inducible Transmembrane (IFITM) Protein Family

Interferon inducible transmembrane (IFITM) proteins are a family of small membrane proteins found in the plasm and endolysosomal membranes, which take a role in cellular resistance to many viruses by preventing the membrane fusion between the host cellular membrane and the outer envelope of viruses. (Yanez et al., 2020; Zhao et al., 2018). IFITM protein family was discovered for the first time as interferon-induced genes in neuroblastoma cells, together with promoter regions of the genes containing interferon-stimulated response elements, make them susceptible to type I and type II interferons (Bzhalava et al., 2012; Friedman et al., 1984). Five *IFITM* genes (*IFITM1, IFITM2, IFITM3, IFITM5, IFITM10*) located on chromosome 11 were identified in humans, while seven *Ifitm* was discovered in mice; six of them (*Ifitm1, Ifitm2, Ifitm3, Ifitm5, Ifitm6, Ifitm10*) are located on chromosome 7, and *Ifitm7* on chromosome 16 (Liao et al., 2019).

IFITM proteins consist of two transmembrane or intramembrane domains extending along the membrane layers (Weston et al., 2014). While the loops found in two transmembrane domains are highly conserved and always found in the intracellular, the N- and C- terminal domains of the proteins can be located in both intracellular and extracellular regions of the cells (Yanez et al., 2020). Although the exact topologies of the IFITM protein family are not elucidated yet thoroughly, suggested that their topologies can be varies based on their function in the cell.

Different roles for members of the IFITM protein family were suggested, such as specification process of germ cells, osteoblast functioning, cell cycle regulation, cancer metabolism, and immune function by demonstrating resistance and restriction to many viruses (Bedford et al., 2019; Yanez et al., 2020). Different IFITM proteins can demonstrate specificity and function against different types of viruses. Although the viral restriction mechanisms of IFITM proteins are not clear, there are various explanations for inhibiting viral entrance, repressing the synthesis of viral proteins, or viral replication.

2.8 Significance of Novel Clock Component Discovery Research

. Especially over 20 years, biochemical, genetic, and computational tools were applied to improve our understanding of molecular clock mechanisms and discover unknown parts of this network by identifying new clock components (Anafi et al., 2014; Cal-Kayitmazbatir et al., 2021; Robles et al., 2010). Most core clock components like *Per* and *Cry* were discovered based on random mutagenesis, one of the forward genetic applications. To gain insight into the molecular clock mechanism of the negative transcription-translation feedback loop, protein complexes interacting with BMAL1 were investigated, whereby RACK1 has been identified as an integral component of the circadian clock in mammalians (Robles et al., 2010). Moreover, potential circadian clock components and modifiers were screened previously by our group and collaborators. In 2014, they aimed to identify new clock components based on the "machine learning" approach to understand molecular clock physiology further. This study targeted genes exhibiting clock-like characteristics such as circadian manner oscillation, expression in different tissues ubiquitously, interaction with other core clock genes, conservation and homology across species, and alterations in circadian rhythmicity derived from manipulations in the gene. Based on this work, they suggested CHRONO (Gm129) as one candidate, which interferes with the function of BMAL1 to recruit CBP (Anafi et al., 2014). Seven years later, one of the other candidates identified in this study, CBS, was characterized as a clock component by enhancing CRY1-mediated repression of the CLOCK: BMAL1 and shortening the circadian period (Cal-Kayitmazbatir et al., 2021)

CHAPTER 3:
MATERIALS AND METHODS

3.1 Plasmid Constructs and Molecular Cloning

Annealed oligo Cloning, PCR Based Cloning, and Cloning by restriction digest techniques were used to generate target constructs. To prevent degradation and increase efficiency, the pJET vector was used as a subcloning vector to clone the genes of interest. Generated constructs were represented. (**Table 4. 1**, **Appendix Table B. 1**)

3.1.1 Annealed Oligo Cloning

Designed sgRNA primers (via GPP sgRNA Designer developed by Broad Institute) to knock out hIFITM1 and hIFITM3 genes were phosphorylated and annealed via T4 PNK enzyme (Thermo) as arranging the thermocycler for the following parameters **(Table 3. 1).**

Table 3. 1: Phosphorylation and Annealing Incubation Times for T4 PNK

Temperature	Incubation Time
37	30 minutes
95	5 minutes then ramp down to 25 at the decreasing 5 in each minute

After diluting obtained oligos at 1:200 with sterile water, it was ligated to Esp3I restricted lentiCRISPR v2-Hygro vector using T4 ligase and transformed into chemically competent bacteria strain NEBst.

3.1.2 PCR Based Cloning

Target coding sequences were cloned into the pJET-v2 vector. To amplify target regions, plasmids containing coding regions or cDNAs from HEK293-T, U2-OS, or

NIH3T3 were used as PCR templates. Q5 High Fidelity DNA Polymerase was used according to the manufacturer's instructions by applying the following Touch-down PCR conditions to amplify the region.

3.1.3 Cloning by Restriction Digest

Both donor plasmids containing the gene of interest and recipient plasmids were restricted with compatible Thermo Scientific Fast Digest Type II Restriction Enzymes to target specific restriction enzyme sites **(Table 4. 1, Appendix Table B. 1)**. To prevent back ligation in the recipient plasmids, phosphate groups in the 5' ends were cleaved via FastAP Thermosensitive Alkaline Phosphatase (1 U/µL) (Cat. No. EF0651) by incubating at 37°C for 1 hour. Restricted fragments were run in 0.8 % agarose gel and isolated to clean up with Macherey Nagel NucleoSpin Gel and PCR Clean-up Kit (Cat. No. MN740609) to the manufacturer's instructions. The isolated fragments were ligated via T4 DNA Ligase (5 U/µL) (Cat. No. EL0011) for 1 hour at room temperature. The ligation was set up without an insert to evaluate background colony formation as a negative control. The ligation products were transformed into chemically competent NEBst strains via Heat-Shock Transformation. The bacterial mix was spread onto LB Agar Plate containing specific antibiotics to the host's antibiotic resistance site.

3.2 Cell Lines and Regular Maintenance Procedure

HEK293 (Human embryonic kidney 293), HEK293-T (Human embryonic kidney 293), U2OS, and U2OS *Bmal1-dluc* cell lines were maintained to the supplier's recommendations in high glucose DMEM supplemented with 10% fetal bovine serum (FBS; Gibco, Cat. No. 11573397) and 100 µg/mL Penicillin and Streptomycin (P/S; Gibco, Cat. No. 15140122) by providing 37°C and 5% CO_2 through the incubator.

3.3 Generation of IFITM1 Overexpressed and CRISPR Knock-out Stable Cell Lines

3.3.1 Determination of Optimal Selection Antibiotic Concentration

U2-OS cells were harvested via trypsin, and a cell suspension was prepared by diluting cells in a 1:5 ratio with DMEM + 10% FBS media. 500 µL of prepared cell suspensions were transferred into a 24-well plate containing 500 µL of media and

antibiotic mix in several concentrations (Hygromycin B: 50 µg/mL to 1 mg/mL, G418: 50 µg/mL to 1 mg/mL) to select the appropriate dose. The cells were incubated at 37°C and 5% CO_2 through the incubator and monitored for 14 days, and the media containing antibiotics were replaced every three days. The viability of the cells was evaluated every two days. The lowest concentration of the antibiotic doses led to massive cell death in 3 days, and killing all the cells within two weeks was determined as the proper antibiotic dose for selection. The appropriate doses of U2-OS and U2-OS *Bmal1-dluc* were determined for Hygromycin B as 300 µg/mL and G418 as 0.8 mg/mL.

3.3.2 Lentivirus Production to Generate IFITM1 Overexpression and CRISPR Knock-out Stable Cell Lines

To get 70-80% confluency for transfection one day later, 2.5-3x10^6 HEK293-T cells were seeded into a 10 cm plate and incubated for about 24 hours at 37°C and 5% CO_2. Lentivirus plasmid mix was prepared and mixed via pipetting. After adding PEI, the transfection mix was incubated for 15-20 minutes at room temperature. 5 mL of 10 mL medium of HEK293-T cells were discarded. The transfection mix was added gently dropwise onto HEK293-T cells after mixing the mixture by pipetting. The cells were incubated overnight at 37°C and 5% CO_2. The next day, 3 mL fresh complete medium was added to the plate by paying attention to not disturbing the transfected cells. After 48 hours of transfection, the medium o cells were discarded, and 8 mL of fresh complete medium was added without disturbing cells. After 72 hours of transfection, an 8 mL medium containing lentiviral particles was harvested and collected in the 50 mL falcon to store at 4°C till the next collection. Again 8 mL of fresh complete medium was added to the cells. After 96 hours of transfection, the medium containing particles was harvested and added to the previously harvested medium. 16 mL of harvested medium was filtered through a 0.45 µm filter to get rid of any cell debris and aliquoted as 750 µL lentivirus particle in 1.5 mL microtubes to store at -80°C for long-term usage.

3.3.3 Establishment of Overexpressed Stable Cell Lines

1.8-2x10^5 U2-OS or U2-OS *Bmal1-dluc* cells were seeded into 6- a well plate. When the cells reached 70% confluency, frozen viral particles carrying IFITM1 or IFITM3 overexpression lentiviral constructs were thawed quickly. After the medium of the cells was discarded, lentiviral particles were introduced onto the cells by supplementing 1 µl

protamine sulfate (8 µg/µL) and 250 µl DMEM to each aliquot. The following day, the media involving viral particles was replaced with a 1.5 mL fresh complete medium for each well. After 48 hours of transduction, fresh complete media consisting of 1 mg/mL G418 were added to the cells to select overexpressed cells.

3.3.4 Establishment of CRISPR Knock-out Stable Cell Lines

To generate *KO* cell lines, the design of sgRNA constructs targeting *IFITM1* and *IFITM3* genes was performed using GPP sgRNA Designer (Broad Institute). Three potential sgRNA candidates that are close to the first AUG (Met) codon were chosen to knock out the target genes **(Table 3. 2)**. After phosphorylation and annealing of sgRNA oligo pairs as mentioned in *Section 3.3.1*, they were inserted into the pLentiCRISPRv2-Hygro vector. After generating the constructs with appropriate gRNAs followed by virus preparation, cell lines were transduced to generate stable cell lines.

Table 3. 2: Sequence of oligo pairs and name of constructs used for knocking out the target gene via CRISPR

Insert	Primer Names	Oligo Pairs	Recipient Plasmids
hIFITM1_GPP_g1	hIFITM1_GPP_g1_F	caccgTGATCACGGTGGACCTTGGA	lentiCRISPR v2 Hygro
	hIFITM1_GPP_g1_R	aaacTCCAAGGTCCACCGTGATCAc	
hIFITM1_GPP_g2	hIFITM1_GPP_g2_F	caaaGCACAAGGAGGAACATGAGG	lentiCRISPR v2 Hygro
	hIFITM1_GPP_g2_R	aaacCCTCATGTTCCTCCTTGTGC	
hIFITM1_GPP_g4	hIFITM1_GPP_g4_F	caccgACAGCACCAGTTCAAGAAGA	lentiCRISPR v2 Hygro
	hIFITM1_GPP_g4_R	aaacTCTTCTTGAACTGGTGCTGTc	
hIFITM3_GPP_g1	hIFITM3_GPP_g1_F	caccGATGCTCAAGGAGGAGCACG	lentiCRISPR v2 Hygro
	hIFITM3_GPP_g1_R	aaacCGTGCTCCTCCTTGAGCATC	
hIFITM3_GPP_g3	hIFITM3_GPP_g3_F	caccgATGTGGATCACGGTGGACGT	lentiCRISPR v2 Hygro
	hIFITM3_GPP_g3_R	aaacACGTCCACCGTGATCCACATc	
hIFITM3_GPP_g5	hIFITM3_GPP_g5_F	caccGGGGGCTGGCCACTGTTGAC	lentiCRISPR v2 Hygro
	hIFITM3_GPP_g5_R	aaacGTCAACAGTGGCCAGCCCCC	

Design of sgRNA regions for knockout of IFITM1 and IFITM3 genes was performed using GPP sgRNA Designer (https://portals.broadinstitute.org/gpp/public/analysis-tools/sgrna-design).

For transduction, 1.8-2x10^5 U2-OS or U2-OS *Bmal1-dluc* cells were seeded into 6-a well plate. When the cells reached 70% confluency, frozen viral particles carrying IFITM1 CRISPR-g1, IFITM1 CRISPR-g4, IFITM3 CRISPR-g1, IFITM3 CRISPR-g3, IFITM3 CRISPR-g5 CRISPR lentiviral constructs were thawed quickly. After the medium of the cells was discarded, lentiviral particles were introduced onto the cells by

supplementing 1 µl protamine sulfate (8 µg/µl) and 250 µl DMEM to each aliquot. The following day, the media involving viral particles was replaced with a 1.5 mL fresh complete medium for each well. After 48 hours of transduction, fresh complete media consisting of 300 ug/mL of Hygromycin were added to cells to select knocked-out cells. Selected cell populations were divided into two plates. One group was used to verify of efficiency of CRISPR, and the other group was separated for monoclonal selection.

3.3.5 Monoclonal Expansion via Limiting Dilution

To prevent selective pressure on heterogeneous populations of knock-out cells and extinguish the possibility of reduced transgene expression over time, monoclonal CRISPR knock-out cell lines were aimed to generate via limiting dilution. A conditional medium was obtained from the medium of 50-60% confluent U2-OS cell lines by filtering through 0.45 µm PES. Heterogenous CRISPR knock-out cell populations were trypsinized from a 10 cm plate. After the cell population was homogenized, 10 mL of new cell suspension at a 5 cells/mL concentration was made. Later, the mixture was seeded into a 96-well plate by transferring 100 µL of the 5 cells/mL solution into each well. The cells were let to incubate without disturb for 7-14 days. After 7 days, the plate was scanned to evaluate cell growth. Until observing colony patches deriving from a single cell, the plate was continued to monitor. When the cells were expanded, they were trypsinized to transfer into new larger dishes. After the monoclonal lines were expanded adequately, obtained cell lines were screened via western blotting and T7 endonuclease assay to evaluate the efficiency of CRISPR.

3.3.6 T7 Endonuclease Assay

To isolate genomic DNA from the cell pellet, harvested cells were resuspended in 100 µL Lysis Buffer (100 mM NaCl, 10 mM Tris-HCl pH 8.0, 25 mM EDTA pH 8.0, 0.5% SDS, 0.1 mg/mL Proteinase K) and incubated for 12-18 hours. After incubation, 100 µL Phenol: Chloroform: Isoamyl Alcohol 25:24:1, Saturated with 10mM Tris, pH 8.0, 1mM EDTA (Cat. No. P3803) was added and vortexed for 10 seconds. The mixture was centrifuged at 2000 g for 5 minutes in a microcentrifuge at room temperature. The upper aqueous phase containing DNA was transferred into a new tube. To precipitate DNA, 100 µL 7.5 M ammonium acetate and 200 µL 100% ethanol were added, and it was

centrifuged at 2000 g for 10 minutes at room temperature. Without disturbing the DNA pellet, the supernatant was discarded carefully, and the pellet was washed 3 times with 1 mL of 70% ethanol. The microcentrifuge tube was centrifuged at 1700 g for 5 minutes at room temperature to precipitate the DNA sample. The supernatant was removed, and the tube was left to air-dry for 30 minutes till the ethanol was completely removed. The DNA pellet was resuspended in TE buffer (10 mM Tris-HCl pH 8.0, 1 mM EDTA pH 8.0). Genome Targeting Efficiency using T7 Endonuclease I was determined manufacturer's instruction accordingly via New England BioLabs T7 Endonuclease I ((Cat. No. M0302S). The reaction products were visualized via running samples in 0.8% Agarose gel at 100V for 20 minutes.

3.4 Cell-Based Circadian Assay

U2-OS *Bmal1-dluc* cell line-derived stable cell lines, U2-OS IFITM1, and U2-OS IFITM1 KO was used to evaluate and monitor the effect of the IFITM1 gene on circadian rhythm by using U2-OS *Bmal1-dluc* as a control group. About $2x10^5$ cells were seeded into 35 mm culture dishes one day before introducing *Bmal1-dluc* lentiviruses via 3rd generation lentiviral system by supplementing protamine sulfate. The following day, the media containing virus was discarded, and a fresh medium was added to the cells. About 60 hours incubation after transduction in an incubator providing 37°C and 5% CO_2, the medium was changed with serum-free DMEM containing 0.1 μM dexamethasone at final (DXM; Sigma Aldrich, Cat. No. D4902) and let to incubation for 2 hours in the incubator to synchronize the cells. After that, the medium was discarded, and added Lumicycle medium containing Luciferin (Promega, Cat. No. 50227). Plates containing Lumicycle Medium were sealed with silicone grease to prevent evaporation and contamination and were replaced with LumiCycle 32 Luminometer (Actimetrics), located a 37°C incubators. The appliance was programmed to record bioluminescence via photomultiplier for 70 seconds every 10 minutes for 7 days.

3.5 Bimolecular Fluorescence Complementation Assay and Colocalization Analysis in Fluorescence Microscope

To understand the physical interaction between CRY1 and IFITM1, N-terminal and C-terminal halves of Venus fluorescence protein was fused with the genes of interest; CRY1 and IFITM1. In the case of the interaction of two proteins, two halves of Venus

protein will constitute a completed VENUS fluorescent protein which gives a signal under a fluorescent microscope (**Figure 4. 1**).

350.000 HEK293 cells were seeded on Poly-D-Lysine coated coverslip in 6-well dishes in high glucose DMEM supplemented with 10% fetal bovine serum and 100 µg/mL Penicillin and Streptomycin to have 70-80% confluency for transient transfection. After 24 hours, the cells were transiently transfected by using PEI. For PEI transfection, plasmids to the desired condition were prepared in Opti-MEM by adding 3 µL PEI for each 1 ug plasmid. Each Venus construct was transferred as 1 ug. After 20 minutes of incubation at room temperature, the transfection mixture was added dropwise by being careful about avoiding detaching from the cover slide. For colocalization analysis, the same procedure with BiFC was performed. For PEI transfection, plasmids to the desired condition were transferred into HEK293 cells as 800 ng of each. After 48 hours post-transfection, the cells were prepared for fixation and visualizing under the microscope.

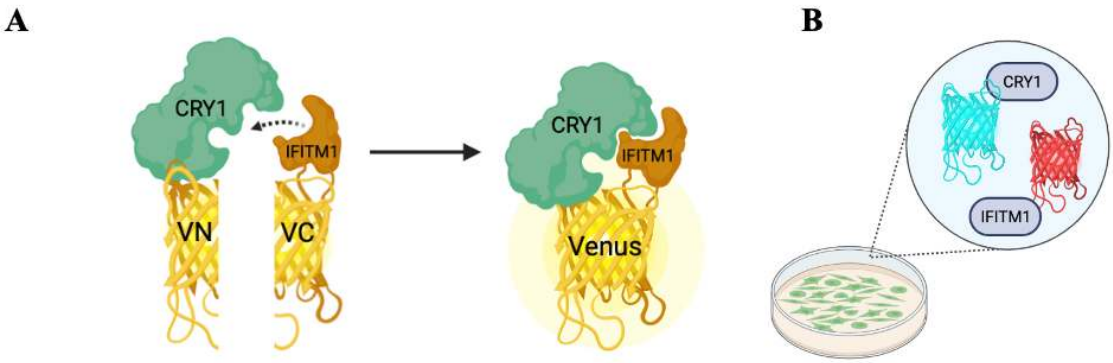

Figure 3. 1: Schematic representation of BiFC (Bimolecular Fluorescent Complementation Assay) and co-localization working principle (A) demonstrates the working mechanism of BiFC (B) shows fluorescent protein fused with target genes to visualize under the microscope.

3.6 Protein Isolation and Western Blotting

3.6.1 Protein Isolation from Mammalian Cells

To isolate proteins from the cell pellet, harvested cells were resuspended in ice-cold RIPA buffer (150 mM NaCl, 50 mM Tris (pH 7.4), 0.1% SDS, 1% Triton-X, 1 mM PMSF, 1% protease inhibitor cocktail (PIC; Cat. No. 78429)). The resuspended samples were incubated in ice for 15 minutes and briefly vortexed for 5 seconds. After that, the samples were incubated in the ice for 15 minutes. The samples were centrifuged for 20

minutes at 15000g in the cold room. The supernatants of the samples were transferred into the new Eppendorf without touching the pellets at the bottom of the tubes. The concentrations of the protein samples were determined via Pierce assay (Thermo Fisher Scientific, Cat. No. 22660) or Bradford Solution (31.67% Ethanol, 58.67% Phosphoric acid, 1.41 M Coomassie Brilliant Blue G-250). Measurements were obtained by Epoch microplate reader at 660 nm for Pierce assay or Thermo Scientific™ Multiskan™ GO Microplate Spectrophotometer at 590 nm for Bradford Assay. Later, protein samples were prepared for SDS-PAGE (Sodium Dodecyl Sulfate Gel Electrophoresis) by mixing with 4X Laemmli Sample Buffer (250 mM Tris-HCl (pH:6.8), 40% Glycerol, 4% SDS, 0.02% Bromophenol Blue and 10% β-mercaptoethanol). After mixing with Laemmli Sample Buffer, protein samples were boiled at 98°C for 10 minutes. The samples were stored at -20°C for long-term usage.

3.6.2 SDS PAGE and Western Blotting

Protein samples were loaded into 8%-15% SDS PAGE gel to the sizes of proteins that were examined to visualize. Stacking gel and separating gels are prepared from 30 % acrylamide mix, 1.5 M Tris HCl (pH 6.8 and 8.8 respectively), 10 % SDS, 10% APS, and TEMED. Proteins were run in the gel systems at 90V for 15 minutes until reaching the stacking phase. After they passed the stacking, the voltage was increased to 120V. When the proteins were separated in the gel, they were transferred into a polyvinylidene fluoride membrane (PVDF, Millipore, Cat. No. IEVH00005) using a wet Western blot transfer system. In this system, the gel was placed into a transfer sandwich pressed with Whatman paper and sponges to provide a suitable environment to transfer proteins from gel to membrane. This transfer sandwich was replaced with a Mini Trans-Blot Cell wet tank blotting system. The complete electric current in the system, the tank was filled with Transfer Buffer (25 mM Tris, 192 mM glycine, 10% Methanol). The transfer was performed for 1.30 hours at 95 V.

After the transfer procedure, the membrane was washed with TBS-T (Tris-buffered saline with 0.15% Tween-20 (Thermo Fischer Scientific, Cat. No. 003005), and the membrane was incubated for blocking with 5% non-fat milk dissolved in TBS-T for 1 hour. After the membrane was blocked entirely, the membrane was incubated overnight at +4°C to detect endogenous proteins. Overexpressed and housekeeping proteins were incubated at room temperature for 1 hour on a shaker with a primary antibody targeting

interested protein Anti-FLAG (Cell Signalling, Cat. No. 14793), Anti-Myc (Cell Signalling. No. 5605), Anti-β-actin (Cell Signalling, Cat. No.4970), IFITM1 (Proteintech,#60074), and IFITM3 (Cell Signalling, Cat. No.59212). Antibodies were prepared in 5% non-fat milk or BSA (Bovine Serum Albumin) solution in TBS with 0.15% Tween-20 to the manufacturer's instructions with proper dilutions. After completion of primary antibody incubation, to remove excess amount of primary antibody in the environment, the PVDF membranes were rinsed in TBS-T solution three times for 5 minutes with a rotator shaker continuously at room temperature. The rinsed membranes were incubated in secondary antibody conjugated with Horseradish Peroxidase (HRP), which recognizes specific primary antibodies (Anti-Mouse: Cell Signalling, Cat. No. 58802; Anti-Rabbit: Cell Signalling, Cat. No. 7074) for 1 hour at room temperature. Before visualization of the protein bands, again, to remove excess amount of non-binding secondary antibodies in the environment, the PVDF membranes were rinsed in TBS-T solution three times for 5 minutes with a rotator shaker. The membranes were prepared for visualization.

3.6.3 Visualizing via Homemade ECL Solution

To visualize the protein bands, the membrane was treated for 1 minute at room temperature with Super-ECL solution, which was prepared by mixing Solution S-A (2.5 mM Luminol, 4 mM IPBA, 100 mM Tris-HCl (pH 8.8) and Solution S-B (10 mM H_2O_2, 100 mM Tris-HCl (pH 8.8)) in 1:1 ratio. The excess amount of solution was blotted off. Luminescence was detected with BioRad ChemiDoc Touch or Azure c300 Gel Imaging System.

3.7 RNA Isolation and Real-Time PCR

3.7.1 RNA Isolation from Cell Pellet

All equipment and working place were cleaned with RNase Zap. The cell pellet collected from 35 cm dishes was thawed in the ice, and 1 mL Trizol Reagent was added to resuspend into each pellet. Then 200 µL chloroform solution was added and mixed by inverting 10 times gently. Cell suspensions were let incubated at room temperature for 5 minutes. After incubation, the samples were centrifuged at 14000g at +4°C for 20 minutes. The supernatants were transferred into new Eppendorfs. To ease the precipitation of RNA, 400 µL ice-cold isopropanol and 0.6 µL glycogen (20 mg/mL) were

added to the transferred aqueous supernatant. After inverting 10 times gently, they were left to incubate at -80°C for two hours. Frozen samples were incubated in ice to thaw, then centrifuged at 14000g at +4°C for 20 minutes. After centrifugation, the supernatant was discarded, and the pellet was washed gently without disturbing it with 75% Ethanol. Washed samples were centrifuged again at 14000g at +4°C for 5 minutes, and these washing steps were repeated three times. When the pellets were washed, they were let to dry to remove excess ethanol, which might inhibit the following processes. The dried pellets were dissolved in 30 µL DEPC treated ddH_2O. The concentration of RNA samples was measured via Nanodrop. The quality of RNA was checked via running samples in 0.8% Agarose gel at 100V for 20 minutes.

3.7.2 cDNA Synthesis from Isolated RNA

To obtain first-strand cDNA from RNA, Thermo Scientific RevertAid First Strand cDNA Synthesis Kit (Cat. No. K1622) was used according to the manufacturer's instructions. In each reaction, 500 ng RNA sample was used to synthesize cDNA. The reverse transcription reaction product was diluted 1:5 ratio with sterile ddH_2O for storage at -20°C.

3.7.3 Real-Time PCR

SYBR Green Real-Time PCR mix was used with real-time PCR primers of target genes, whose stock solutions are prepared as 10 µM. The real-time PCR primer was listed (**Appendix Table B. 2)**.

3.8 Cytosol-Nuclear Fractionation

To understand the subcellular location of the target proteins, cytosol-nuclear fractionation was performed. *IFITM1* OE, KO, and WT U2-OS *Bmal1-dluc* cells were seeded into a 10 cm plate. When a cell line reaches about 90-100% confluency, they were harvested 1 mL ice-cold 1X PBS and centrifuged at 5000 g for 5 minutes at 4°C. After removing supernatants, cells were dissolved with 300 µL Cytosolic Lysis Buffer (CLB) containing 10 mM HEPES pH 7.9, 10 mM KCl, 0.1 mM EDTA pH 8.0, 0.05% NP-40, 1X PIC, and then the tubes were incubated on ice for 10 minutes. After incubation, the samples were centrifuged at 5000 g for 5 minutes at 4°C. The supernatants of each tube were separated to isolate the cytosolic fraction; the pelleted were washed with 200 µL

CLB 3 times to remove the unwanted cytosolic fraction proteins. At the end of each wash, the samples were centrifuged at 5000 g for 5 minutes at 4°C. Later, cell pellets collected at the bottom of the tubes were resuspended with Nuclear Lysis Buffer (NLB) (20mM HEPES pH 7.9, 0.4M NaCl, 1mM EDTA, 10% Glycerol, 1X PIC) and exposed to sonication (60% power, 10 seconds, 3 cycles) (BANDELIN SONOPULS HD 2070 homogenizer) for 2 times. After it was burst via pipetting and sonication, the samples were centrifuged at 15000xg for 5 minutes with the cytosolic fractions. Each cytosolic and nuclear fragment was transferred into the new tubes, and the amount of the protein was verified. For Western blot analysis following antibodies were used: anti-CRY1(Bethyl, A302-614A), anti-CRY2 (Bethyl, A302-614A), Histone H3 (Proteintech,#17168), and anti-αTUBULIN (Proteintech, #11224) antibodies. Histone H3 and α-Tubulin were loading control for the nucleus and cytosol, respectively.

3.9 Poly(I: C) Induction

Poly(I: C) HMW is provided lyophilized and dissolved in sterile endotoxin-free physiological water (NaCl 0.9%). Stocks were prepared at 1 mg/m Land added medium used in the experiment. The cells were stimulated with 30 ng-10 µg/ml Poly(I: C) HMW for 6 to 24 hours. They can be stored at -20 °C for one year.

CHAPTER 4:
RESULTS

4.1 The Expression Profile of IFITM1 Shows the Oscillation in Synchronized Cells

In 2014, Ron Anafi and his collaborators discovered new circadian clock components using a machine learning-based strategy. They identified 25 prominent candidates exhibiting common features of core clock genes, such as periodicity, genetic conservation, and functional interaction with other clock genes (Anafi et al., 2014). Among these novel clock gene candidates, cystathionine beta synthetase (CBS) has been previously characterized in our lab and shown to be a part of the core clock machinery (Cal-Kayitmazbatir et al., 2021). Another candidate, interferon-inducible transmembrane protein 1 (Ifitm1), was shown to physically interact with Cry1 based on co-immunoprecipitation and mammalian two-hybrid assay using recombinant mouse proteins (Kulkoyluoglu, 2015). For my thesis study, I have further characterized *IFITM1* to elucidate its role as a clock component.

My initial step in this endeavor was to deduce whether IFITM1 itself exhibits clock-like characteristics. In this sense, I first demonstrated using reverse-transcription-quantitative polymerase chain reaction (RT-qPCR) that *IFITM1* exhibits a rhythmic expression profile in a circadian-dependent manner, which is one of the critical features of core clock genes **(Figure 4. 1)**. My results also correlate with the CircaDB database, where *Ifitm1* exhibited a circadian expression profile in different mouse tissues **(Figure 4. 2)**. These results collectively suggest that IFITM1 is being transcribed under circadian control. Hence, this motivated me to evaluate other common features of core clock genes displayed in IFITM1 to identify whether IFITM1 is a circadian clock component.

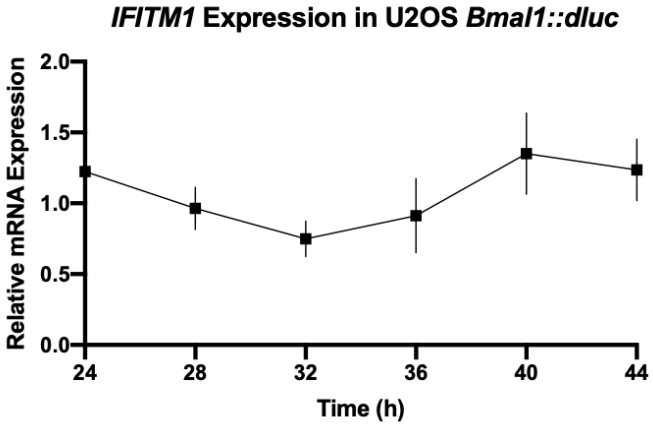

Figure 4. 1: RT-qPCR detection of *IFITM1* mRNA amount oscillation in 4 hours intervals for 20 hours after synchronization with Dexamethasone. Reverse-transcription-quantitative polymerase chain reaction (RT-qPCR) was performed for the WT U2-OS *Bmal1-dluc* cell lines, which were synchronized with 0.1µM dexamethasone. After 24 h of dexamethasone, the samples were harvested in 4 hours period at the indicated time. mRNA levels were normalized to RPLP0 levels. Quantitative results represent the oscillation of *IFITM1*. The expression level of genes was normalized according to the expression level of that gene at 28th h. Data represent the mean ± SEM, n=3 with duplicates. To verify oscillation, EJTK_CLASSIC algorithm was used at BioDare2, *p-value <0.1.

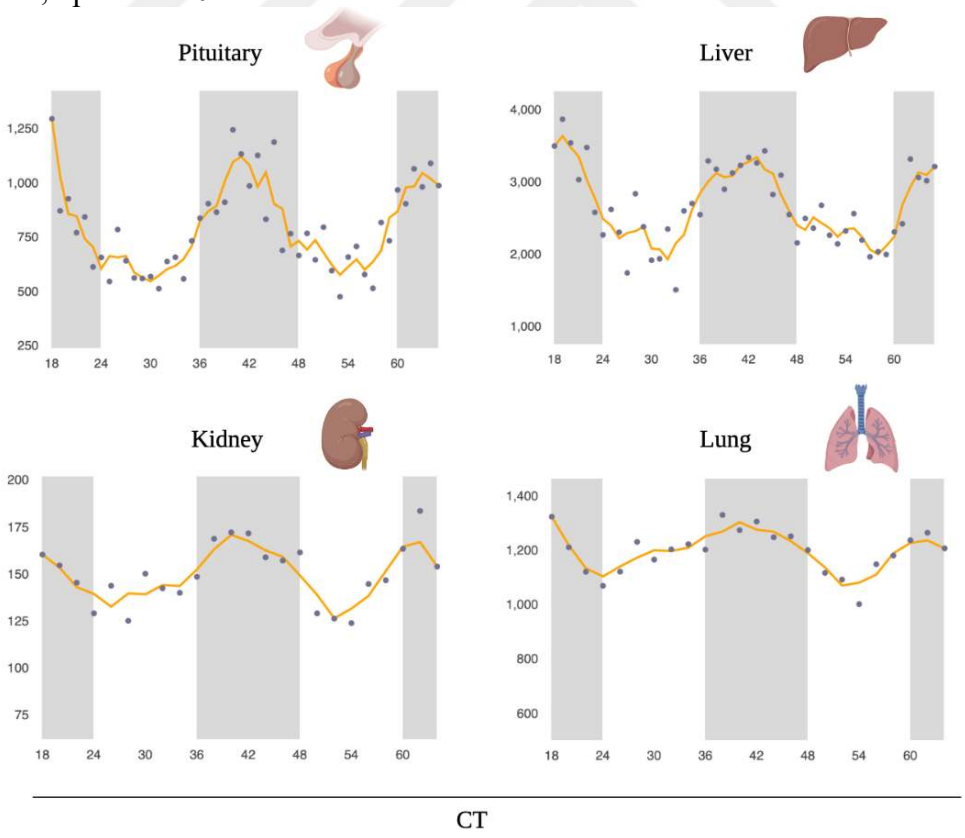

Figure 4. 2: The circadian expression pattern of *Ifitm1* in mouse tissues. These results were adopted from the CircaDB database and illustrated via BioRender.

4.2 Cloning of Human cDNAs of *IFITM*s and *CRY*s into Mammalian Expression Vector

In order to study the role of IFITM1 in the circadian rhythm as a candidate clock component, especially human recombinant *IFITM* and *CRY* constructs were generated (**Table 4. 1)**. Although in previous clock gene discovery research (Anafi et al., 2014; Cal-Kayitmazbatir et al., 2021; Kulkoyluoglu, 2015), mouse constructs were preferred to identify the function of the clock candidates, in this work we used human recombinant system on purpose. This is because the xenogenic nature of recombinant mouse protein might lead to a considerable risk of recognition by immune system elements (Bresser et al., 2020). With the intent to eliminate this phenomenon while using U2-OS and HEK293-T cell lines and to generate models which are as far as similar to the human physiological system in functional studies, human recombinant constructs were generated.

To generate plasmids, DNA regions encoding human *IFITM1*, *IFITM3*, *CRY1,* and *CRY2* were amplified from cDNA obtained from U2-OS cells by using touch-down PCR with appropriate primers. Amplified products were sub-cloned into the pJET vector and later transferred into the recipient vector. Recipient vectors, which were selected based on the intended use, were listed **(Table 4. 1)**. In order to generate stable cell lines, lenti backbones which are compatible with 3rd generation system; pLenti-CMV-Neo-DEST for overexpression and lentiCRISPR v2 Hygro for knockout systems were generated. The overexpression lenti plasmids encode flag tagged *IFITM*s.

Several pCMV-Sport6 constructs were used to overexpress *IFITM*s because they are compatible with our overexpression core clock plasmid library, which can be used for understanding the consequences of functional interactions of *IFITM*s in overexpressed systems. The verification of pCMV-Sport6 vectors carrying Flag-tagged *IFITM*s at the protein level was performed via western blotting **(Figure 4. 4)**. While pBiFC-VC155, with HA-tagged, and VN173 with Flag-tagged were generated to understand protein-protein interaction via BiFC (Bimolecular Fluorescent Complementation Assay. Plasmids having *Scarlet* and *Turquoise* fluorescent proteins were used for intracellular localization of CRYs and IFITMs. After the generation of constructs, colonies carrying desired plasmids were picked, and plasmid DNAs were purified. After DNA purification, diagnostic restriction digest analyses were performed to verify the presence and

orientation of the cloned inserts **(Figure 4. 3)**. After verification by restriction, recombinant plasmids were sequenced (Macrogen Europe) to check for mutations that could be introduced during PCR amplification. Constructs that possessed wild-type sequences were used in further studies.

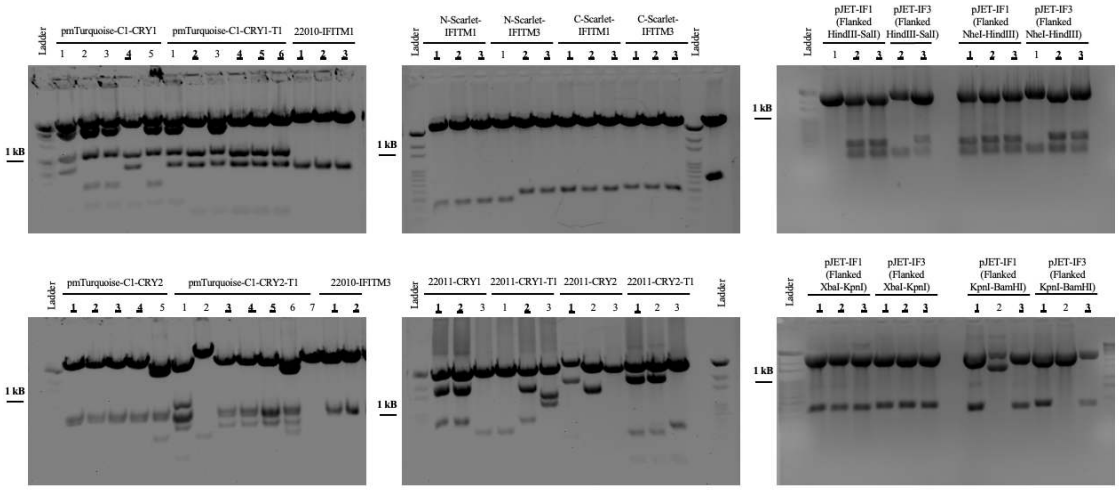

Figure 4. 3: Diagnostic restriction digest products were run on an 0.8% agarose gel to verify the correct orientation and as well as a correct insert in the plasmids. In the figure, the plasmid names are written above each gel. The colony number of each plasmid is represented below the name of the plasmid. The plasmids that give the correct diagnostic bands are signed in bold and underlined.

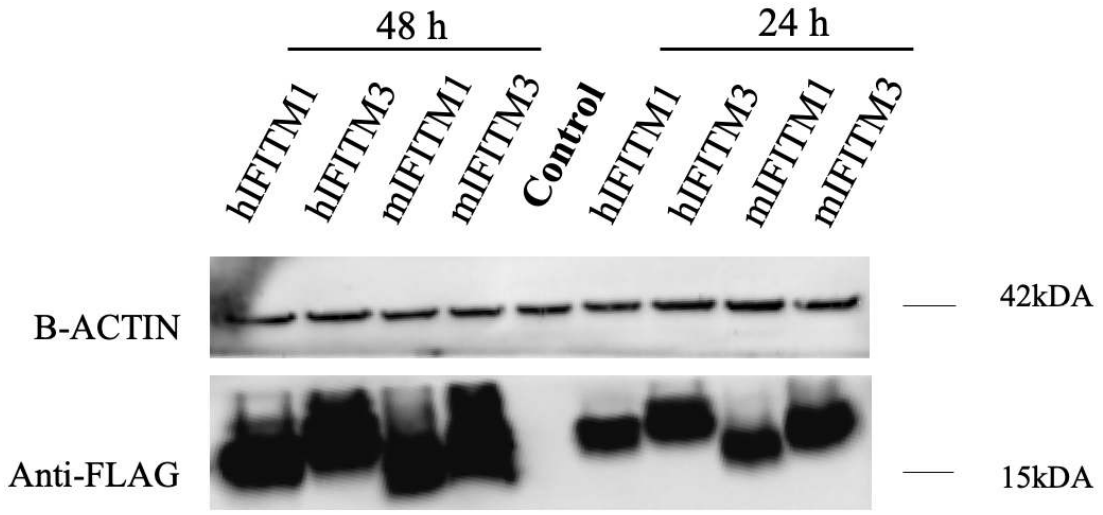

Figure 4. 4: Western Blot verification of pCMV-Sport6-FLAG-*IFITM* recombinant constructs. In samples collected 24 and 48 hours after transfection, it was observed that IFITM protein expression increased over time. The empty pCMV-Sport6 vector was transfected as a control.

Table 4. 1: Plasmids and genes that used in the clonings of this study.

Donor Plasmid or Source	Gene of Interest	Restriction Sites	Cloning Technique	Recipient Plasmids
Primers Encoding Flag Epitope	Flag Epitope	SalI/SalI	Oligo Cloning	pENTR1A no ccdB (w48-1) (#17398)
pJET-v2-hIFITM1	hIFITM1	Donor: BamHI/XhoI Recipient: BamHI/XhoI	Restriction Digest	pENTR1A-Flag
pJET-v2-hIFITM3	hIFITM3	Donor: BamHI/XhoI Recipient: BamHI/XhoI	Restriction Digest	pENTR1A-Flag
pJET-v2-mIfitm1	mIfitm1	Donor: BamHI/XhoI Recipient: BamHI/XhoI	Restriction Digest	pENTR1A-Flag
pJET-v2-mIfitm3	mIfitm3	Donor: BamHI/XhoI Recipient: BamHI/XhoI	Restriction Digest	pENTR1A-Flag
lentiCRISPR v2 (#52961)	U6 promototer + gRNA scaffold region	Donor: KpnI/NheI Recipient: KpnI/NheI	Restriction Digest	lenti-SpCas9 hygro (#104995)
pENTR1A-Flag-hIFITM1	hIFITM1-Flag	Donor: DraI/Eco32I Recipient: SmaI/BoxI	Restriction Digest	pLenti-CMV-Neo-DEST (#17392)
pENTR1A-Flag-hIFITM3	hIFITM3-Flag	Donor: DraI/Eco32I Recipient: SmaI/BoxI	Restriction Digest	pLenti-CMV-Neo-DEST (#17392)
pENTR1A-Flag-mIFITM1	mIFITM1-Flag	Donor: DraI/Eco32I Recipient: SmaI/BoxI	Restriction Digest	pLenti-CMV-Neo-DEST (#17392)
pENTR1A-Flag-mIFITM3	mIFITM3-Flag	Donor: DraI/Eco32I Recipient: SmaI/BoxI	Restriction Digest	pLenti-CMV-Neo-DEST (#17392)
pENTR1A-Flag-hIFITM1	hIFITM1-Flag	Donor: DraI/XhoI Recipient: XhoI/Eco32I	Restriction Digest	pCMV-Sport6
pENTR1A-Flag-hIFITM3	hIFITM3-Flag	Donor: DraI/XhoI Recipient: XhoI/Eco32I	Restriction Digest	pCMV-Sport6
pENTR1A-Flag-mIFITM1	mIFITM1-Flag	Donor: DraI/XhoI Recipient: XhoI/Eco32I	Restriction Digest	pCMV-Sport6
pENTR1A-Flag-mIFITM3	mIFITM3-Flag	Donor: DraI/XhoI Recipient: XhoI/Eco32I	Restriction Digest	pCMV-Sport6
pJET-v2-hCRY1	hCRY1	Donor: KpnI/XbaI Recipient: KpnI/XbaI	Restriction Digest	pmTurquoise-C1 (#60558)
pJET-v2-hCRY1	hCRY1	Donor: KpnI/KpnI Recipient: KpnI/KpnI	Restriction Digest	pBiFC-VC155 (#22011)
pJET-v2-hCRY1-T1	hCRY1-T1	Donor: KpnI/XbaI Recipient: KpnI/XbaI	Restriction Digest	pmTurquoise-C1 (#60558
pJET-v2-hCRY1-T1	hCRY1-T1	Donor: KpnI/KpnI Recipient: KpnI/KpnI	Restriction Digest	pBiFC-VC155 (#22011)
pJET-v2-hCRY2	hCRY2	Donor: KpnI/XbaI Recipient: KpnI/XbaI	Restriction Digest	pmTurquoise-C1 (#60558
pJET-v2-hCRY2	hCRY2	Donor: KpnI/KpnI Recipient: KpnI/KpnI	Restriction Digest	pBiFC-VC155 (#22011)
pJET-v2-hCRY2-T1	hCRY2-T1	Donor: KpnI/XbaI Recipient: KpnI/XbaI	Restriction Digest	pmTurquoise-C1 (#60558
pJET-v2-hCRY2-T1	hCRY2-T1	Donor: KpnI/KpnI Recipient: KpnI/KpnI	Restriction Digest	pBiFC-VC155 (#22011)
pCMV-Sport6-Flag-hIFITM1	hIFITM1	Donor: HindIII/SalI Recipient: HindIII/SalI	Restriction Digest	pBiFC-VN173 (#22010)
pCMV-Sport6-Flag-hIFITM3	hIFITM3	Donor: HindIII/SalI Recipient: HindIII/SalI	Restriction Digest	pBiFC-VN173 (#22010
pCMV-Sport6-Flag-hIFITM1	hIFITM1	Donor: KpnI/BamHI Recipient: KpnI/BamHI	Restriction Digest	pmScarlet_C1 (#85042)
pCMV-Sport6-Flag-hIFITM3	hIFITM3	Donor: KpnI/BamHI Recipient: KpnI/BamHI	Restriction Digest	pmScarlet_C1 (#85042)
pCMV-Sport6-Flag-hIFITM1	hIFITM1	Donor: HindIII/PstI Recipient: HindIII/PstI	Restriction Digest	pScarlet-N1 (#128060)
pCMV-Sport6-Flag-hIFITM3	hIFITM3	Donor: HindIII/PstI Recipient: HindIII/PstI	Restriction Digest	pScarlet-N1 (#128060)

Donor Plasmid or Source are vectors used as templates to obtain the target gene. The gene of interest is the name of the target coding sequence. Restriction sites are the regions which recognized by restriction enzymes to restrict the target fragments and ligate. These specific sites used in the cloning were defined for both donor plasmid and recipient plasmid. Cloning techniques represent the technique used to create recipient plasmid. The recipient plasmid is the host-vector which are desired to insert the gene of interest into it. Plasmids that were provided by Addgene were stated with their Addgene catalog numbers (e. g. #17398).

30

4.3 Generating and Verifying *IFITM1* Overexpression and CRISPR/Cas9 Knock-out Stable Cell Lines

After observing the circadian oscillation of *IFITM1* gene expression at the mRNA level, I investigated how overexpression or knock-out of *IFITM1* affects circadian rhythm, which is a critical parameter in identifying circadian clock components. Therefore I generated two distinct cell lines using both wildtype U2-OS and U2-OS *Bmal1-dluc* cells. The first cell line was generated using overexpression constructs for stable IFITM1 overexpression and the second using CRISPR/Cas9-mediated knockout constructs for IFITM1 knockout. *IFITM3* overexpression and knock-out cell lines were generated as negative controls because our previous results using recombinant mouse constructs of *Ifitm3* and *Cry1* showed no interaction in co-IP assays. (Kulkoyluoglu, 2015). However, after the *IFITM3* was knocked-out via CRISPR/Cas9, drastic morphological changes such as shrinkage in the cells and death at the end were observed.

After I generated the overexpression pLenti constructs, explained in **Section 4. 2** and **Table 4. 1**, I transiently transfected HEK293-T cells with these pLenti-CMV-Neo-DEST-*IFITM*s via PEI to verify encoded functional proteins by using western blotting (**Figure 4. 5 A)**. Also, the efficiency of *IFITM1* CRISPR constructs was confirmed in U2-OS and U2-OS *Bmal1-dluc* lines at the protein level (**Figure 4. 5 B)**.

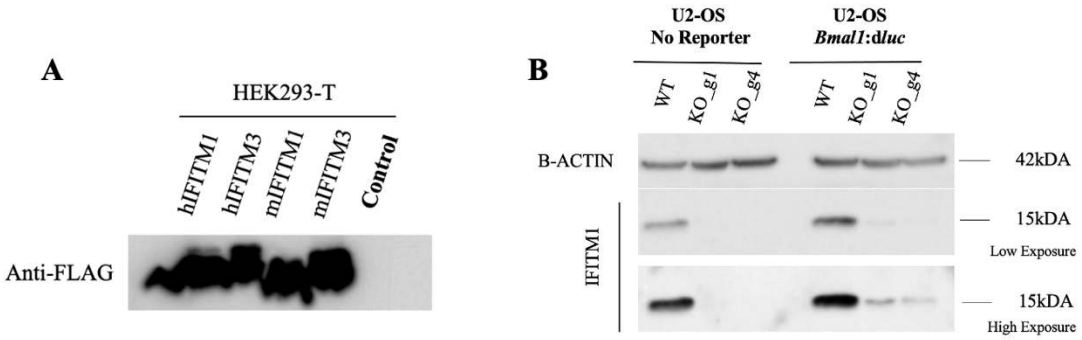

Figure 4. 5: Protein Level Verification of Overexpression and CRISPR/Cas9 constructs by Western Blot (A) Western results of pLenti-CMV-Neo-DEST-*IFITM*s recombinant constructs in transiently transfected into unsynchronized HEK293-T cells after 24 hours of transfection. **h**IFITMs represent human proteins, and **m**IFITMs represent mouse proteins. (B) After introducing pLentiCRISPRv2-Hygro-*IFITM1*-KO-g1 and g4 via 3rd generation lentivirus to U2-OS and U2-OS *Bmal1-dluc,* Hygromycin selection was made to eliminate the undesired population from the cell pool. The

efficiency of CRISPR in bulk populations was evaluated via western blotting before performing the monoclonal selection.

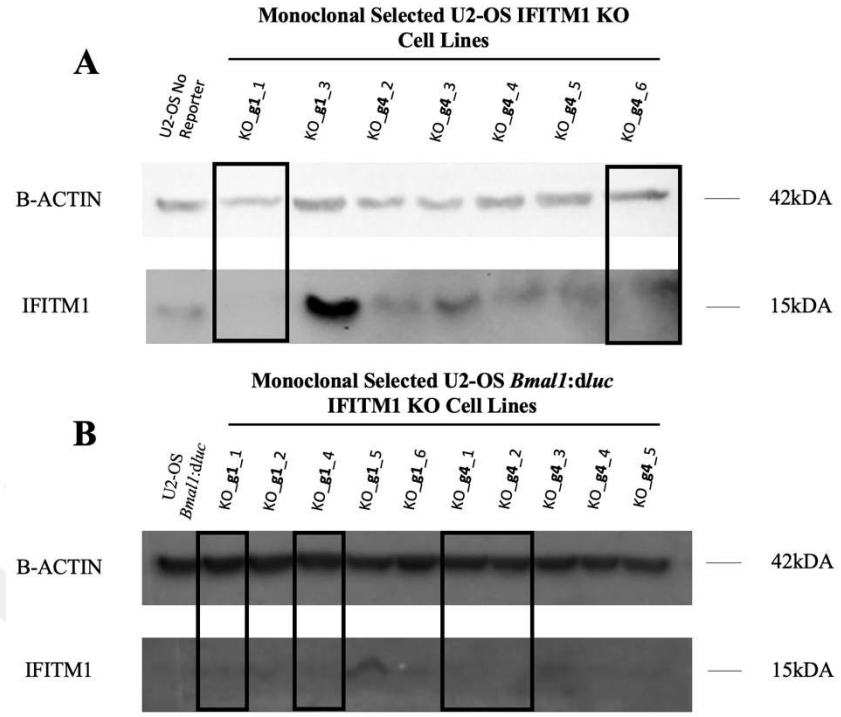

Figure 4. 6: Western Blot verification of monoclonal selected colonies from *IFITM1* KO U2-OS and U2-OS *Bmal1-dluc* bulk population. Rectangles indicate successfully knocked out colonies. g1 and g4 are the names of constructs used to knock out *IFITM1*. The cell lines that derived from single-cell were designated. KO_g1_1 means colony number 1, which was knocked out via the g1 construct. (A) demonstrate the colonies obtained from U2-OS (B) from U2-OS *Bmal1-dluc.*

To eliminate the effect of genetic variance in the heterogeneous cell population, monoclonal cell lines were generated by the limiting dilution method. After monoclonal selection and expansion, cell lines were verified by western blotting **(Figure 4. 6)** and T7 endonuclease assay to knockout cell line **(Figure 4. 7)**. For U2-OS *Bmal1-dluc* cell lines, two colonial populations were selected for each individual sgRNA knockout vector (denoted g1_1 and g1_4 for hIFITM1_GPP_g1 construct, and g4_1 and g4_5 for hIFITM1_GPP_g4 construct respectively). I have selected two distinct populations per sgRNA to negate the effect of random knockout of off-target genes, which may alter cellular function and produce false results. By comparing two distinct populations, we can ensure that the downstream effect observed is consistent with the knockout of target gene. For wildtype U2-OS cells, only one colonial population was selected and propagated (g1_1 for hIFITM1_GPP_g1 and g4_6 for hIFITM1_GPP_g4).

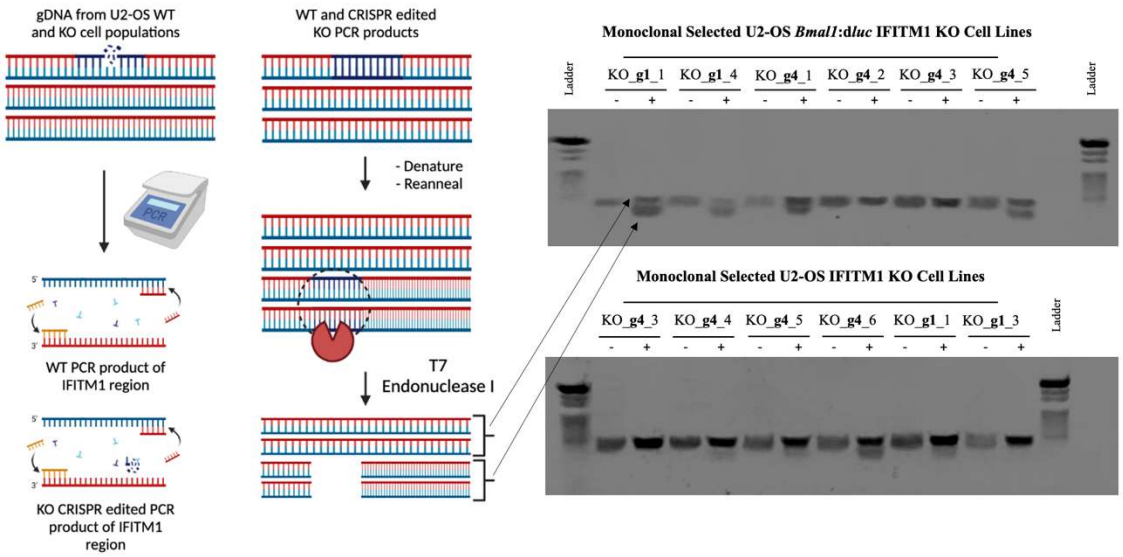

Figure 4. 7: Schematic and result of T7 Endonuclease I assay to verify CRISPR *IFITM1* KO U2-OS cell lines. PCR amplification targets the *IFITM1* site by using genomic DNA isolated from cells containing wild-type and CRISPR edited DNA (represented with darker blue) as a template. After denaturation and annealing of PCR products from wild-type and CRISPR edited, DNA creates mismatches cleaved by T7 Endonuclease I. The right panel shows these cleaved products and full-length DNA from U2-OS and U2-OS *Bmal1-dluc* CRISPR KO cell lines were separated on the 0.8% agarose gel. The gel demonstrates untreated (-) and cells edited with Cas9 and sgRNA (+). The schema was illustrated via BioRender.

4.4 *IFITM1* KO affects the circadian rhythmicity of U2-OS *Bmal1-dluc* by extending the period and dampening the amplitude.

Using verified U2-OS *Bmal1*:d*luc* CRISPR g1_1 and g4_1 KO cell lines, I evaluated the effect of *IFITM1* knockout on *in vitro* circadian rhythms. Knockdown of *Ifitm1* causes dampening in the amplitude and lengthening in the period in NIH 3T3 cells (Anafi et al., 2014). Also, knock-down *IFITM1* via siRNA in U2-OS *Bmal1*:d*luc* dampened the amplitude and lengthened the period (Kulkoyluoglu, 2015). In line with these results, I analyzed the period and amplitude of *IFITM1* KO cell lines compared to U2-OS *Bmal1*:d*luc* as a control. As expected, *IFITM1* knock-out extended the circadian period by 1.28 h and 0.625 h in U2-OS *Bmal1*:d*luc* g1_1 and g4_1 KO cells, respectively. Also, their amplitude significantly decreased compared to WT in U2-OS *Bmal1*:d*luc* **(Figure 4. 8 A)**. On the other hand, U2-OS *Bmal1*:d*luc* overexpressing IFITM1 stably exhibited significantly shorter circadian period, as expected, but severely reduced amplitude **(Figure 4. 8 B).** The reason for this severe dampening at overexpressing cells might be due to metabolic toxicity and cell death induced by overexpression of the

IFITM1 protein (Park et al., 2016). Nevertheless, lengthening of the circadian period and the dampening of the amplitude due to *IFITM1* knockout in U2-OS cells hint that IFITM1 can be a core clock component.

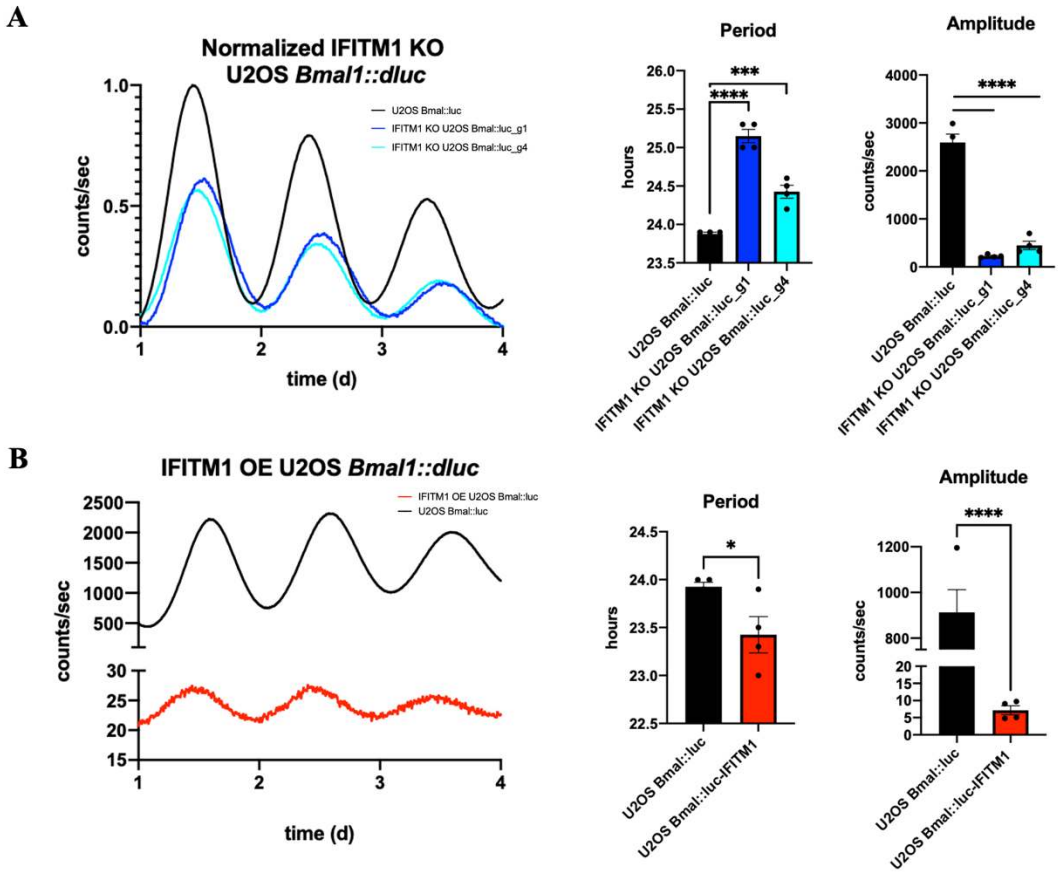

Figure 4. 8: *IFITM1* KO and OE modulate the rhythmicity of U2-OS *Bmal1-dluc* cell lines. (A) The period and amplitude of *IFITM1* KO U2-OS *Bmal1*:d*luc*_g1 (darker blue) and *IFITM1* KO U2-OS *Bmal1*:d*luc*_g4 (lighter blue) were compared to WT U2-OS *Bmal1-dluc* (black). While the period was extended when IFITM1 depleted around 24.5-25 hours, the amplitudes were significantly reduced. Data represent mean ± SEM; n=4, independent experiments. *p-value <0.05; **p-value <0.01; ***p-value <0.001; ****p-value <0.0001. (B) The period and amplitude of *IFITM1* OE U2-OS *Bmal1-dluc* (red) were compared to WT U2-OS *Bmal1-dluc* (black). While the period was shortened in the case of *IFITM1* overexpressed around 23.5 hours, the amplitudes were drastically reduced. After seeding, the cells were synchronized with 0.1 µM dexamethasone. Then, dishes were replaced in Lumicycle to collect data of luminescence signals for 5-7 days each 10 minutes. The data recorded on the first day were excluded. Data represent mean ± SEM; n=3, independent experiments. Data represent mean ± SEM; n=4, independent experiments. *p-value <0.05; **p-value <0.01; ***p-value <0.001; ****p-value <0.0001.

4.5 IFITM1 and CRY1 physically interact and co-localize in the nucleus, but not CRY2.

The physical interaction between Cry and Ifitm1 was shown based on co-immunoprecipitation and mammalian two-hybrid assay using recombinant mouse proteins. What is more, the fact that the C-terminal of CRY1 in this interaction is critical was demonstrated. However, it is not known where CRY1 and IFITM1 interact in vivo and whether the interaction is specific between CRY1 and IFITM1. To understand the role of IFITM1 on the molecular clock, I aimed to investigate whether IFITM1 interacts physically with CRY1 and CRY2. In order to test this, I have used two different methods, namely bimolecular fluorescence complementation (BiFC) and sub-cellular fractionation techniques.

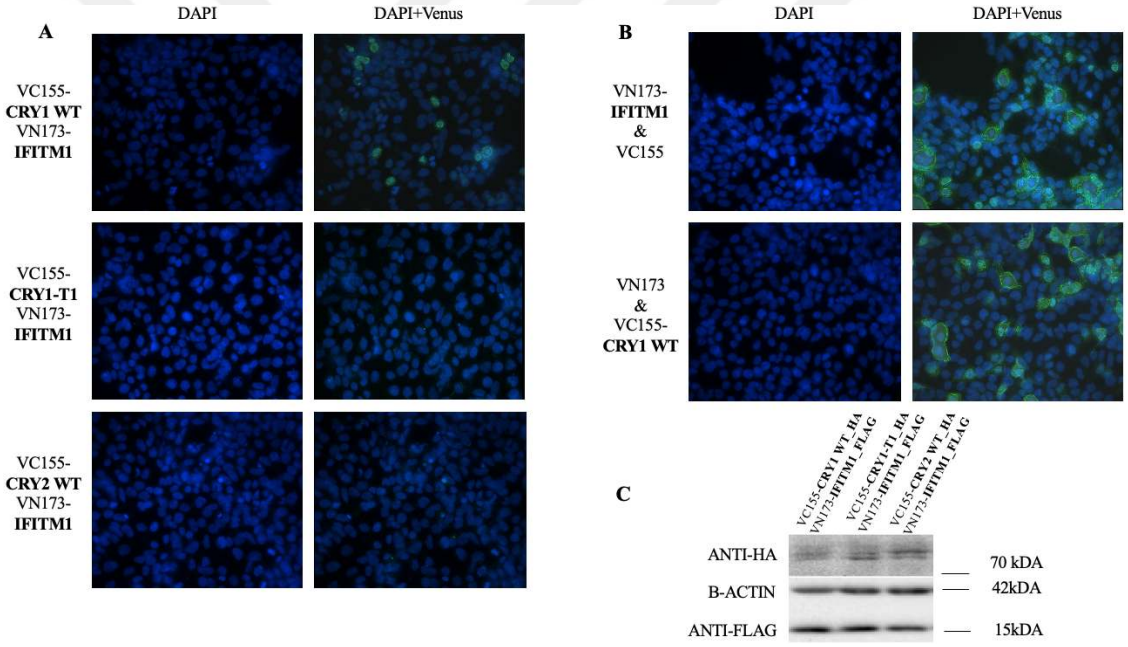

Figure 4. 9: Bi-FC (Bimolecular Fluorescent Complementation) assay shows IFITM1 interacts with CRY1 in the nucleus but not CRY2. (A) The plasmids written right side of Panel A indicate the name of plasmids that were transiently transfected into HEK293 cells. Images of DAPI and Venus + DAPI merged signals are shown, and the Venus signal could be detected only in the "CRY1-WT and IFITM1" condition. (B) Empty vectors VC155 and VN173 give non-specific signals due to random collisions. (C) Protein expression of CRYs and IFITM1 in the "CRY1-WT and IFITM1", "CRY1-T1 and IFITM1", and "CRY2-WT and IFITM1" samples were verified via western blotting.

BiFC is used to detect the protein-protein interaction in the cell and the localization of this interaction. BiFC is based on reassembling two complementary non-

fluorescent fragments of Venus protein when an interaction takes place between two proteins that are each fused to these fragments. When these complementary interaction partners interact, the N- and C-terminal regions of Venus come together and reconstitute the Venus protein, which emits a fluorescent signal when excited. In our study, the C-terminal section of Venus protein was fused with different CRY constructs (CRY1-WT-VC, CRY1-T1-VC, CRY2-WT-VC), and the N-terminal half of it was conjugated with IFITM1 (IFITM-VN).

One issue about BiFC assays is the propensity to generate non-specific signals due to the random collision of the N- and C-terminal Venus parts (Kodama & Hu, 2012). This phenomenon can also be observed in our experiments. When "CRY1-WT-VC155 / empty VN173" and "empty VC155 / IFITM1-VN173" pairs were co-transfected to HEK 293 cells and observed under a microscope, the non-specific fluorescence signal was detected in the cytosol **(Figure 4. 9 B).** It is necessary to include an appropriate non-interacting negative control to solve this. Here, I used CRY-T1-VC155 / IFITM1-VN173 pair as a negative control since our earlier experiments indicate that *Cry1-T1* and *Ifitm1* do not interact in vitro (Kulkoyluoglu, 2015). When these non-interacting pairs were transfected to HEK 293 cells and monitored under a microscope, I did not observe a significant Venus signal even if "CRY-T1-VC155 and IFITM1-VN173" constructs were expressed, as evident from Western blots **(Figure 4. 9 C).**

In the first column of **Figure 4. 9 A,** DAPI staining was represented to specify nuclear fragments. The second column represents the merged version of DAPI and Venus signals. Venus signal (yellow-greenish one) was detected in the first row of **Figure 4. 9 A** in the nucleus indicating CRY1-IFITM1 interaction. However, the signal disappeared when CRY-T1-VC155 and IFITM1-VN173 were introduced into HEK 293 cells. In addition, the signal could not be detected in the CRY2-WT and IFITM1 transfected samples demonstrated in the third row of **Figure 4. 9 A**.

First of all, these results confirm that IFITM1 and CRY1 interact physically, and the interaction is through the C-terminal intrinsically disordered domain of CRY1. While CRY1-WT interacts with IFITM1, CRY1-T1 does not interact with IFITM1. The last 20 amino acids in the C terminal of CRY1 that are absent from CRY1-T1 indicate a critical role in CRY1-IFITM1 interaction. Secondly, IFITM1-CRY1 interaction is specific since

no Venus fluorescence was observed for IFITM1-CRY2 pairing. Finally, CRY1-IFITM1 interaction occurs in the nucleus. Although CRY1 is a repressor regulating the negative feedback loop and mainly works in the nucleus, IFITM1 can be found commonly in the plasma membrane and the early endosomes (Narayana et al., 2015). The localization of IFITM1 in the nucleus has not been observed before. Considering the known function of IFITM1 in inhibiting the virus uncoating mechanism by altering the membrane topology, the biological importance of this nuclear colocalization should be investigated with further experiments to suggest a potential role for IFITM1 nuclear localization.

To further support our microscope results and verify the location of IFITM1 *in vitro*, I performed a subcellular fractionation assay using *IFITM1* OE, KO, and WT U2-OS *Bmal1*:d*luc* cell lines. IFITM1 was found in the nucleus at high levels in OE and WT cells **(Figure 4. 10 A)**. These results confirm BIFC studies and support the perinuclear or nuclear localization of IFITM1 in the cells (**Figure 4. 10 A, Appendix A. 1**). In addition, CRY1 did not localize to the nucleus *IFITM1* KO U2-OS *Bmal1:dluc*. The CRY1 level is significantly higher in the cells overexpressing the IFITM1. These results suggest that IFITM1 may require for the stability of the in the nucleus. I therefore wish to investigate this hypothesis in next section.

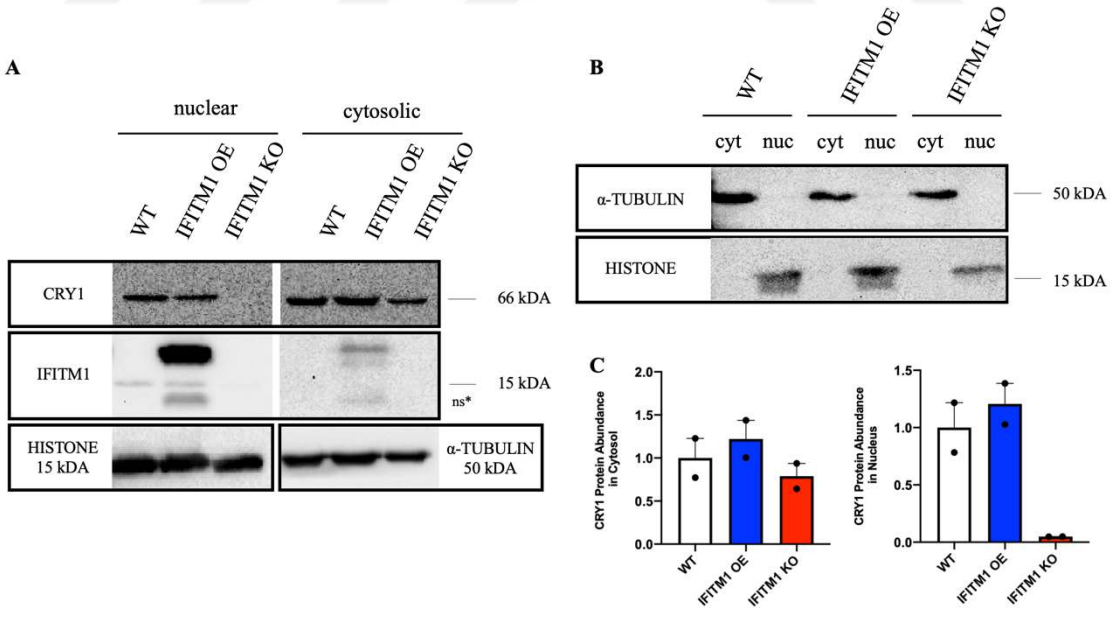

Figure 4. 10: The subcellular fractionation shows IFITM1 is found in the nuclear field to a large extent. (A) I performed subcellular fractionation in *IFITM1* OE, KO, and WT U2-OS *Bmal1*:d*luc*. IFITM1 is mainly found in the nuclear fraction in both WT and OE samples. Although CRY1 can be found in both nuclear and cytosolic fractions in WT and OE cell lines, in the nuclear part of the KO cell, CRY1 could not be detected. (B) Control for the accomplishment of subcellular fractionation experiment. The amount of

tubulin and Histone-H3 was evaluated in all fractions. n=2, independent experiments. *ns=non-specific band in western blot.

4.6 The effect of IFITM1 on the half-life of CRY1.

The aforementioned nuclear colocalization of CRY1-IFITM1 in BiFC and depletion of CRY1 in the nucleus in KO cell lines prompted us to investigate how CRY1-IFITM1 interaction affects the stability of CRY1 and the expression of other core clock genes. Therefore, I performed a cycloheximide chase assay to understand the impact of this BiFC-identified IFITM1-CRY1 interaction on the half-life of CRY1 and CRY2. Cycloheximide inhibits protein synthesis by binding to ribosomes and preventing eEF2-mediated translocation, hence blocking the elongation step of translation in eukaryotes. (Schneider-Poetsch et al., 2010). In this experiment, I evaluated how the stability of CRY1 is affected by elevated IFITM1 expression in *IFITM1* OE cell lines compared to WT U2-OS *Bmal1:dluc*. Notably, the half-life of CRY1 was augmented to around 16 hours, while there was no significant change in CRY2 when IFITM1 was overexpressed **(Figure 4. 11 A, B)**. While the half-life of CRY1 increases, we could not observe a significant alteration in CRY2. This phenomenon implies that the rise in the stability of CRY1 is a result of its association with IFITM1.

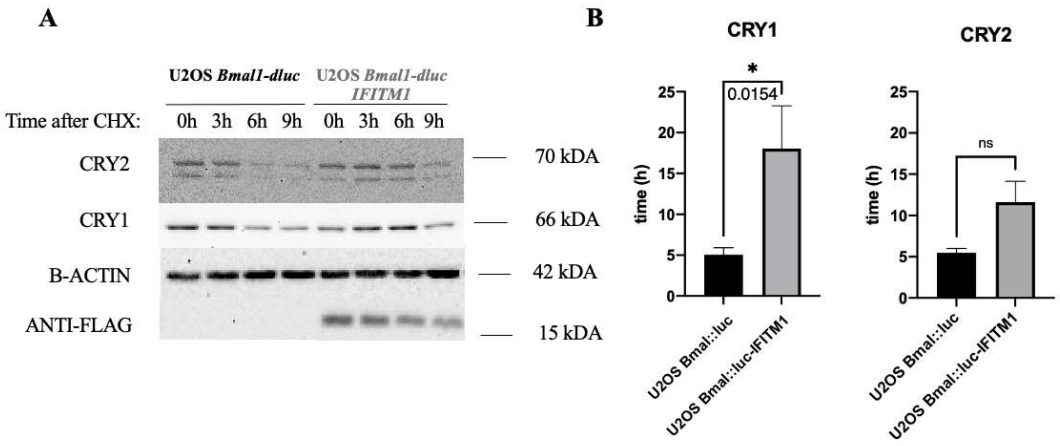

Figure 4. 11: CRY1 is more stable when IFITM1 is overexpressed in the *IFITM1* OE and WT U2-OS *Bmal1*:d*luc*. (A) After cycloheximide treatment, IFITM1 OE and WT U2-OS *Bmal1-dluc* samples were harvested every 3 hours. The amount of the protein was visualized to calculate the half-lives of the target proteins via Western blotting (B). The half-lives ($t_{1/2}$) of CRY1 and CRY2 were calculated using a one-phase exponential decay function. Comparisons were made between WT CRY1 and CRY2. Data represents mean $t_{1/2}$ values ± SEM; n=3, independent experiments (student's t-test ; *p-value <0.05; **p-value <0.01).

4.7 The relative mRNA expressions of core clock genes are altered in *IFITM1* overexpressed (OE) and knock-out (KO) cell lines.

Based on the results presented earlier, I hypothesized that increased stability of CRY1 through CRY1-IFITM1 association in the nucleus could enhance CRY1-mediated repression on BMAL1/CLOCK-driven transcription. This phenomenon, in turn, should decrease the expression level of circadian clock output genes, e.g., *PER2* and *DBP.* Hence, I tested this hypothesis by evaluating the mRNA expressions of other core clock genes in synchronized *IFITM1* OE, KO, and WT U2-OS *Bmal1:dluc* cell lines. Therefore, I analyzed the effect of *IFITM1* overexpression and knock-out on mRNA level of circadian clock output genes *PER2* and *DBP,* plus *CRY1* and *CRY2.* In line with CRY1-IFITM1 co-localization in the nucleus **(Figure 4.9 A)** and increased stability of CRY1 **(Figure 4. 11)**, we observed a significant decrease in the expression level of *PER2*, *DBP,* and *CRY1* at the 24th hour **(Figure 4.12 A)**. On the other hand, the mRNA levels of *PER2* and *CRY1* significantly increase compared to WT at all-time points **(Figure 4.12 B)**. All these results suggest that IFITM1 increases the nuclear stability of the CRY1 and, in turn, altering CRY1 stability enforces the negative arm and changes the expression of clock-controlled genes.

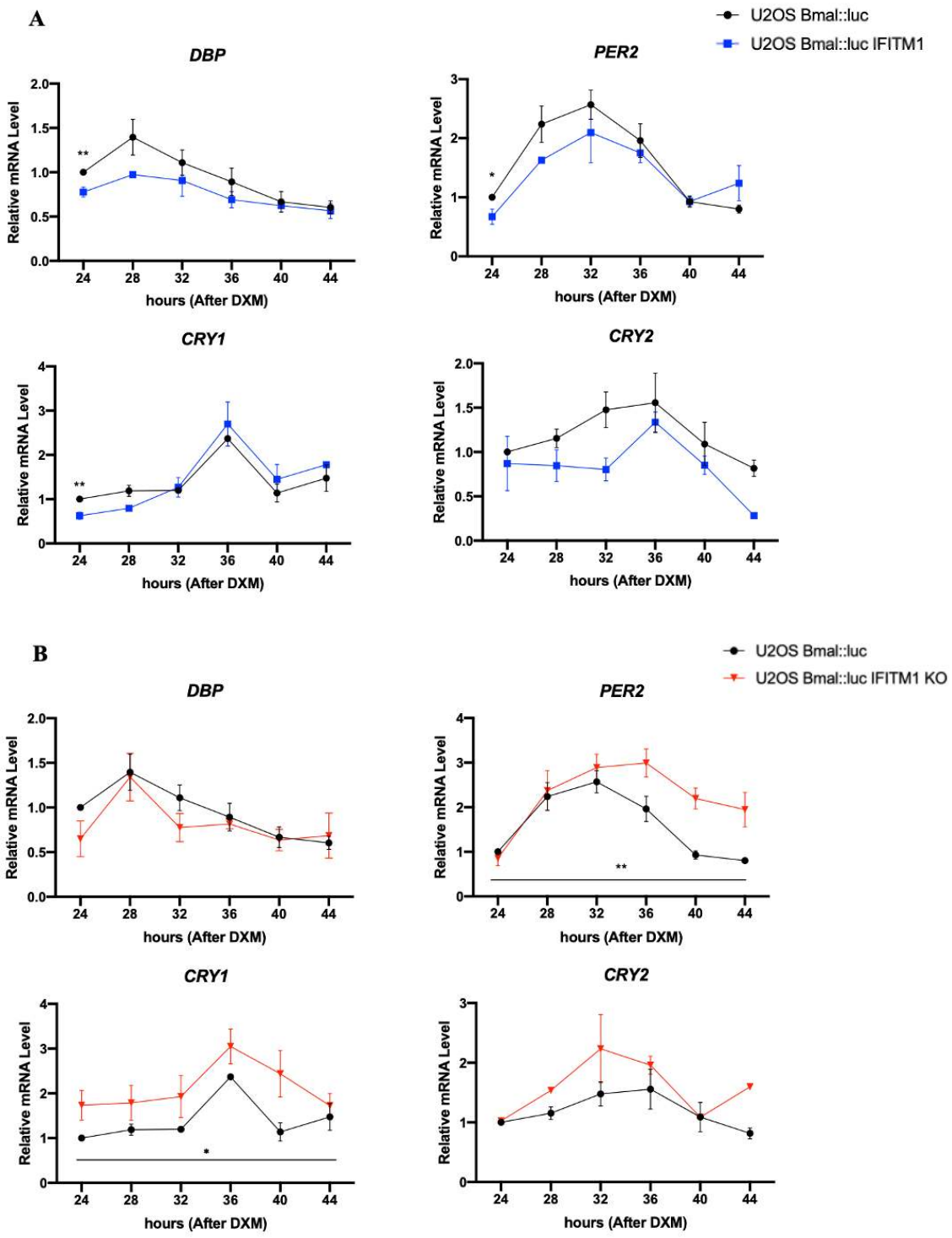

Figure 4. 12: The mRNA expressions of core clock genes are modulated when IFITM1 is overexpressed or knockout. Reverse-transcription-quantitative polymerase chain reaction (RT-qPCR) was performed for the *IFITM1* OE, KO, and WT U2-OS *Bmal1-dluc* cell lines which were synchronized with 0.1μM dexamethasone. After 24 h of dexamethasone, the samples were harvested every 4 hours at the indicated time. mRNA levels were normalized to RPLP0 levels. (A) *DBP*, *PER*, *CRY1*, and *CRY2* results of IFITM1 OE samples compared to WT, (B) results of IFITM1 KO samples compared to WT. While IFITM1 overexpression affects *DBP*, *CRY1,* and *PER2* levels at 24th h (student's t-test, *p-value <0.05; **p-value <0.01), *IFITM1* KO alters overall *CRY1* and

PER2 levels compared to WT (*p-value <0.05; **p-value <0.01 WT versus KO by two-way ANOVA). The expression level of genes was normalized according to the expression level of that gene at 24th h. Data represent the mean ± SEM, n=3 with duplicates.

4.8 IFITM1 is strongly upregulated by type I and type II IFNs through Poly(I: C) in induced *U2-OS Bmal1-dluc.*

To summarize my findings briefly, I have shown that IFITM1 and CRY1 specifically interact and colocalize in the nucleus. Notably, the terminal 20 amino acids in the C-terminal of CRY1 play a critical role. Moreover, the stability of CRY1 is increased due to the IFITM1-CRY1 interaction, and the negative arm is strengthened; thus, some clock output genes are downregulated.

Up to this point, I have primarily focused on the effect of IFITM1 gene expression on the core clock machinery. However, as we know, the major role of IFITM1 is to restrict virus entry to cells by altering membrane topology. How IFITM1-CRY1 interaction connects viral restriction to circadian clock alteration has not been elucidated until now. In order to assess the role of IFITM1 in this potential communication, I have approached this question from the immune system view this time. Here I have utilized Poly(I: C), which is a synthetic double-strand RNA analog, to investigate this association under pathogenic stress by stimulating viral infection.

Poly(I: C) is a chemical compound that is a synthetic double-strand RNA analog. Natural and synthetic analogs of double-stranded RNAs are eligible to induce type I interferons (IFN) and other cytokine production. It activates different antiviral pattern recognition receptors such as TLR3, RIG-I/MDA5, and PKR; in that way, it plays a role in inducing signaling through many inflammatory pathways, including NF-κB and IRF (Alexopoulou et al., 2001). Since IFITM1 was regulated by the expression of type I and type II IFNs, a rise in IFITM1 protein amount is expected after Poly(I: C) treatment (Zhao et al., 2014). High Molecular Weight Poly(I: C), which was used in this study, contains long strands of inosine poly(I) homopolymer annealed to strands of cytidine poly(C) homopolymer. The dose range of HMW Poly(I: C) was determined accordingly to the manufacturer's order. When 10 μg/mL Poly(I: C) HMW, the highest dose which is not toxic, was introduced into *U2-OS Bmal1-dluc* cells, I observed 30 times rise in the amount of IFITM1 protein compared to WT. Thus, I decided to use 10 μg/mL Poly(I: C) HMW as a working concentration for future experiments since the effective dose led to the

expression of IFITM1 at the highest level **(Figure 4. 13).** However, significant changes in the amounts of CRY1 and CRY2 could not be detected among the doses.

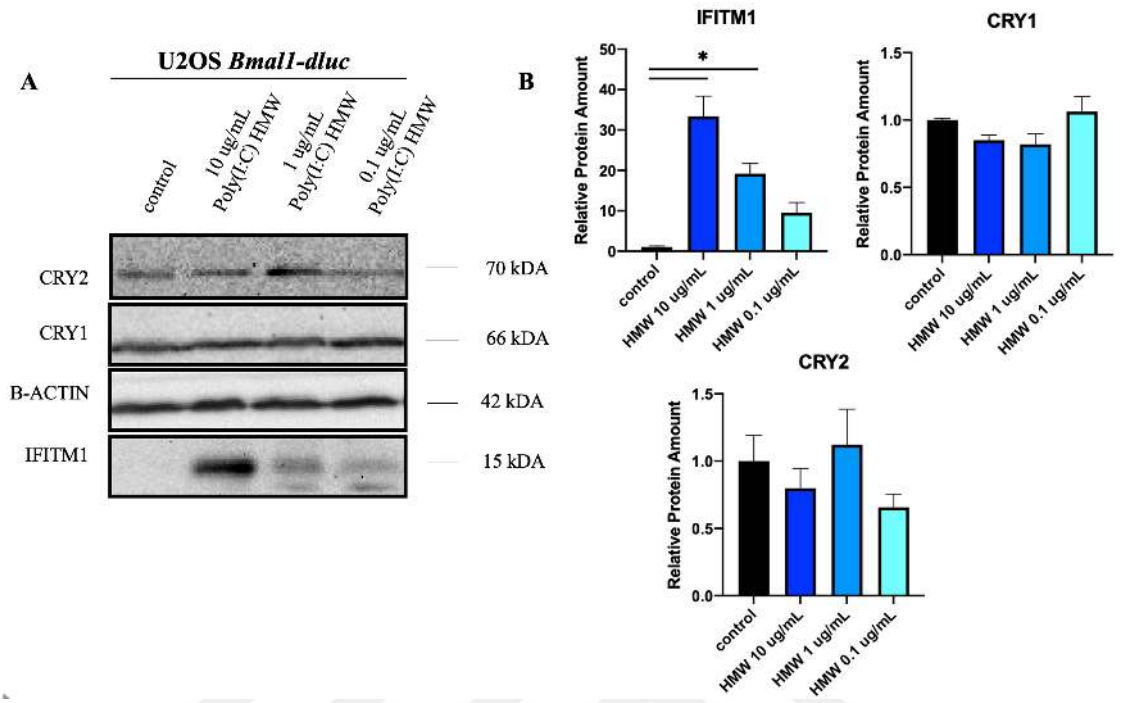

Figure 4. 13: Poly(I: C) induces the expression of IFITM1 significantly in *U2OS Bmal1-dluc.* (A) Poly(I: C) HMW mimics the viral stress in the cells, which leads to an increase in IFITM1 dose-dependent manner. This effect on the protein level was shown via western blotting. (B) The amount of the proteins was quantified compared to the control group. The amount of IFITM1 was significantly elevated after treatment of 10 µg/mL and 1 µg/mL Poly(I:C) HMW (student's t-test, *p-value <0.05; **p-value <0.01). Data represent mean ± SEM; n=3, independent experiments.

4.9 When the immune system is triggered via Poly(I: C), circadian oscillations are modulated.

All the data that I presented so far suggest IFITM1 specifically interacts with CRY1 and regulates its stability. It is known that the IFITM1 level increased in response to the virus through induces type I and II interferons (IFN) (Narayana et al., 2015; Zhao et al., 2014). I hypothesized that challenging U2-OS with Poly(I: C) induces type I interferons (IFN) and IFITM1 levels and, in turn, circadian rhythm. To test that, *IFITM1* knockout and WT *U2-OS Bmal1-dluc* were exposed to 10 µg/mL Poly(I: C) HMW treatment, while control groups were treated with only sterile endotoxin-free physiological water (NaCl 0.9%) for 7 days. In fact, the level of IFITM1 level was increased in response to Poly(I:

C) treatment in a dose-dependent manner (**Figure 4.13**). Expectedly (**Figure 4. 8 A**), the period of *IFITM1* knockout was lengthened, and the amplitude was dampened significantly compared to WT *U2OS Bmal1*-d*luc*. Cells treated with Poly(I: C) HMW exhibited a significant decrease in the period and enhancement in the amplitude, while *IFITM1* knockout cell lines did not display any circadian period changes in response to Poly(I: C) HMW. A severe rise in amplitude was observed after Poly(I: C) HMW treatment in *IFITM1* KO *U2-OS Bmal1-dluc*.

After Poly(I: C) HMW treatment in *U2-OS Bmal1-dluc* elevated IFITM1 level can stabilize CRY1 more. This shortening in the period of *U2-OS Bmal1-dluc* can be associated with increased CRY1 stability, as observed from studies where CRY1 stability was enhanced using small molecules (Kavakli, Gul, et al., 2022; Oshima et al., 2015). On the other hand, a significant increase in amplitude at KO cell lines compared to non-treated ones may suggest an alternative role for IFITM1 that should be investigated further.

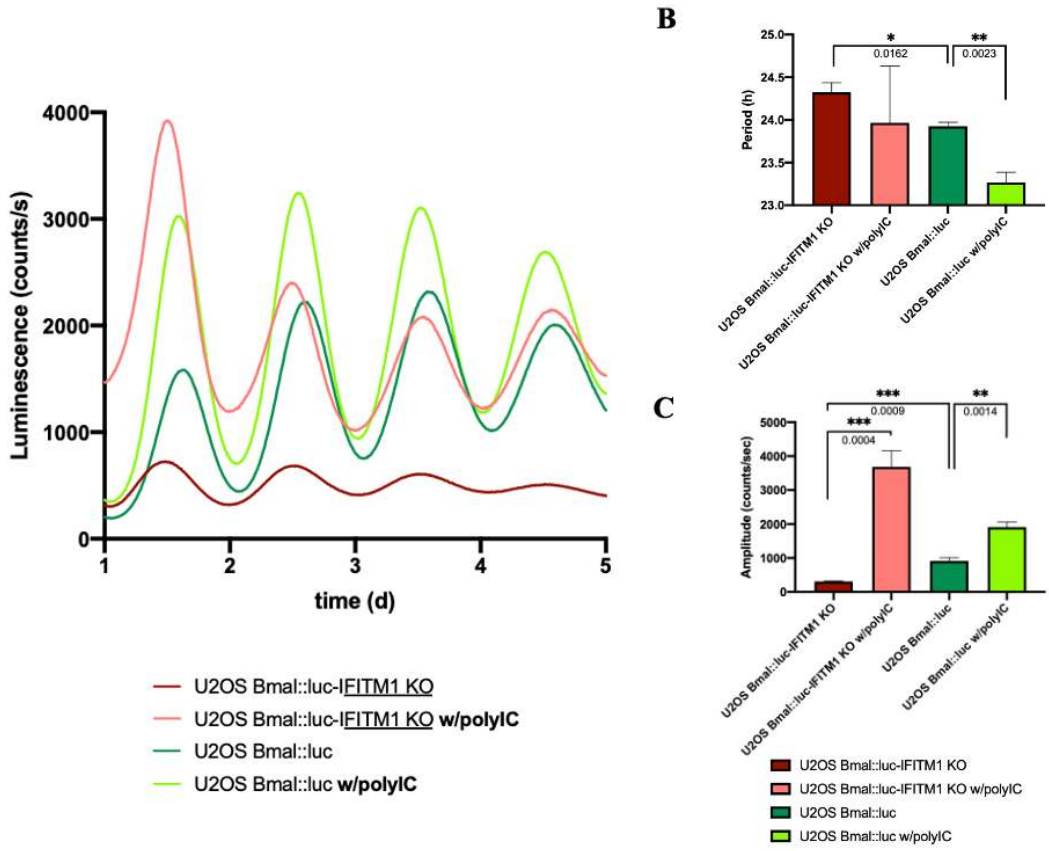

Figure 4. 14: Circadian phenotype was altered because of immune response stimulated by Poly(I: C) (A) Continuous monitoring of circadian oscillations in HMW Poly(I: C) treated and non-treated *IFITM1* KO and WT *U2-OS Bmal1-dluc* by using Lumicycle, Actimetrics. (B) Period and (C) amplitude results from circadian oscillations. After seeding, the cells were synchronized with 0.1 µM dexamethasone and treated with 10 ug/mL HMW Poly(I: C). Then, dishes were replaced in Lumicycle to collect data of luminescence signals for 5-7 days each 10 minutes. The data recorded on the first day were excluded. (student's t-test, *p-value <0.05; **p-value <0.01; ***p-value <0.01). Data represent mean ± SEM; n=3, independent experiments.

4.10 When the immune system is triggered via Poly(I: C), mRNA expression of core clock genes is changed.

After evaluating the physiological response in *IFITM1* KO and WT *U2-OS Bmal1-dluc*, to understand the reason for the changes in circadian phenotype and core clock genes, I performed RT-qPCR in unsynchronized Poly(I: C) treated and non-treated *IFITM1,* OE, KO, and WT *U2-OS Bmal1-dluc.* After Poly(I: C) treatment, *CRY1* transcription was significantly increased in the KO cells compared to non-treated ones. In agreement with this, a decline in *DBP* transcription was observed in Poly(I: C) treated

IFITM1 KO *U-2OS Bmal1-dluc* cells. These results suggest that IFITM stabilizes the level CRY1 and, therefore, causes the reduction of DBP.

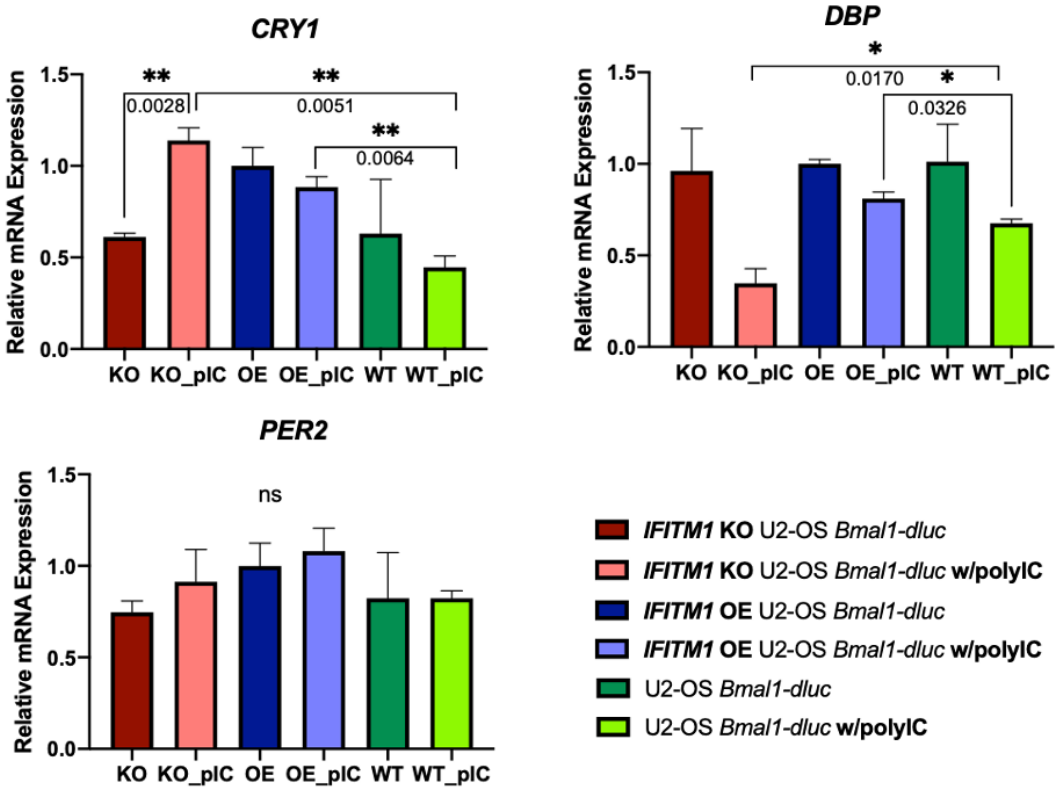

Figure 4. 15: The mRNA expressions of core clock genes are modulated when viral stress was mimicked via Poly(I: C) in *IFITM1* OE, KO, and WT U2-OS *Bmal1-dluc* cell lines. Reverse-transcription-quantitative polymerase chain reaction (RT-qPCR) was performed for the *IFITM1* OE, KO, and WT U2-OS *Bmal1-dluc* cell lines which were unsynchronized. After 24 h of seeding, the samples were harvested, and mRNA was isolated and used to synthesize cDNA. mRNA levels were normalized to RPLP0 levels. *DBP*, *PER2*, and *CRY1* results of *IFITM1* OE and KO samples compared to WT were represented. (student's t-test, *p-value <0.05; **p-value <0.01).The expression level of genes was normalized according to the expression level of that gene of WT. Data represent the mean ± SEM, n=3 with duplicates.

CHAPTER 5:
DISCUSSION

The circadian rhythm regulates gene expression at transcriptional and post-transcriptional levels in mammals. For this reason, any disruption in the biological clock can cause a significant increase in susceptibility to diseases such as cancer and immune disorders (Haspel et al., 2020; Sulli et al., 2019). Hence, discovering novel circadian clock components carries the considerable potential to illuminate the mechanisms underlying circadian clock-regulated immune physiology and to suggest therapeutic strategies. In this thesis, I have presented direct evidence regarding IFITM1 as a circadian clock candidate by identifying its clock-like characteristics. In this sense, I have shown that IFITM1 and CRY1 interact physically in the nucleus, but not CRY2, contributing to the regulation of the core-clock machinery. The effect of IFITM1 on CRY1 stability is also likely to be significant for controlling circadian oscillation at the cellular level and possibly play a role in pathogenic stress-induced circadian alteration in the organism.

IFITM1 is a member of the interferon-inducible transmembrane protein family that could restrict the entrance of several BSL3 and BSL4 levels pathogenic viruses such as Influenza A Virus (IAV), Dengue Virus (DENV), West Nile Virus (WNV), Zika Virus (ZIKV), Ebola Virus (EBOV), Marburg Virus (MARV), Rift Valley Fever Virus (RVFV), Hantaan Virus (HTNV), Hepatitis C Virus (HCV), Human Immunodeficiency Virus (HIV) and Severe Acute Respiratory Syndrome Coronavirus (SARS-CoV) (Yanez et al., 2020). Although IFITM1 is expressed ubiquitously in human tissues without interferon induction, it can be up-regulated by different types of interferons (Zhao et al., 2014). Even though the mechanism of IFITM1 inhibition of viral fusion and cell entrance has not been elucidated yet, IFITM1 matters as a novel circadian clock component (Anafi et al., 2014) in discovering a previously unexplored link between the biological clock and the immune system.

In this study, I further characterized the function of IFITM1 as a novel circadian clock component (Kulkoyluoglu, 2015), which performs its role by interacting with the core clock protein, CRY1. Sequence alignment studies demonstrate that CRYs have an intrinsically disordered region (IDR) along their C-terminal domains that enable them to interact with various proteins, promoting tissue and organism-dependent functions (Kavakli et al., 2017). Our study demonstrated that IFITM1 interacts with the C-terminal of CRY1 in the nucleus **(Figure 4. 9)**. This functional physical interaction was supported by a co-IP assay in *IFITM1* OE and KO U2-OS *Bmal1-dluc* **(Appendix A.2)**. Especially last 20 amino acids in the C-terminal tail of CRY1 are critical in this interaction, as evident from BiFC results **(Figure 4. 9)**. As a result of this physical interaction, when the IFITM1 level is upregulated, the stability of CRY1 is increased **(Figure 4. 11)** as transcription of clock genes are downregulated **(Figure 4. 12)**. Despite increased stability of CRY1, period shortening was observed in the cells when IFITM1 level is elevated under Poly(I: C) induced pathogenic stress **(Figure 4. 14)**. Altogether, the results suggest that IFITM1 can play an essential role in the regulation of circadian rhythm system by modulating CRY1 levels under pathogenic stress.

Previous studies showed that IFITM1 was mainly distributed to the plasma membrane and co-localized to early endo-lysosomal bodies in the cytoplasm, even though the precise subcellular localization of IFITM1 remains ambiguous (Sun et al., 2020; Yanez et al., 2020; Zhao et al., 2014). Here, interestingly, I observed that IFITM1 was localized to the nuclear fraction when it was overexpressed (**Figure 4. 10**). However, I could not observe a significant increase in the CRY1 level in the nucleus based on its interaction with IFITM1 when IFITM1 was overexpressed in the total cell lysate, despite a notable decrease in the KO U2-OS *Bmal1:dluc* (**Figure 4. 10**). A complete understanding of this phenomena will possibly require a detailed time-resolved investigation on synchronized samples to study the distribution of both proteins to nuclear and cytoplasmic fractions. Indeed, it can be hypothesized that minor immune alterations may underestimate large-scale changes observed at the cellular level. *Ifitm1*$^{-/-}$ mice models subjected to viral infection, on the other hand, would allow us to demonstrate these dynamic changes at the physiological level.

Notably, our results showed that IFITM1 and CRY1 interact in the nucleus. This means that a transmembrane protein, IFITM1, could enter the nucleus due to its

interaction with a core clock repressor, CRY1. Recent studies showed that about 10% of eukaryotic transmembrane proteins could be located on the nuclear membrane even if their localization in the nucleus is in case of a dispute (Mudumbi et al., 2020). Because of the mechanistic challenges considering intranuclear localization of a transmembrane protein, transmembrane proteins having multiple transmembrane domains are rarely found in the nucleus for a good reason (Huang et al., 2021). This reason might be relieving the tension derived from pathogenic stress during a viral attack by modulating the stability of CRY1 and enforcing the negative feedback loop by retaining it in the nucleus (**Figure 5. 1**).

A significant increase in the half-life of the CRY1 to approximately 16 hours from 4.5-5 hours is a result of the interaction between IFITM1 and CRY1 through the CRY1 C terminus **(Figure 4. 11)**. As a result of this interaction, communication of CRY1 with FBXL3 through the coiled-coil helix in the C-terminus might be modulated in the nucleus. Hence, the CRY1 becomes more stable. In accordance with this, an increase in period length should have been present because of reduced interaction between CRY1 and FBXL3 (Hirota et al., 2012). However, after Poly(I: C) treatment in WT U2-OS *Bmal1:dluc* cells, elevated IFITM1 caused period shortening **(Figure 4. 14)**. This might be the result of not only increased IFITM1 levels but also the cumulative response of other Poly(I: C) induced genes. Alternatively, this might indicate other mechanisms for IFITM1-dependent period alterations.

Period determination in the mammalian clock is affected by the turnover rate of transcription factors regulating the negative arm of the core clock TTFL, CRY, and PER (Yoo et al., 2013). Period lengthening in *IFITM1* KO U2-OS *Bmal1:dluc* cells and, conversely, shortening in Poly(I: C) treated WT U2-OS *Bmal1:dluc* can be explained by several regulation mechanisms. Thus, IFITM1 probably regulates the circadian period not only by altering the rate of CRY1 degradation but also through some other undiscovered processes intervened by CRY, as suggested in period-shortening molecules (Oshima et al., 2015). In essence, IFITM1-CRY1 mediated period alterations under pathogenic stress have to be studied further to illuminate other potential key players in this interesting phenomenon.

There is a direct effect of immune response elements on the central circadian clock at the molecular level and affects the rhythmicity. IFN- γ treated mice SCN cells exhibit reduced amplitude based on *Per1*-luciferase activity (Kwak et al., 2008). IFITM1 is upregulated by IFN-γ (Yang et al., 2007). In line with these findings, we observed period shortening and severely reduced amplitude in U2-OS *Bmal1-dluc* overexpressing *IFITM1* **(Figure 4. 8 B).** The reason for this severe dampening at overexpressing cells might be related to metabolic toxicity and cell death induced by the expression of IFITM1 protein (Park et al., 2016) or inflammatory mediators (Yang et al., 2007). However, the effect of bacterial and viral products directly and indirectly on the molecular clock by inflammatory mediators should be investigated more to understand the underlying mechanism.

In addition to alterations in circadian rhythmicity derived from inflammation and pathogenic stress, *in vivo* and *in vitro* studies show modulations in the expression of core clock genes after applications of several immune stimulators (Okada et al., 2008). TNFα application diminish the expression of *Dbp* in mice SCN (Cavadini et al., 2007). Peripheral LPS injection into rats cause suppression of *Per2* and *Dbp* at mRNA level (Okada et al., 2008). In both mouse liver and hepatocytes, IFN-α administration downregulates the *Per1* and *Dbp* based on qPCR (Koyanagi & Ohdo, 2002). All these findings from previous studies support our results of a significant reduction in the expression level of *PER2*, *DBP,* and *CRY1,* in U2-OS *Bmal1-dluc* cell lines overexpressing *IFITM1* **(Figure 4. 12 A)**.

With the application of molecules exhibiting pathogen-associated molecules such as Poly(I: C), a TLR3 agonist, into splenocytes, a significant decrease in the levels of *Per2, Bmal1, Rev-erbα, and Dbp* in ZT1 (but not ZT13) were demonstrated (Silver, 2017). In the light of this finding, our results show a decreasing trend in the mRNA level of *DBP* in *IFITM1* OE, KO, and WT U2-OS *Bmal1-dluc* cells after Poly(I: C) treatment are expected **(Figure 4. 15)**. However, there was a significant increase in the *CRY1* level after application in *IFITM1* KO U2-OS *Bmal1-dluc,* whereas, in OE and WT cell lines, a reverse effect was observed. This could be explained by two potential mechanisms. First, because CRYs also operate as anti-inflammatory proteins, they can regulate the intensity of immune responses by dampening several cytokines (Hergenhan et al., 2020). In the absence of IFITM1, CRY1 might try to compensate for the anti-inflammatory function of

IFITM1 by raising its mRNA level. Second, this may indicate other intertwined mechanisms between circadian rhythm and the immune system aside from IFITM1. On the other hand, the application time of Poly(I: C) can affect the TLR pathways, which also regulate the IFITM levels; thus, the time of responsiveness could cause distinctive influences on the different time points on the molecular clock (Keller et al., 2009). The reason why significant changes at the *CRY1* and *PER2 levels* could not be observed in WT and OE U2-OS *Bmal1-dluc* cells after Poly(I: C) treatment can be explained by this phenomenon. To eliminate the alterations in the expression level masked because of time-dependent variations and to bare the effect of Poly(I: C), the core clock expression should be evaluated in the synchronized cells with dexamethasone.

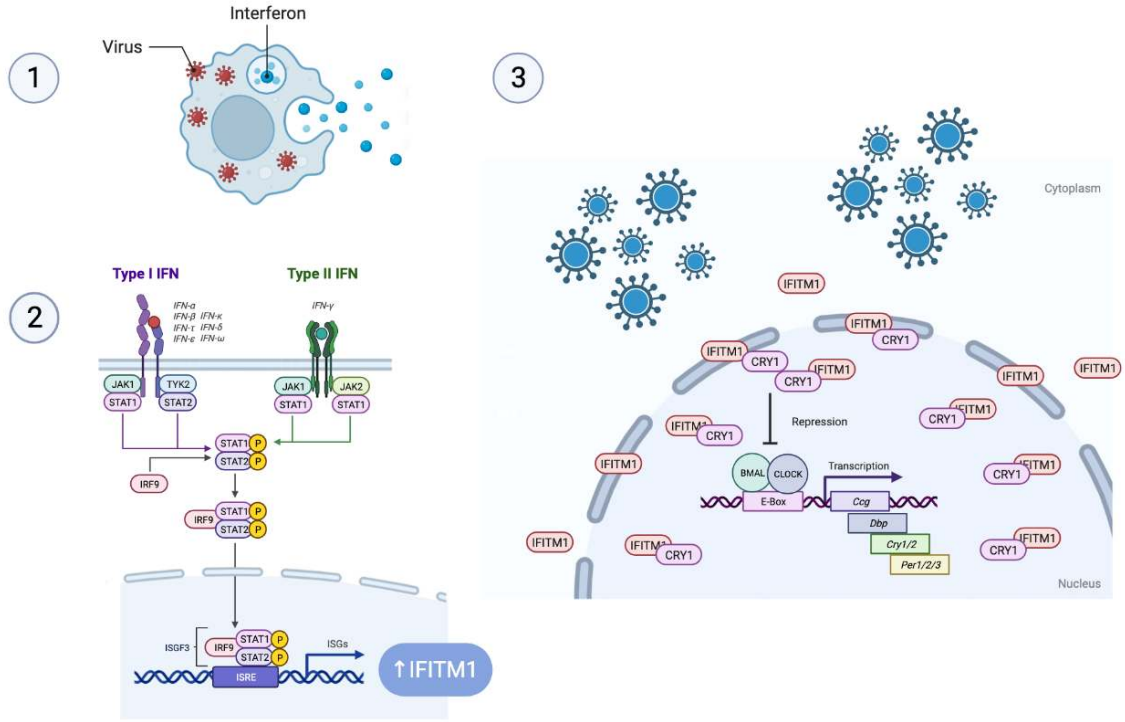

Figure 5. 1: Schematic representation of IFITM1 and CRY1 communication under pathogenic stress. After a viral attack on the organism, the Type I and II interferons are released (1), and they are recognized by receptors initiating cell signaling through JAK/STAT pathways. In that way, transcription of IFITM1, which is one of the interferons stimulated genes, is initiated (2). Elevated IFITM1 levels as a response to pathogenic stress caused increased stability of CRY1 and enforced the negative feedback loop (3). The schema was illustrated via BioRender.

In conclusion, we contribute to understanding molecular clock mechanisms more comprehensively by identifying the function of a circadian clock candidate, *IFITM1*. Moreover, we present an insight into how the biological clock is affected by viral stress for the first time at the molecular level by focusing on the interaction of IFITM1 and CRY1 that occurred in the nucleus but not CRY2. In addition to the cycloheximide assay,

increased stability of CRY1 specifically through this association was demonstrated. Under pathogenic stress, rising at IFITM1 level trigger increased stability of CRY1 in the nucleus and strengthen the effect of CRY1 on the negative arm of the transcription and translation feedback loop. In summary, our results attribute a new role for IFITM1 as a clock component that modulates the circadian rhythm by regulating CRY1 stability and indicates potential mechanisms for circadian clock-immune system communication. The details of this communication will be necessary to investigate more thoroughly especially targeting the alterations derived from IFITM1-CRY1 communication on the immune system elements with *in vivo* and *in vitro* studies. Through this project, a progression has been made for the study of IFITM1 and the treatment of immune system-circadian rhythm-related disease.

BIBLIOGRAPHY

Alexopoulou, L., Holt, A. C., Medzhitov, R., & Flavell, R. A. (2001). Recognition of double-stranded RNA and activation of NF-κB by Toll-like receptor 3. *Nature*, *413*(6857), 732-738. https://doi.org/10.1038/35099560

Anafi, R. C., Lee, Y., Sato, T. K., Venkataraman, A., Ramanathan, C., Kavakli, I. H., Hughes, M. E., Baggs, J. E., Growe, J., Liu, A. C., Kim, J., & Hogenesch, J. B. (2014). Machine learning helps identify CHRONO as a circadian clock component. *PLoS Biol*, *12*(4), e1001840. https://doi.org/10.1371/journal.pbio.1001840

Aschoff, J. (1960). Exogenous and endogenous components in circadian rhythms. Cold Spring Harbor symposia on quantitative biology,

Aschoff, J. (1965). Circadian rhythms in man: a self-sustained oscillator with an inherent frequency underlies human 24-hour periodicity. *Science*, *148*(3676), 1427-1432.

Asher, G., Reinke, H., Altmeyer, M., Gutierrez-Arcelus, M., Hottiger, M. O., & Schibler, U. (2010). Poly(ADP-Ribose) Polymerase 1 Participates in the Phase Entrainment of Circadian Clocks to Feeding. *Cell*, *142*(6), 943-953. https://doi.org/https://doi.org/10.1016/j.cell.2010.08.016

Bedford, J. G., O'Keeffe, M., Reading, P. C., & Wakim, L. M. (2019). Rapid interferon independent expression of IFITM3 following T cell activation protects cells from influenza virus infection. *PLoS One*, *14*(1), e0210132. https://doi.org/10.1371/journal.pone.0210132

Bellet, M. M., Zocchi, L., & Sassone-Corsi, P. (2012). The RelB subunit of NFκB acts as a negative regulator of circadian gene expression. *Cell cycle (Georgetown, Tex.)*, *11*(17), 3304-3311. https://doi.org/10.4161/cc.21669

Brass, A. L., Huang, I. C., Benita, Y., John, S. P., Krishnan, M. N., Feeley, E. M., Ryan, B. J., Weyer, J. L., van der Weyden, L., Fikrig, E., Adams, D. J., Xavier, R. J., Farzan, M., & Elledge, S. J. (2009). The IFITM proteins mediate cellular resistance to influenza A H1N1 virus, West Nile virus, and dengue virus. *Cell*, *139*(7), 1243-1254. https://doi.org/10.1016/j.cell.2009.12.017

Bresser, K., Dijkgraaf, F. E., Pritchard, C. E. J., Huijbers, I. J., Song, J.-Y., Rohr, J. C., Scheeren, F. A., & Schumacher, T. N. (2020). A mouse model that is

immunologically tolerant to reporter and modifier proteins. *Communications Biology*, *3*(1), 273. https://doi.org/10.1038/s42003-020-0979-0

Brown, S. A., Zumbrunn, G., Fleury-Olela, F., Preitner, N., & Schibler, U. (2002). Rhythms of mammalian body temperature can sustain peripheral circadian clocks. *Curr Biol*, *12*(18), 1574-1583. https://doi.org/10.1016/s0960-9822(02)01145-4

Busino, L., Bassermann, F., Maiolica, A., Lee, C., Nolan, P. M., Godinho, S. I., Draetta, G. F., & Pagano, M. (2007). SCFFbxl3 controls the oscillation of the circadian clock by directing the degradation of cryptochrome proteins. *Science*, *316*(5826), 900-904.

Bünning, E. (1960). Opening address: biological clocks. Cold Spring Harbor Symposia on Quantitative Biology,

Bzhalava, D., Ekström, J., Lysholm, F., Hultin, E., Faust, H., Persson, B., Lehtinen, M., de Villiers, E.-M., & Dillner, J. (2012). Phylogenetically diverse TT virus viremia among pregnant women. *Virology*, *432*(2), 427-434.

Cal-Kayitmazbatir, S., Kulkoyluoglu-Cotul, E., Growe, J., Selby, C. P., Rhoades, S. D., Malik, D., Oner, H., Asimgil, H., Francey, L. J., Sancar, A., Kruger, W. D., Hogenesch, J. B., Weljie, A., Anafi, R. C., & Kavakli, I. H. (2021). CRY1-CBS binding regulates circadian clock function and metabolism. *FEBS J*, *288*(2), 614-639. https://doi.org/10.1111/febs.15360

Cavadini, G., Petrzilka, S., Kohler, P., Jud, C., Tobler, I., Birchler, T., & Fontana, A. (2007). TNF-alpha suppresses the expression of clock genes by interfering with E-box-mediated transcription. *Proc Natl Acad Sci U S A*, *104*(31), 12843-12848. https://doi.org/10.1073/pnas.0701466104

Cuninkova, L., & Brown, S. A. (2008). Peripheral Circadian Oscillators. *Annals of the New York Academy of Sciences*, *1129*(1), 358-370. https://doi.org/https://doi.org/10.1196/annals.1417.005

Curtis, A. M., Bellet, M. M., Sassone-Corsi, P., & O'Neill, L. A. (2014). Circadian clock proteins and immunity. *Immunity*, *40*(2), 178-186. https://doi.org/10.1016/j.immuni.2014.02.002

Daan, S. (2000). The Colin S. Pittendrigh Lecture. Colin Pittendrigh, Jürgen Aschoff, and the natural entrainment of circadian systems. *J Biol Rhythms*, *15*(3), 195-207. https://doi.org/10.1177/074873040001500301

Damiola, F., Le Minh, N., Preitner, N., Kornmann, B., Fleury-Olela, F., & Schibler, U. (2000). Restricted feeding uncouples circadian oscillators in peripheral tissues

from the central pacemaker in the suprachiasmatic nucleus. *Genes Dev*, *14*(23), 2950-2961. https://doi.org/10.1101/gad.183500

de Mairan, J.-J. (1729). Observation botanique. *Histoire de l'Académie Royale des Sciences Paris*.

Druzd, D., Matveeva, O., Ince, L., Harrison, U., He, W., Schmal, C., Herzel, H., Tsang, A. H., Kawakami, N., & Leliavski, A. (2017). Lymphocyte circadian clocks control lymph node trafficking and adaptive immune responses. *Immunity*, *46*(1), 120-132.

Dunlap, J. C., Loros, J. J., & DeCoursey, P. J. (2004). *Chronobiology: biological timekeeping*. Sinauer Associates.

Eckel-Mahan, K. L., & Storm, D. R. (2009). Circadian rhythms and memory: not so simple as cogs and gears. *EMBO Rep*, *10*(6), 584-591. https://doi.org/10.1038/embor.2009.123

Evans, J. A., & Davidson, A. J. (2013). Chapter Ten - Health Consequences of Circadian Disruption in Humans and Animal Models. In M. U. Gillette (Ed.), *Progress in Molecular Biology and Translational Science* (Vol. 119, pp. 283-323). Academic Press. https://doi.org/https://doi.org/10.1016/B978-0-12-396971-2.00010-5

Fortier, E. E., Rooney, J., Dardente, H., Hardy, M.-P., Labrecque, N., & Cermakian, N. (2011). Circadian variation of the response of T cells to antigen. *The Journal of Immunology*, *187*(12), 6291-6300.

Franken, P., & Dijk, D. J. (2009). Circadian clock genes and sleep homeostasis. *Eur J Neurosci*, *29*(9), 1820-1829. https://doi.org/10.1111/j.1460-9568.2009.06723.x

Friedman, R. L., Manly, S. P., McMahon, M., Kerr, I. M., & Stark, G. R. (1984). Transcriptional and posttranscriptional regulation of interferon-induced gene expression in human cells. *Cell*, *38*(3), 745-755. https://doi.org/10.1016/0092-8674(84)90270-8

Fuhr, L., Abreu, M., Pett, P., & Relogio, A. (2015). Circadian systems biology: When time matters. *Comput Struct Biotechnol J*, *13*, 417-426. https://doi.org/10.1016/j.csbj.2015.07.001

Gachon, F., Nagoshi, E., Brown, S. A., Ripperger, J., & Schibler, U. (2004). The mammalian circadian timing system: from gene expression to physiology. *Chromosoma*, *113*(3), 103-112.

Gamble, K. L., Berry, R., Frank, S. J., & Young, M. E. (2014). Circadian clock control of endocrine factors. *Nature reviews. Endocrinology*, *10*(8), 466-475. https://doi.org/10.1038/nrendo.2014.78

Gauger, M. A., & Sancar, A. (2005). Cryptochrome, circadian cycle, cell cycle checkpoints, and cancer. *Cancer research*, *65*(15), 6828-6834.

Haspel, J. A., Anafi, R., Brown, M. K., Cermakian, N., Depner, C., Desplats, P., Gelman, A. E., Haack, M., Jelic, S., Kim, B. S., Laposky, A. D., Lee, Y. C., Mongodin, E., Prather, A. A., Prendergast, B. J., Reardon, C., Shaw, A. C., Sengupta, S., Szentirmai, É., Thakkar, M., Walker, W. E., & Solt, L. A. (2020). Perfect timing: circadian rhythms, sleep, and immunity - an NIH workshop summary. *JCI insight*, *5*(1), e131487. https://doi.org/10.1172/jci.insight.131487

Henrici, R. C., Pecen, T. J., Johnston, J. L., & Tan, S. (2017). The pPSU plasmids for generating DNA molecular weight markers. *Scientific reports*, *7*(1), 1-9.

Hergenhan, S., Holtkamp, S., & Scheiermann, C. (2020). Molecular Interactions Between Components of the Circadian Clock and the Immune System. *J Mol Biol*, *432*(12), 3700-3713. https://doi.org/10.1016/j.jmb.2019.12.044

Herzog, E. D., Hermanstyne, T., Smyllie, N. J., & Hastings, M. H. (2017). Regulating the Suprachiasmatic Nucleus (SCN) Circadian Clockwork: Interplay between Cell-Autonomous and Circuit-Level Mechanisms. *Cold Spring Harbor perspectives in biology*, *9*(1), a027706. https://doi.org/10.1101/cshperspect.a027706

Hirano, A., Fu, Y. H., & Ptacek, L. J. (2016). The intricate dance of post-translational modifications in the rhythm of life. *Nat Struct Mol Biol*, *23*(12), 1053-1060. https://doi.org/10.1038/nsmb.3326

Hirano, A., Yumimoto, K., Tsunematsu, R., Matsumoto, M., Oyama, M., Kozuka-Hata, H., Nakagawa, T., Lanjakornsiripan, D., Nakayama, K. I., & Fukada, Y. (2013). FBXL21 regulates oscillation of the circadian clock through ubiquitination and stabilization of cryptochromes. *Cell*, *152*(5), 1106-1118. https://doi.org/10.1016/j.cell.2013.01.054

Hirota, T., Lee, J. W., John, P. C. S., Sawa, M., Iwaisako, K., Noguchi, T., Pongsawakul, P. Y., Sonntag, T., Welsh, D. K., Brenner, D. A., Doyle, F. J., Schultz, P. G., & Kay, S. A. (2012). Identification of Small Molecule Activators of Cryptochrome. *Science*, *337*(6098), 1094-1097. https://doi.org/doi:10.1126/science.1223710

Hogenesch, J. B., Chan, W. K., Jackiw, V. H., Brown, R. C., Gu, Y. Z., Pray-Grant, M., Perdew, G. H., & Bradfield, C. A. (1997). Characterization of a subset of the

basic-helix-loop-helix-PAS superfamily that interacts with components of the dioxin signaling pathway. *J Biol Chem*, *272*(13), 8581-8593. https://doi.org/10.1074/jbc.272.13.8581

Horst, G. T. J. v. d., Muijtjens, M., Kobayashi, K., Takano, R., Kanno, S.-i., Takao, M., Wit, J. d., Verkerk, A., Eker, A. P. M., Leenen, D. v., Buijs, R., Bootsma, D., Hoeijmakers, J. H. J., & Yasui, A. (1999). Mammalian Cry1 and Cry2 are essential for maintenance of circadian rhythms. *Nature*, *398*(6728), 627-630. https://doi.org/10.1038/19323

Huang, Y., Li, J., Du, W., Li, S., Li, Y., Qu, H., Xv, J., Yu, L., Zhu, R., & Wang, H. (2021). Nuclear translocation of the 4-pass transmembrane protein Tspan8. *Cell Res*, *31*(11), 1218-1221. https://doi.org/10.1038/s41422-021-00522-9

Janse van Rensburg, D. C., Jansen van Rensburg, A., Fowler, P. M., Bender, A. M., Stevens, D., Sullivan, K. O., Fullagar, H. H. K., Alonso, J. M., Biggins, M., Claassen-Smithers, A., Collins, R., Dohi, M., Driller, M. W., Dunican, I. C., Gupta, L., Halson, S. L., Lastella, M., Miles, K. H., Nedelec, M., Page, T., Roach, G., Sargent, C., Singh, M., Vincent, G. E., Vitale, J. A., & Botha, T. (2021). Managing Travel Fatigue and Jet Lag in Athletes: A Review and Consensus Statement. *Sports Med*, *51*(10), 2029-2050. https://doi.org/10.1007/s40279-021-01502-0

Kavakli, I. H., Baris, I., Tardu, M., Gül, Ş., Öner, H., Çal, S., Bulut, S., Yarparvar, D., Berkel, Ç., Ustaoğlu, P., & Aydın, C. (2017). The Photolyase/Cryptochrome Family of Proteins as DNA Repair Enzymes and Transcriptional Repressors. *Photochemistry and Photobiology*, *93*(1), 93-103. https://doi.org/https://doi.org/10.1111/php.12669

Kavakli, I. H., Gul, S., & Turkay, M. (2022). Identification of novel small molecules targeting core clock proteins to regulate circadian rhythm. *Current Opinion in Chemical Engineering*, *35*. https://doi.org/10.1016/j.coche.2021.100730

Kavakli, I. H., Ozturk, N., & Baris, I. (2022). Protein interaction networks of the mammalian core clock proteins.

Kavakli, I. H., & Sancar, A. (2002). Circadian photoreception in humans and mice. *Mol Interv*, *2*(8), 484-492. https://doi.org/10.1124/mi.2.8.484

Keller, M., Mazuch, J., Abraham, U., Eom, G. D., Herzog, E. D., Volk, H.-D., Kramer, A., & Maier, B. (2009). A circadian clock in macrophages controls inflammatory

immune responses. *Proceedings of the National Academy of Sciences*, *106*(50), 21407-21412.

Ko, C. H., Yamada, Y. R., Welsh, D. K., Buhr, E. D., Liu, A. C., Zhang, E. E., Ralph, M. R., Kay, S. A., Forger, D. B., & Takahashi, J. S. (2010). Emergence of noise-induced oscillations in the central circadian pacemaker. *PLoS biology*, *8*(10), e1000513.

Kodama, Y., & Hu, C.-D. (2012). Bimolecular fluorescence complementation (BiFC): A 5-year update and future perspectives. *BioTechniques*, *53*(5), 285-298. https://doi.org/10.2144/000113943

Kofuji, P., Mure, L. S., Massman, L. J., Purrier, N., Panda, S., & Engeland, W. C. (2016). Intrinsically Photosensitive Retinal Ganglion Cells (ipRGCs) Are Necessary for Light Entrainment of Peripheral Clocks. *PLoS One*, *11*(12), e0168651. https://doi.org/10.1371/journal.pone.0168651

Konopka, R. J., & Benzer, S. (1971). Clock Mutants of Drosophila melanogaster. *Proceedings of the National Academy of Sciences*, *68*(9), 2112-2116. https://doi.org/doi:10.1073/pnas.68.9.2112

Koyanagi, S., & Ohdo, S. (2002). Alteration of intrinsic biological rhythms during interferon treatment and its possible mechanism. *Mol Pharmacol*, *62*(6), 1393-1399. https://doi.org/10.1124/mol.62.6.1393

Kuhlman, S. J., Craig, L. M., & Duffy, J. F. (2018). Introduction to Chronobiology. *Cold Spring Harb Perspect Biol*, *10*(9). https://doi.org/10.1101/cshperspect.a033613

Kulkoyluoglu, E. (2015). *Interferon Induced Transmembrane Protein 1 as a Candidate Clock Regulator Gene*

Koç University].

Kume, K., Zylka, M. J., Sriram, S., Shearman, L. P., Weaver, D. R., Jin, X., Maywood, E. S., Hastings, M. H., & Reppert, S. M. (1999). mCRY1 and mCRY2 are essential components of the negative limb of the circadian clock feedback loop. *Cell*, *98*(2), 193-205.

Kwak, Y., Lundkvist, G. B., Brask, J., Davidson, A., Menaker, M., Kristensson, K., & Block, G. D. (2008). Interferon-gamma alters electrical activity and clock gene expression in suprachiasmatic nucleus neurons. *J Biol Rhythms*, *23*(2), 150-159. https://doi.org/10.1177/0748730407313355

Kyriacou, C. P., & Hastings, M. H. (2010). Circadian clocks: genes, sleep, and cognition. *Trends Cogn Sci*, *14*(6), 259-267. https://doi.org/10.1016/j.tics.2010.03.007

Lamont, E. W., & Amir, S. (2017). Circadian and Ultradian Clocks/Rhythms. In *Encyclopedia of Behavioral Neuroscience, 2nd edition* (pp. 746-751). https://doi.org/10.1016/b978-0-12-809324-5.00283-2

Liao, Y., Goraya, M. U., Yuan, X., Zhang, B., Chiu, S. H., & Chen, J. L. (2019). Functional Involvement of Interferon-Inducible Transmembrane Proteins in Antiviral Immunity. *Front Microbiol*, *10*, 1097. https://doi.org/10.3389/fmicb.2019.01097

Liu, C., Weaver, D. R., Strogatz, S. H., & Reppert, S. M. (1997). Cellular construction of a circadian clock: period determination in the suprachiasmatic nuclei. *Cell*, *91*(6), 855-860.

Lloyd, D., & Murray, D. B. (2005). Ultradian metronome: timekeeper for orchestration of cellular coherence. *Trends in biochemical sciences*, *30*(7), 373-377. https://www.sciencedirect.com/science/article/pii/S0968000405001507?via%3Dihub

McClung, C. R. (2006). Plant Circadian Rhythms. *The Plant Cell*, *18*(4), 792-803. https://doi.org/10.1105/tpc.106.040980

McIntosh, B. E., Hogenesch, J. B., & Bradfield, C. A. (2010). Mammalian Per-Arnt-Sim proteins in environmental adaptation. *Annu Rev Physiol*, *72*(1), 625-645.

Merrow, M., Spoelstra, K., & Roenneberg, T. (2005). The circadian cycle: daily rhythms from behaviour to genes. *EMBO Rep*, *6*(10), 930-935. https://doi.org/10.1038/sj.embor.7400541

Mohawk, J. A., Green, C. B., & Takahashi, J. S. (2012). Central and Peripheral Circadian Clocks in Mammals. *Annual Review of Neuroscience*, *35*(1), 445-462. https://doi.org/10.1146/annurev-neuro-060909-153128

Moszczynski, A., & Murray, B. J. (2012). Neurobiological aspects of sleep physiology. *Neurologic clinics*, *30*(4), 963-985.

Mudumbi, K. C., Czapiewski, R., Ruba, A., Junod, S. L., Li, Y., Luo, W., Ngo, C., Ospina, V., Schirmer, E. C., & Yang, W. (2020). Nucleoplasmic signals promote directed transmembrane protein import simultaneously via multiple channels of nuclear pores. *Nat Commun*, *11*(1), 2184. https://doi.org/10.1038/s41467-020-16033-x

Nangle, S. N., Rosensweig, C., Koike, N., Tei, H., Takahashi, J. S., Green, C. B., & Zheng, N. (2014). Molecular assembly of the period-cryptochrome circadian

transcriptional repressor complex. *Elife*, *3*, e03674. https://doi.org/10.7554/eLife.03674

Narayana, S. K., Helbig, K. J., McCartney, E. M., Eyre, N. S., Bull, R. A., Eltahla, A., Lloyd, A. R., & Beard, M. R. (2015). The Interferon-induced Transmembrane Proteins, IFITM1, IFITM2, and IFITM3 Inhibit Hepatitis C Virus Entry. *J Biol Chem*, *290*(43), 25946-25959. https://doi.org/10.1074/jbc.M115.657346

Nguyen, K. D., Fentress, S. J., Qiu, Y., Yun, K., Cox, J. S., & Chawla, A. (2013). Circadian gene Bmal1 regulates diurnal oscillations of Ly6Chi inflammatory monocytes. *Science*, *341*(6153), 1483-1488.

Nobis, C. C., Dubeau Laramée, G., Kervezee, L., Maurice De Sousa, D., Labrecque, N., & Cermakian, N. (2019). The circadian clock of CD8 T cells modulates their early response to vaccination and the rhythmicity of related signaling pathways. *Proceedings of the National Academy of Sciences*, *116*(40), 20077-20086.

Okada, K., Yano, M., Doki, Y., Azama, T., Iwanaga, H., Miki, H., Nakayama, M., Miyata, H., Takiguchi, S., Fujiwara, Y., Yasuda, T., Ishida, N., & Monden, M. (2008). Injection of LPS causes transient suppression of biological clock genes in rats. *J Surg Res*, *145*(1), 5-12. https://doi.org/10.1016/j.jss.2007.01.010

Oshima, T., Yamanaka, I., Kumar, A., Yamaguchi, J., Nishiwaki-Ohkawa, T., Muto, K., Kawamura, R., Hirota, T., Yagita, K., Irle, S., Kay, S. A., Yoshimura, T., & Itami, K. (2015). C-H activation generates period-shortening molecules that target cryptochrome in the mammalian circadian clock. *Angew Chem Int Ed Engl*, *54*(24), 7193-7197. https://doi.org/10.1002/anie.201502942

Park, H.-J., Lee, W.-Y., Jeong, H.-Y., Kang, H.-S., Kim, J.-B., & Song, H. (2016). Mitochondrial interferon-induced transmembrane protein-1 is a critical regulator of cell death in MPRO cells. *Biotechnology and Bioprocess Engineering*, *21*(4), 561-566. https://doi.org/10.1007/s12257-016-0253-y

Pittendrigh, C. S. (1954). On temperature independence in the clock system controlling emergence time in Drosophila. *Proceedings of the National Academy of Sciences*, *40*(10), 1018-1029.

Pittendrigh, C. S. (1960). Circadian rhythms and the circadian organization of living systems. Cold Spring Harbor symposia on quantitative biology,

Preitner, N., Damiola, F., Lopez-Molina, L., Zakany, J., Duboule, D., Albrecht, U., & Schibler, U. (2002). The orphan nuclear receptor REV-ERBalpha controls

circadian transcription within the positive limb of the mammalian circadian oscillator. *Cell*, *110*(2), 251-260. https://doi.org/10.1016/s0092-8674(02)00825-5

Ralph, M. R., Foster, R. G., Davis, F. C., & Menaker, M. (1990). Transplanted suprachiasmatic nucleus determines circadian period. *Science*, *247*(4945), 975-978. https://doi.org/10.1126/science.2305266

Reppert, S. M., & Weaver, D. R. (2002). Coordination of circadian timing in mammals. *Nature*, *418*(6901), 935-941.

Richards, J., & Gumz, M. L. (2012). Advances in understanding the peripheral circadian clocks. *FASEB journal : official publication of the Federation of American Societies for Experimental Biology*, *26*(9), 3602-3613. https://doi.org/10.1096/fj.12-203554

Robles, M. S., Boyault, C., Knutti, D., Padmanabhan, K., & Weitz, C. J. (2010). Identification of RACK1 and Protein Kinase Cα as Integral Components of the Mammalian Circadian Clock. *Science*, *327*(5964), 463-466. https://doi.org/doi:10.1126/science.1180067

Scheiermann, C., Kunisaki, Y., & Frenette, P. S. (2013). Circadian control of the immune system. *Nat Rev Immunol*, *13*(3), 190-198. https://doi.org/10.1038/nri3386

Schmutz, I., Ripperger, J. A., Baeriswyl-Aebischer, S., & Albrecht, U. (2010). The mammalian clock component PERIOD2 coordinates circadian output by interaction with nuclear receptors. *Genes Dev*, *24*(4), 345-357. https://doi.org/10.1101/gad.564110

Schneider-Poetsch, T., Ju, J., Eyler, D. E., Dang, Y., Bhat, S., Merrick, W. C., Green, R., Shen, B., & Liu, J. O. (2010). Inhibition of eukaryotic translation elongation by cycloheximide and lactimidomycin. *Nat Chem Biol*, *6*(3), 209-217. https://doi.org/10.1038/nchembio.304

Schwartz, G. J., & Zeltser, L. M. (2013). Functional organization of neuronal and humoral signals regulating feeding behavior. *Annual review of nutrition*, *33*, 1-21. https://doi.org/10.1146/annurev-nutr-071812-161125

Shi, G., Kenney, A. D., Kudryashova, E., Zani, A., Zhang, L., Lai, K. K., Hall-Stoodley, L., Robinson, R. T., Kudryashov, D. S., Compton, A. A., & Yount, J. S. (2021). Opposing activities of IFITM proteins in SARS-CoV-2 infection. *EMBO J*, *40*(3), e106501. https://doi.org/10.15252/embj.2020106501

Siepka, S. M., Yoo, S.-H., Park, J., Lee, C., & Takahashi, J. S. (2007). Genetics and neurobiology of circadian clocks in mammals. Cold Spring Harbor symposia on quantitative biology,

Silver, A. C. (2017). Pathogen-associated molecular patterns alter molecular clock gene expression in mouse splenocytes. *PLoS One*, *12*(12), e0189949. https://doi.org/10.1371/journal.pone.0189949

Silver, A. C., Arjona, A., Walker, W. E., & Fikrig, E. (2012). The circadian clock controls toll-like receptor 9-mediated innate and adaptive immunity. *Immunity*, *36*(2), 251-261. https://doi.org/10.1016/j.immuni.2011.12.017

Spengler, M. L., Kuropatwinski, K. K., Comas, M., Gasparian, A. V., Fedtsova, N., Gleiberman, A. S., Gitlin, I. I., Artemicheva, N. M., Deluca, K. A., Gudkov, A. V., & Antoch, M. P. (2012). Core circadian protein CLOCK is a positive regulator of NF-κB-mediated transcription. *Proceedings of the National Academy of Sciences of the United States of America*, *109*(37), E2457-E2465. https://doi.org/10.1073/pnas.1206274109

Sulli, G., Lam, M. T. Y., & Panda, S. (2019). Interplay between Circadian Clock and Cancer: New Frontiers for Cancer Treatment. *Trends in cancer*, *5*(8), 475-494. https://doi.org/10.1016/j.trecan.2019.07.002

Sun, F., Xia, Z., Han, Y., Gao, M., Wang, L., Wu, Y., Sabatier, J. M., Miao, L., & Cao, Z. (2020). Topology, Antiviral Functional Residues and Mechanism of IFITM1. *Viruses*, *12*(3). https://doi.org/10.3390/v12030295

Takahashi, J. S. (2017). Transcriptional architecture of the mammalian circadian clock. *Nat Rev Genet*, *18*(3), 164-179. https://doi.org/10.1038/nrg.2016.150

Toh, K. L., Jones, C. R., He, Y., Eide, E. J., Hinz, W. A., Virshup, D. M., Ptácek, L. J., & Fu, Y. H. (2001). An hPer2 phosphorylation site mutation in familial advanced sleep phase syndrome. *Science*, *291*(5506), 1040-1043. https://doi.org/10.1126/science.1057499

Van Gelder, R. N. (2003). Making (a) sense of non-visual ocular photoreception. *Trends Neurosci*, *26*(9), 458-461. https://doi.org/10.1016/s0166-2236(03)00211-x

Vielhaber, E. L., Duricka, D., Ullman, K. S., & Virshup, D. M. (2001). Nuclear export of mammalian PERIOD proteins. *Journal of Biological Chemistry*, *276*(49), 45921-45927.

Vitaterna, M. H., King, D. P., Chang, A. M., Kornhauser, J. M., Lowrey, P. L., McDonald, J. D., Dove, W. F., Pinto, L. H., Turek, F. W., & Takahashi, J. S. (1994).

Mutagenesis and mapping of a mouse gene, Clock, essential for circadian behavior. *Science*, *264*(5159), 719-725. https://doi.org/10.1126/science.8171325

Vitaterna, M. H., Selby, C. P., Todo, T., Niwa, H., Thompson, C., Fruechte, E. M., Hitomi, K., Thresher, R. J., Ishikawa, T., Miyazaki, J., Takahashi, J. S., & Sancar, A. (1999). Differential regulation of mammalian period genes and circadian rhythmicity by cryptochromes 1 and 2. *Proc Natl Acad Sci U S A*, *96*(21), 12114-12119. https://doi.org/10.1073/pnas.96.21.12114

Vitaterna, M. H., Takahashi, J. S., & Turek, F. W. (2001). Overview of circadian rhythms. *Alcohol Research & Health*, *25*(2), 85-93.

Wang, T., Wang, Z., Yang, P., Xia, L., Zhou, M., Wang, S., Du, J., & Zhang, J. (2016). PER1 prevents excessive innate immune response during endotoxin-induced liver injury through regulation of macrophage recruitment in mice. *Cell Death Dis*, *7*(4), e2176. https://doi.org/10.1038/cddis.2016.9

Welsh, D. K., Logothetis, D. E., Meister, M., & Reppert, S. M. (1995). Individual neurons dissociated from rat suprachiasmatic nucleus express independently phased circadian firing rhythms. *Neuron*, *14*(4), 697-706.

Weston, S., Czieso, S., White, I. J., Smith, S. E., Kellam, P., & Marsh, M. (2014). A membrane topology model for human interferon inducible transmembrane protein 1. *PLoS One*, *9*(8), e104341. https://doi.org/10.1371/journal.pone.0104341

Wever, R. A. (1986). Characteristics of circadian rhythms in human functions. *J Neural Transm Suppl*, *21*, 323-373.

Wirz-Justice, A. (2006). Biological rhythm disturbances in mood disorders. *Int Clin Psychopharmacol*, *21 Suppl 1*, S11-15. https://doi.org/10.1097/01.yic.0000195660.37267.cf

Yamazaki, S., Numano, R., Abe, M., Hida, A., Takahashi, R., Ueda, M., Block, G. D., Sakaki, Y., Menaker, M., & Tei, H. (2000). Resetting central and peripheral circadian oscillators in transgenic rats. *Science*, *288*(5466), 682-685. https://doi.org/10.1126/science.288.5466.682

Yanez, D. C., Ross, S., & Crompton, T. (2020). The IFITM protein family in adaptive immunity. *Immunology*, *159*(4), 365-372. https://doi.org/10.1111/imm.13163

Yang, G., Xu, Y., Chen, X., & Hu, G. (2007). IFITM1 plays an essential role in the antiproliferative action of interferon-γ. *Oncogene*, *26*(4), 594-603. https://doi.org/10.1038/sj.onc.1209807

Yi, J. S., Diaz, N. M., D'Souza, S., & Buhr, E. D. (2022). The molecular clockwork of mammalian cells. *Semin Cell Dev Biol*, *126*, 87-96. https://doi.org/10.1016/j.semcdb.2021.03.012

Yoo, S. H., Mohawk, J. A., Siepka, S. M., Shan, Y., Huh, S. K., Hong, H. K., Kornblum, I., Kumar, V., Koike, N., Xu, M., Nussbaum, J., Liu, X., Chen, Z., Chen, Z. J., Green, C. B., & Takahashi, J. S. (2013). Competing E3 ubiquitin ligases govern circadian periodicity by degradation of CRY in nucleus and cytoplasm. *Cell*, *152*(5), 1091-1105. https://doi.org/10.1016/j.cell.2013.01.055

Yoo, S. H., Yamazaki, S., Lowrey, P. L., Shimomura, K., Ko, C. H., Buhr, E. D., Siepka, S. M., Hong, H. K., Oh, W. J., Yoo, O. J., Menaker, M., & Takahashi, J. S. (2004). PERIOD2::LUCIFERASE real-time reporting of circadian dynamics reveals persistent circadian oscillations in mouse peripheral tissues. *Proc Natl Acad Sci U S A*, *101*(15), 5339-5346. https://doi.org/10.1073/pnas.0308709101

Yu, X., Rollins, D., Ruhn, K. A., Stubblefield, J. J., Green, C. B., Kashiwada, M., Rothman, P. B., Takahashi, J. S., & Hooper, L. V. (2013). TH17 cell differentiation is regulated by the circadian clock. *Science*, *342*(6159), 727-730. https://doi.org/10.1126/science.1243884

Zhao, X., Guo, F., Liu, F., Cuconati, A., Chang, J., Block, T. M., & Guo, J.-T. (2014). Interferon induction of IFITM proteins promotes infection by human coronavirus OC43. *Proceedings of the National Academy of Sciences*, *111*(18), 6756-6761.

Zhao, X., Li, J., Winkler, C. A., An, P., & Guo, J. T. (2018). IFITM Genes, Variants, and Their Roles in the Control and Pathogenesis of Viral Infections. *Front Microbiol*, *9*, 3228. https://doi.org/10.3389/fmicb.2018.03228

APPENDICES

APPENDIX A : SUPPLEMENTARY DATA

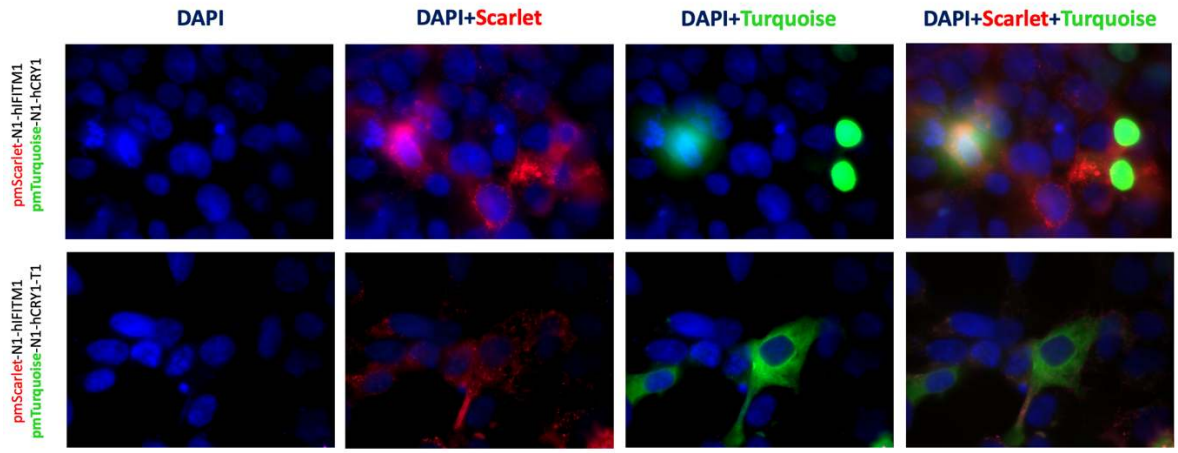

Figure A. 1 Subcellular localization of IFITM and CRY in HEK 293 cell lines. Cellular localization of IFITM1 and CRY1 was evaluated by co-transfecting transiently HEK 293 cells with "pmScarlet-N1-hIFITM1 and pmTurquoise-N1-hCRY1" and "pmScarlet-N1-hIFITM1 and pmTurquoise-N1-hCRY1-T1". DAPI was used as a nuclear marker. WT CRY1 mainly localizes in the nucleus in the presence of IFITM1, while IFITM1 is located around the nucleus. On the other hand, when the last 20 amino acids of CRY1 were absent, CRY1-T1 and IFITM1 localized in the cytosol.

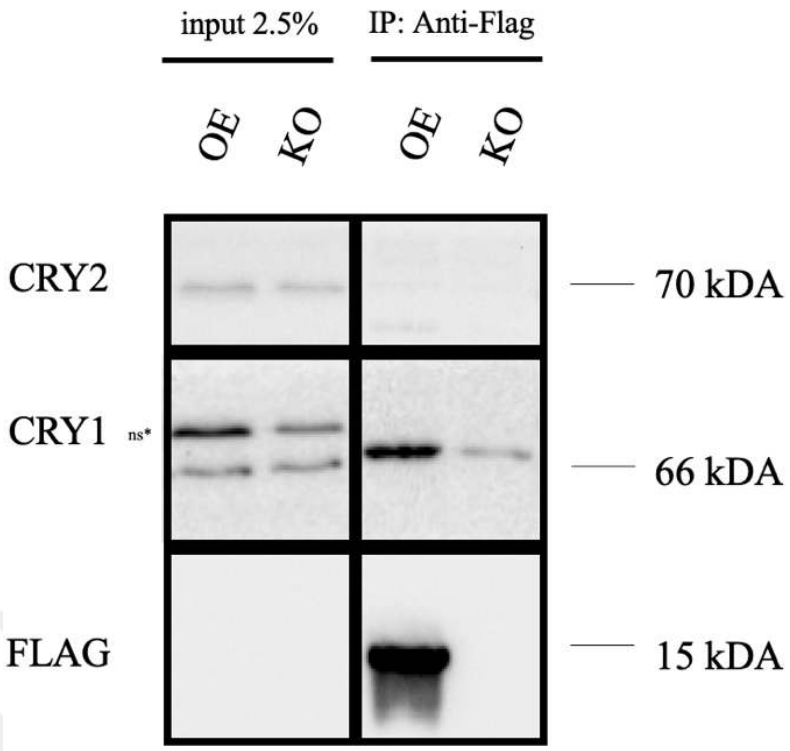

Figure A. 2 IFITM1 physically interacts with CRY1 but not CRY2 by co-Immunoprecipitation in IFITM1 OE and KO U2-OS Bmal1-*dluc* cell lines. Interaction between IFITM1 and CRY1 was assessed via co-IP assay.FLAG-IFITM1 overexpressed in *IFITM1* OE U2-OS *Bmal1-dluc* cell lines predicated by anti-FLAG resin, and the amounts of CRY1 and CRY2 it came with were analyzed with western blotting. *IFITM1* OE U2-OS *Bmal1-dluc 1:dluc* were used in the experiment as a negative control.

APPENDIX B PRIMER SEQUENCES

Table A. 3 The regions were amplified via PCR by adding specific Restriction Sites for subcloning into pJET-v2.

Appendix 1: The regions were amplified via PCR by adding specific Restriction Sites for subcloning into pJET-v2

Donor Plasmid or Source	Gene of Interest	Restriction Sites Added via PCR	Primer Names	Sequence	Recipient Plasmids
pMU2_hCry1	hCRY1	KpnI/XbaI	F: KpnI_hCRY1_For(v2)	GGTACCatgggggtgaacgccgtg	pJET-v2
			R: XbaI_hCRY1_Rev	TCTAGActaattagtgctctgtctctggacttag	
pMU2_hCry1	hCRY1	KpnI/KpnI	F: KpnI_hCRY1_For(v2)	GGTACCatgggggtgaacgccgtg	pJET-v2
			R: KpnI_hCRY1_NoSTOP_Rev	GGTACCattagtgctctgtctctggacttag	
pMU2_hCry1	hCRY1-T1	KpnI/XbaI	F: KpnI_hCRY1_For(v2)	GGTACCatgggggtgaacgccgtg	pJET-v2
			R: XbaI_hCRY1_T1_Rev	TCTAGActaacgtttcccaccactgagacc	
pMU2_hCry1	hCRY1-T1	KpnI/KpnI	F: KpnI_hCRY1_For(v2)	GGTACCatgggggtgaacgccgtg	pJET-v2
			R: KpnI_hCRY1_NoSTOP_T1_Rev	GGTACCacgtttcccaccactgagacc	
HEK293-T cDNA	hCRY2	KpnI/XbaI	F: KpnI_hCRY2_For(v2)	GGTACCatggcggcgactgtggcgacg	pJET-v2
			R: XbaI_hCRY2_Rev	TCTAGAtcaggcatccttgctcggcag	
HEK293-T cDNA	hCRY2	KpnI/KpnI	F: KpnI_hCRY2_For(v2)	GGTACCatggcggcgactgtggcgacg	pJET-v2
			R: KpnI_hCRY2_NoSTOP_Rev	GGTACCggcatccttgctcggcag	
HEK293-T cDNA	hCRY-T1	KpnI/XbaI	F: KpnI_hCRY2_For(v2)	GGTACCatggcggcgactgtggcgacg	pJET-v2
			R: XbaI_hCRY2_T1_Rev	TCTAGAtcattcttcaccaggtgttcctcgg	
HEK293-T cDNA	hCRY2-T1	KpnI/KpnI	F: KpnI_hCRY2_For(v2)	GGTACCatggcggcgactgtggcgacg	pJET-v2
			R: KpnI_hCRY2_NoSTOP_T1_Rev	GGTACCttcttcaccaggtgttcctcgg	
U2-OS cDNA	hIFITM1	BamHI/XhoI	F: BamHI_hIFITM1_F	GGATCCatgcacaaggaggaacatgagg	pJET-v2
			R: XhoI_hIFITM1_R	CTCGAGctagtaaccccgttttttcctgtattatc	
U2-OS cDNA	hIFITM3	BamHI/XhoI	F: BamHI_hIFITM3_F	GGATCCatgaatcacactgtccaaacttcttc	pJET-v2
			R: XhoI hIFITM3_R	CTCGAGctatccataggcctgggaagatcag	
NIH 3T3	mIfitm1	BamHI/XhoI	F: BamHI_mIfitm1_F	GGATCCatgcctaaggagcagcaagag	pJET-v2
			R: XhoI_mIfitm1_R	CTCGAGtcatctaatggcacagacaacgatg	
NIH 3T3	mIfitm3	BamHI/XhoI	F: BamHI_mIfitm3_F	GGATCCatgaaccacacttctcaagccttc	pJET-v2
			R: XhoI_mIfitm3_R	CTCGAGttaagtgtgaaggtttgagcgttaag	
pCMV-Sport6-Flag-hIFITM1	hIFITM1-Flag	HindIII/SalI	F: N-hIF1_HindIII/PstI_For	AAGCTTatgcacaaggaggaacatgagg	pJET-v2
			R: BiFC_VN173_hIF1_HindIII/SalI_Rev	GTCGACgtaaccccgttttttcctgtattatc	
pCMV-Sport6-Flag-hIFITM3	hIFITM3-Flag	HindIII/SalI	F: N-hIF3_HindIII/PstI_For	AAGCTTatgaatcacactgtccaaacttcttc	pJET-v2
			R: BiFC_VN173_hIF3_HindIII/SalI_Rev	GTCGACtccatggcctggaagatcag	
pCMV-Sport6-Flag-hIFITM1	hIFITM1-Flag	HindIII/PstI	F: N-hIF1_HindIII/PstI_For	AAGCTTatgcacaaggaggaacatgagg	pJET-v2
			R: N-hIF1_HindIII/PstI_Rev	CTGCAGgtaaccccgttttttcctgtattatc	
pCMV-Sport6-Flag-hIFITM3	hIFITM3-Flag	HindIII/PstI	F: N-hIF3_HindIII/PstI_For	AAGCTTatgaatcacactgtccaaacttcttc	pJET-v2
			R: N-hIF3_HindIII/PstI_Rev	CTGCAGtccatggcctggaagatcag	
pCMV-Sport6-Flag-hIFITM1	hIFITM1-Flag	KpnI/BamHI	F: C-hIF1_KpnI/BamHI_For	GGTACCatgcacaaggaggaacatgagg	pJET-v2
			R: C-hIF1_KpnI/BamHI_Rev	GGATCCctagtaaccccgttttttcctgtattatc	
pCMV-Sport6-Flag-hIFITM3	hIFITM3-Flag	KpnI/BamHI	F: C-hIF3_KpnI/BamHI_For	GGTACCatgaatcacactgtccaaacttcttc	pJET-v2
			R: C-hIF3_KpnI/BamHI_Rev	GGATCCctatccataggcctgggaagatcag	

Donor Plasmid or Source are vectors used as templates to obtain the target gene. The gene of interest is the name of the target coding sequence. Restriction sites which were added via PCR are the regions which recognized by restriction enzymes to restrict the target fragments and ligate. Primer Names are the recorded names of used primers for this project in our stock system. Primer sequences of these primers were represented in the Sequence column. The recipient plasmid is the host-vector which are desired to insert the gene of interest into it.

Table A. 4: qRT-PCR Primer List

Gene Name	Sequences (from 5' to 3')
hCRY1	F: 5'-ACAGGTGGCGATTTTTGCTTC-3' R: 5'-TCCAAAGGGCTCAGAATCATACT-3'
hCRY2	F: 5′-CTACCGGGGACTCTGTCTACT-3′ R: 5′-ACTGGGTAGTGGTCTTGGGC-3′
hDBP	F: 5'-GAGGAACTTAAGCCCCAGCC-3' R: 5'-CTCGTTGTTCTTGTACCGCC-3'
hPER2	F: 5'-GCGTGTTCCACAGTTTCACC-3' R: 5'-GGCTTTTCCGGACACTGACA-3'
hRPLP0	F: 5'-TGTGGGAGCAGACAATGTGG-3' R: 5'-CATTCCCCCGGATATGAGGC-3'
hIFITM1	F: 5'-ACACCCTCTTCTTGAACTGGTG -3' R: 5'-AATCAGGGCCCAGATGTTCAG -3'

APPENDIX C: DNA and Protein Ladder

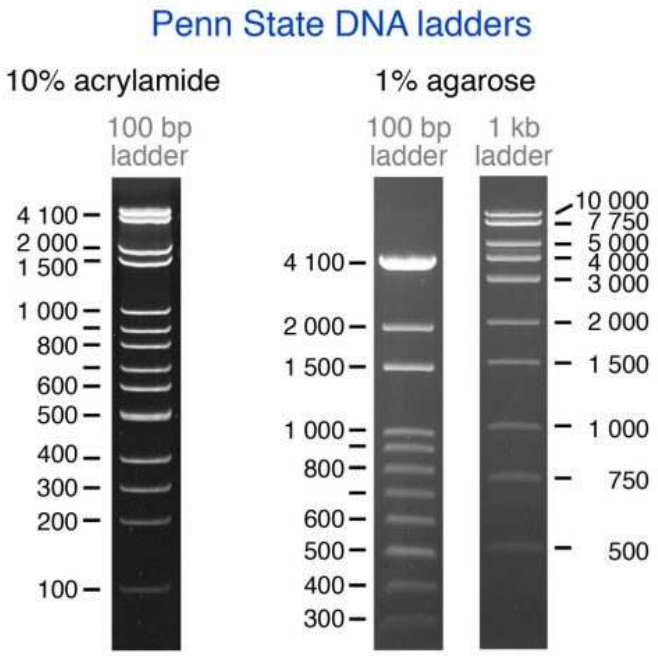

Figure C. 1 1 kb and 100 bp DNA Ladder for agarose gel electrophoresis. (Henrici et al., 2017)

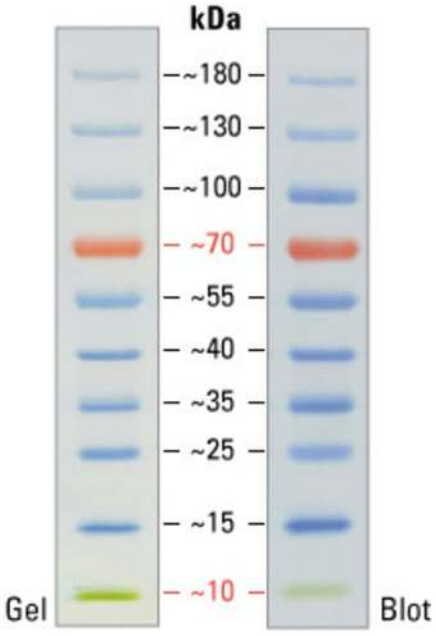

Figure C. 2 Protein ladder for SDS-PAGE and Western Blotting.

APPENDIX D: Plasmid Maps

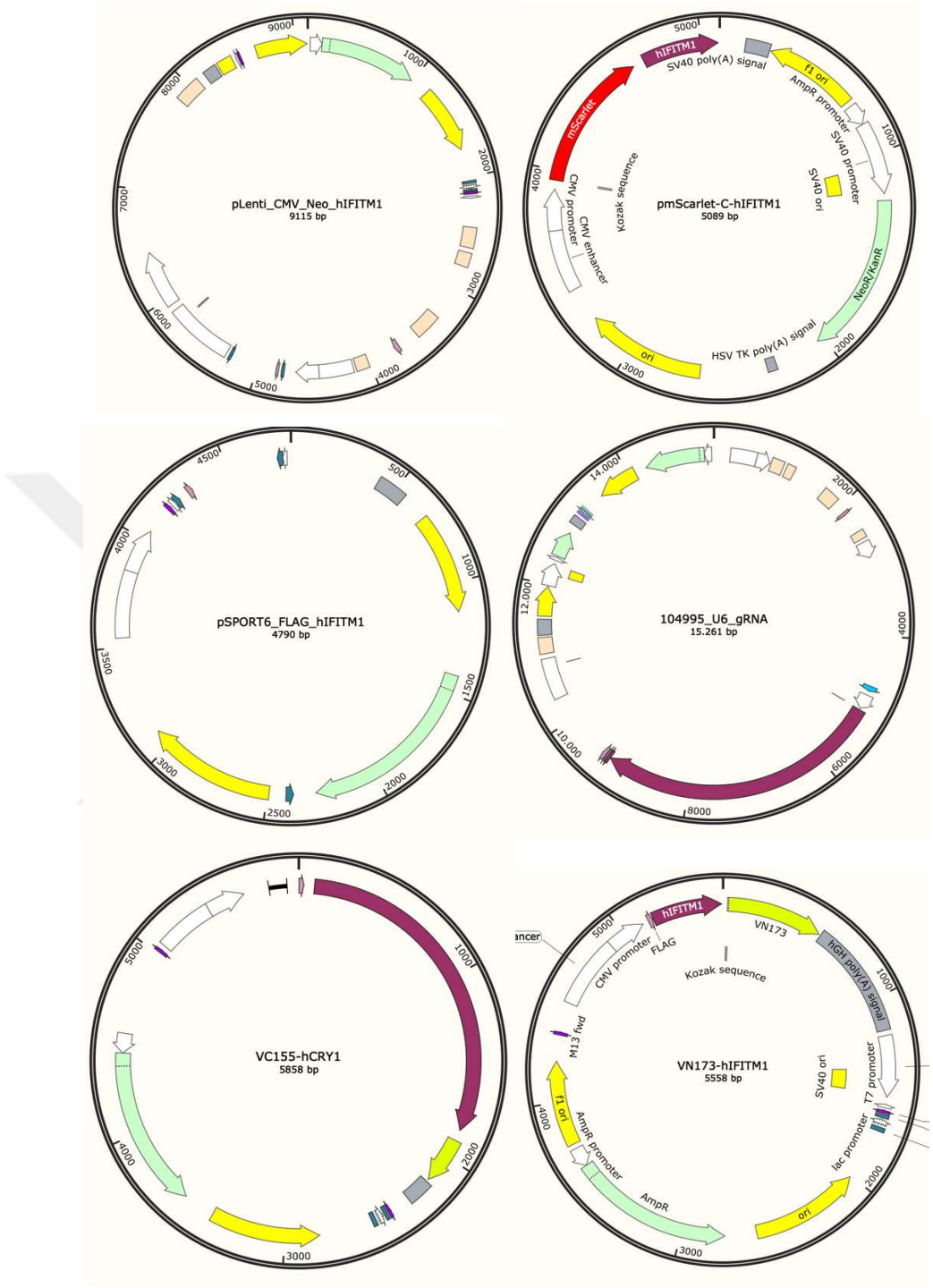

Figure D. 1: Some plasmid constructs in the project. The maps of all plasmids which were used in this study were shared in the below link: https://drive.google.com/drive/folders/13WMqr_7F3SPlANYSTCfyz8ligXhbKsQE?usp=sharing

APPENDIX E: Permissions and Copyrights

SPRINGER NATURE LICENSE
TERMS AND CONDITIONS

Jul 14, 2022

This Agreement between Ms. Melis Çelik ("You") and Springer Nature ("Springer Nature") consists of your license details and the terms and conditions provided by Springer Nature and Copyright Clearance Center.

License Number	5347730830425
License date	Jul 14, 2022
Licensed Content Publisher	Springer Nature
Licensed Content Publication	Nature Reviews Genetics
Licensed Content Title	Transcriptional architecture of the mammalian circadian clock
Licensed Content Author	Joseph S. Takahashi
Licensed Content Date	Dec 19, 2016
Type of Use	Thesis/Dissertation
Requestor type	academic/university or research institute
Format	print and electronic
Portion	figures/tables/illustrations
Number of figures/tables/illustrations	1
High-res required	no
Will you be translating?	no

SPRINGER NATURE LICENSE
TERMS AND CONDITIONS

Jul 15, 2022

This Agreement between Ms. Melis Çelik ("You") and Springer Nature ("Springer Nature") consists of your license details and the terms and conditions provided by Springer Nature and Copyright Clearance Center.

License Number	5350070571361
License date	Jul 15, 2022
Licensed Content Publisher	Springer Nature
Licensed Content Publication	Sports Medicine
Licensed Content Title	Managing Travel Fatigue and Jet Lag in Athletes: A Review and Consensus Statement
Licensed Content Author	Dina C. Janse van Rensburg et al
Licensed Content Date	Jul 14, 2021
Type of Use	Thesis/Dissertation
Requestor type	academic/university or research institute
Format	print and electronic
Portion	figures/tables/illustrations
Number of figures/tables/illustrations	1